

## LATE TRIASSIC (CARNIAN) UNCONFORMITY IN A BLOCK OF THE LATEST CRETACEOUS VOLCANIC OLISTOSTROME UNIT IN THE IZMIR-ANKARA ZONE

Orhan KAYA\*; Walid SADEDDİN\*\*; Demir ALTINER\* and Güssun AKAY\*

ABSTRACT.- In a huge block within the Latest Cretaceous volcanic olistostrome Unit in the Izmir-Ankara zone, nonmetamorphic epidastic and carbonate Late Triassic (Carnian) strata rest unconformably on metacarbonate. Abundant sand-sized detritus of serpentinite occur in the Late Triassic strata. The unconformity is comparable, with respect to stratigraphic setting, with that in the northerly-lying Late Triassic turbidite-olistostrome zone, between the low-grade metamorphic basement and the Late Triassic sedimentary cover.

### INTRODUCTION

The redefined Izmir-Ankara zone is charac-

terized by an outcrop belt of the Latest Cretaceous volcanic olistostrome unit bounded by steepened thrust faults (Kaya, 1992). In the Izmir-Ankara zone,

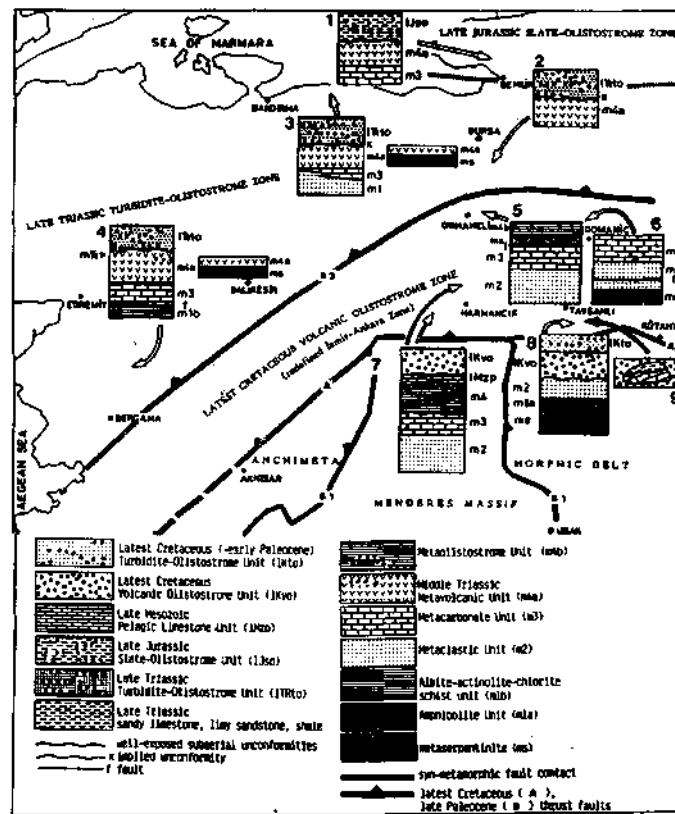


Fig. 1- Structural-stratigraphic settings of the low-grade metamorphic (greenschist and blueschist fades) rocks in the northwestern parts of Anatolia (Kaya 1992). 1- Kaya and Kozur (1987); 2- Kaya Özkoçak and Lisenbee (1989); 4- Kaya and Mostler (1992); 3-8- Kaya in prep.; 9- this report. Arrows indicate the type localities.

the Latest Cretaceous volcanic olistostrome unit overlies unconformably the low-grade metamorphics and serpentized ultramafic tectonites, and the faults separating these basement entities. In the northerly-lying Late Triassic turbidite-olistostrome zone, the Late Triassic turbidite-olistostrome unit rests unconformably on the low-grade metamorphics with an early termination of Middle Triassic (Kaya and Mostler, 1992), and serpentinites.

The objective of this report is to describe the

internal stratigraphy of a composite block within the Latest-Cretaceous volcanic olistostrome and to make an approach to its provenance. W. Sadeddin and D. Altiner investigated the conodonts and foraminifers, respectively. Preparatory works were done by G. Akay.

## REGIONAL GEOLOGY

Major rock units in the report area (fig.2) include the ultramafic unit, the amphibolite unit and the Latest Cretaceous volcanic olistostrome unit.

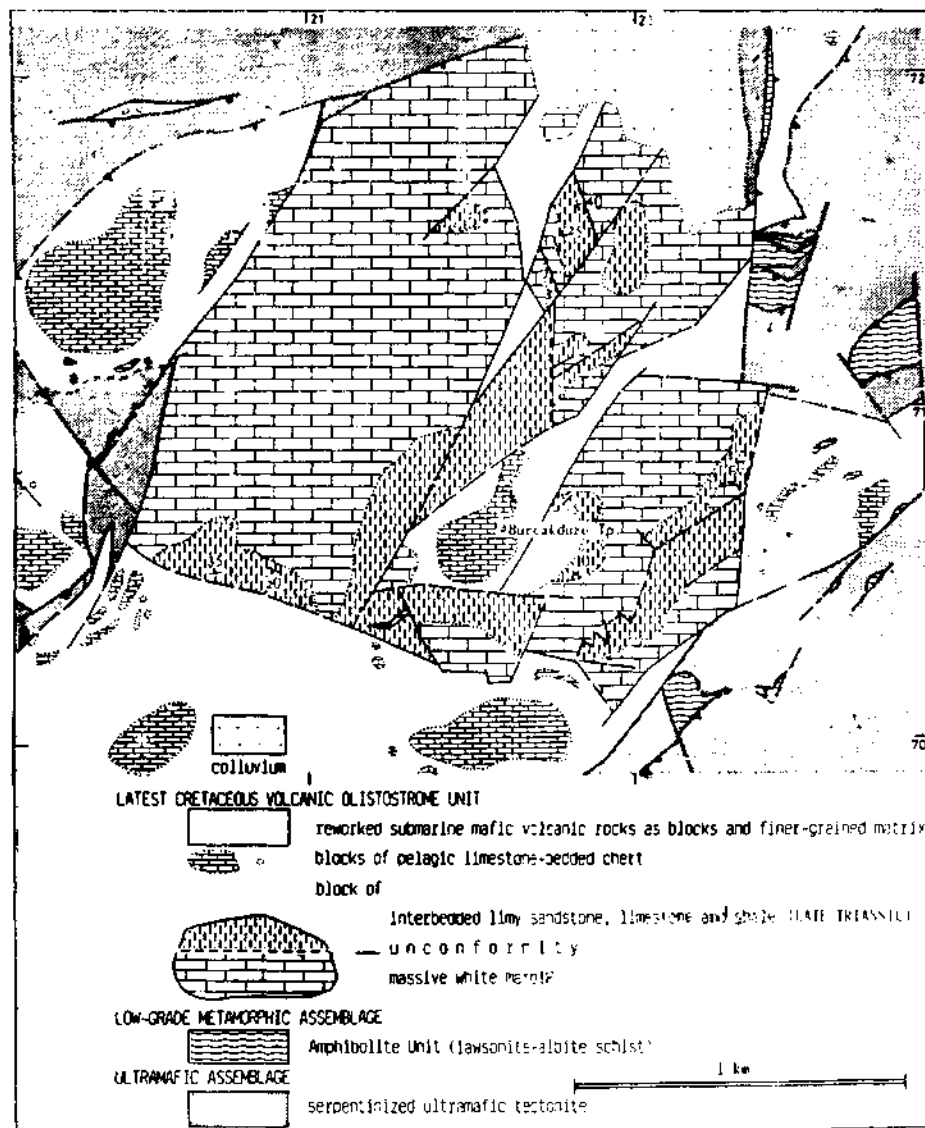


Fig. 2- Geological setting and internal stratigraphy of the studied block in the Latest Cretaceous volcanic olistostrome unit. See Fig. 1, sequence 9. Topographic sheet: J23-a1

### Ultramafic unit

The ultramafic rock, are dunite and harzburgite tectonites that are penetratively serpentinized and pervasively sheared. Jasperoid masses, alteration products of the serpentinites, are widespread.

### Amphibolite unit

Amphibolites exhibit a well developed layering caused by predominating dark colored laminae and thinner and laterally discontinuous light colored laminae, which are less than a millimeter width. Principle components are barroisitic Ca-amphibole, glaucophane-crossite, chlorite, plagioclase, lawsonite and quartz. Other minerals that may be present locally in large amounts, are white mica, epidote-clinozoisite, garnet, sphene and opaques. An earlier Low-grade greenschist mineral assemblage appears to have retrograded to the blueschist assemblage (Kaya, 1981). The amphibolites occur as thrust slices bounded by serpentinites and their silicified varieties.

### Latest Cretaceous volcanic olistostrome unit

This unit consists of green to reddish brown volcanogenic shale and sand to pebble-sized reworked submarine mafic volcanic rocks, and floating or intimately admixed blocks. The blocks include primarily mafic volcanic rocks and subordinately pelagic limestones, bedded cherts, amphibolites, metavolcanic and metaclastic rocks, metacarbonates, and in still smaller amounts, platform-type limestones and lithic sandstone-shale magasequences. The supporting matrix rocks are barren of fossils. Unconformable contact between the volcanic olistostrome unit and the underlying ultramafic and low-grade metamorphic rocks is exposed outside the report area. On the basis of rows of blocks of comparable lithologies and long axis orientations of blocks an internal stratigraphy can be established for this unit.

The studied composite block of metacarbonate and Late Triassic sedimentary rocks is closely associated with various carbonate blocks, and bounded from top and sides by the supporting matrix rocks. In the adjoining areas metacarbonates acting as basement are absent.

### INTERNAL STRATIGRAPHY AND AGE OF THE BLOCK

The huge block (Fig. 2) in the volcanic olistostrome unit consists of two parts: (1) the metacarbonate and (2) the unconformably overlying sedimentary assemblage of epiclastic and carbonate rocks. The metacarbonate is light gray to white, massive, homogeneous and coarse to very coarse-grained calcite-marble. Complexely intersecting planar calcite veins up to 0.5 cm in width related to its dynamometamorphic history, are widespread. The sedimentary part of the block consists, in a generalized ascending order, of pale red, thinly and unevenly bedded sandy limestone, limestone pebble conglomerate with clasts of metacarbonates up to 20 cm in size; dark gray to yellowish gray, thinly interbedded shale and sandy limestone with minor pink limestone interlayers; greenish gray and thin to medium-bedded limy lithic sandstone with abundant intrastratal, sinuous feeding traces up to 1 cm in width and 30 cm in length, and, lenticular gray limestone. The lithic sandstones and in parts sandy limestones contain sand-sized detrital serpentinite, chloritized serpentinite and related opaques. The above stratigraphic horizons show remarkable variation in lateral extent. The basal strata a/6 given in Fig. 3.

The interbedded shale and limestone part of the sedimentary sequence carries abundant severely recrystallized algae and foraminifers. The latter include *Aulotortus* sp. and *Involutinidae*, indicating a

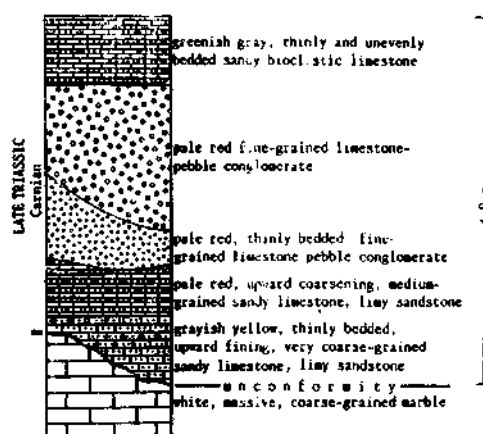


Fig. 3- Well-exposed unconformity between the Late Triassic sedimentary assemblage and underlying metacarbonate (J23-a1, 21.73:71.37).

broad age of Triassic. The conodont fauna comprises *Epigondolella pseudodiebeli* (Kozur), *Gondolella auriformis* Kovacs, *G. noah* (Hayashi), transitional form between *G. noah* (Hayashi) and *G. polygnathiformis* Budurov and Stefanov, *Crathognathodus kochi* (Huckriede), *Enantiognathus* sp. ? Comudina cf. *breviramulis* and *Gondolella* sp. (plate). *G. auriformis*, *E. pseudodiebeli* and *G. noah*, as a whole, are indicative of a Carnian age.

#### POSSIBLE PROVENANCE FOR THE BLOCK

In the Late Triassic turbidite-olistostrome zone (Fig.1), the Middle Triassic (Anisian/Ladinian boundary) early termination of the low-grade metamorphic sequence to the north of Bergama (Kaya and Mostler, 1992), on the ground of conodont evidence, points out to the pre-Carnian stratigraphic setting of the metacarbonate unit (Fig. 1, sequence 4). The Carnian unconformity can be compared with the unconformity between the Middle Triassic and earlier sequence of low-grade metamorphic rocks and the Late Triassic turbidite-olistostrome unit. The abundant sand-sized detritus of serpentinite in the sedimentary part of the studied block correlates with the metaserpentinites and less affected ultramafics, which occur as structurally concordant and syntectonically metamorphosed thrust slices in the low-grade metamorphic sequence (Kaya, 1988, 1992). The turbidite-olistostrome unit contains several blocks of low-grade metaclastics enclosing blocks of metaserpentinite (into block-in-block relationship) supporting the presence of pre-Late Triassic ultramafics (Kaya and Kozur, in prep.).

In conclusion, the metacarbonate part of the studied block may correlate, with respect to its relative age, with the metacarbonate unit to the north of the Izmir-Ankara zone. The sedimentary part may

suggest either to have once preceded the Late Triassic turbidite-olistostrome unit, or to be its facies equivalent.

*Manuscript received November 19, 1992*

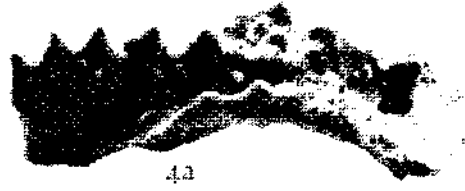
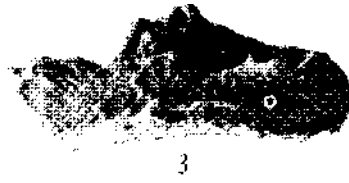
#### REFERENCES

- Kaya, O., 1981, Preliminary study on the Paragenetic relationships in the polymetamorphic blueschist rocks of the Tavşanlı area, West Anatolia: Aegean Earth Sciences, 1, 27-43.
- , 1988, Significance of the contact relationships between the ultramafic and low-grade metamorphic rocks in the western parts of Turkey. Symposium for the 20th Anniversary of Earth Sciences at Hacettepe University, Abstracts, p.9.
- , 1992, Constraints on the age, stratigraphic and structural significance of the ophiolitic and adjoining rocks in the western parts of Turkey: In, Savaşçın, Y. and Donat, H. (eds.), International Earth Sciences Congress on Aegean Regions (IESCA 1990), Proceedings II, 193-209.
- and Kozur, H., 1987, A new and different Jurassic to Early Cretaceous sedimentary assemblage in northwestern Turkey (Gemlik, Bursa): Implications for the pre-Jurassic to Early Cretaceous tectonic evolution: *Yerbilimleri, H. Üniv.*, 14, 253-268.-
- ; Özkoçak, O. and Lisenbee, A., 1989, Stratigraphy of the pre-Jurassic blocky sedimentary rocks to the south of Bursa, NW Turkey: *Bull. Min. Res. Expl. Inst.*, 109, 15-24, Turkey.
- and Mostler, H., 1992, A Middle Triassic age for low-grade greenschist facies metamorphic sequence in Bergama (Izmir): the first paleontological age assignment and structural-stratigraphic implications. *Newsl. Stratigr.*, 26, 1-17.

PLATE

**PLATE -I**

- Fig. 1- *Epigondolella pseudodiebeli* (Kozur)  
a) lateral view, b) lower view, X90
- Fig. 2- *Gondolella auriformis* Kovacs  
a) lateral view, b) lower view, c) upper view,  
X160  
d) lower view, X220, e) lateral view, X128  
f) upper view, g) lower view, X175  
h) upper view, i) lateral view, X220  
j) upper view, k) lower view, X175
- Fig. 3- *Gondolella noah* (Hayashi), juvenile, lateral  
view, X150
- Fig. 4- *G. cf. noah* (Hayashi)  
a) lateral view, b) lower view, c) upper view,  
X150
- Fig. 5- Transitional form between *G. noah* (Hayashi)  
and *G. polygnathiformis* Budurov and Stefanov  
a) lateral view, b) lower view, X120
- Fig. 6- *Gondolella* sp.  
a) lateral view, b) lower view, X140
- Fig. 7- *Cratognathodus kochi* (Huckriede), X110
- Fig. 8- *Enantiognathus* sp., X175
- Fig. 9- ? *Comudina cf. breviramulis*, X145



STRATIGRAPHIC AND STRUCTURAL SETTING OF THE ANCHIMETAMORPHIC ROCKS TO THE SOUTH OF TAVŞANLI (KÜTAHYA, WESTERN TURKEY): RELATION TO THE İZMİR-ANKARA ZONE

Orhan KAYA\*; Walid SADEDDİN\*\*, Demir ALTINER\*\*\*; Engin MERİÇ\*\*\*\*; İzver TANSEL\*\*\*\* and Aylin VURAL\*

ABSTRACT.- In western Anatolia, a belt of anchimetamorphic rocks that are characterized by penetratively developed slaty deavage, extensive mineral overgrowths and formation of new phyllosilicate minerals extends between the Izmir-Ankara zone and the northernmost schist and gneiss masses of the Menderes massif. In the report area, the anchimetamorphic assemblage is divisible into three stratigraphic units. The Middle Triassic lower slate unit consists mainly of slates representing fine-grained silicic and basic tuffs, and subordinately of silicic lava, quartz-conglomerate, quartzofeldspathic sandstone, gray and red limestones, thinly bedded lithic sandstone and red bedded chert. The Middle Triassic to probably Early Liassic upper slate unit consists mainly of slates representing illitic mudrocks and lithic wackes, and subordinately of lithic arenite, lithic conglomerate, gray limestone and coarse-grained mafic tuff. The Middle Liassic limestone unit is made up of gray bioclastic limestones. The Latest Cretaceous (to Paleocene) turbidite-olistostrome unit, which is widely spread in the Izmir-Ankara zone, overlies unconformably the southerly-tying anchimetamorphic rocks and the steep boundary fault separating these rocks from the older entities of the zone. The exposure of the relative allochthon of the anchimetamorphic rocks of a southern origin, the steepening of the fault and the onlap of the turbidite-olistostrome unit onto the anchimetamorphic basement seem to be Latest Cretaceous events.

INTRODUCTION

Separate exposures of penetratively sheared and

pervasively recrystallized sedimentary and volcanic rocks between the redefined İzmir-Ankara zone (IAZ) and the northernmost schist and gneiss masses of

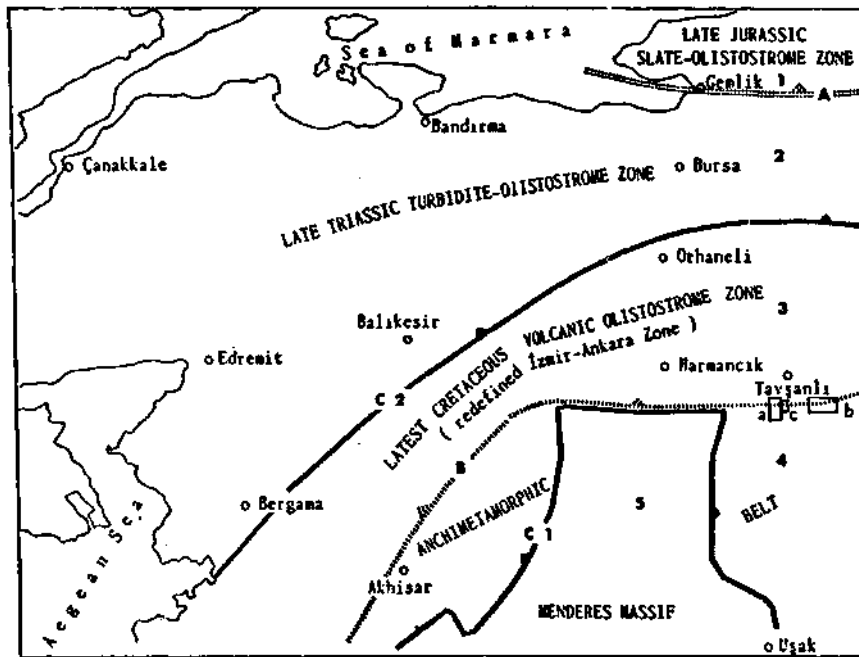


Fig. 1- Major structural-stratigraphic subdivisions of the northwestern parts of Anatolia (Kaya, 1992). 'a'-'c', Report areas.

the Menderes massif are distinguished and delimited as an anchimetamorphic assemblage (Kaya, 1992) (Figs. 1-3).

In the report area, The Latest Cretaceous (to

Paleocene) turbidite-olistostrome unit of the Izmir-Ankara zone overlies unconformably the anchimetamorphic rocks and the boundary fault separating the older rocks of the IAZ (i.e. ultramafics, low-grade greenschist and blueschist rocks, and The

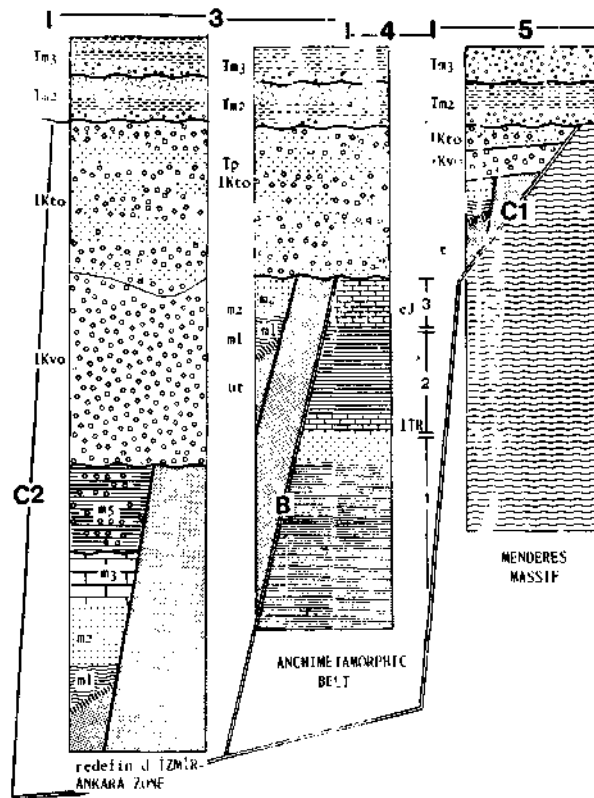


Fig. 2- Structural-stratigraphic setting of the anchimetamorphic rocks in western Anatolia. ITR-eJ, anchimetamorphic assemblage: 1- Lower slate unit, 2- Upper slate unit, 3- Limestone unit, m, Low-grade (greenschist and blueschist facies) metamorphic rocks (1 Amphibolite unit, 2- Metadastic unit, 3- Metacarbonate unit, 4- Metaolistostrome unit), ut, serpentinized ultramafic tectonites. 1kvo, Latest Cretaceous volcanic olistostrome unit. 1kto, Latest Cretaceous (to Paleocene) turbidite olistostrome unit. Tm2, Middle Miocene; Tm3, Late Miocene. B, Boundary fault of an implied Latest Cretaceous age, separating the redefined Izmir-Ankara zone from the anchimetamorphic assemblage. C1, Late Paleocene thrust fault bounding the anchimetamorphic assemblage against the relative allochthonous crystalline masses of the Menderes massif. C2, Thrust fault defining the northern boundary of the redefined Izmir-Ankara zone, contemporary with C1.

Latest Cretaceous volcanic olistostrome unit) from the anchimetamorphic assemblage (Kaya, 1972,1992).

The anchimetamorphic rocks were first described by Canet and Jaoul (1946) in the surroundings of Akhisar and called "the probably Permo-Carboniferous Akhisar schist". Arpat and Norman

(1961) recorded these rocks as "least metamorphic schists". Kaya (1972) reported the anchimetamorphic rocks to the south of Tavşanlı, dated them as Jurassic on the basis of inconclusive evidence and established a lower clastic unit (Üyücek fm.) and an upper limestone unit (Kayaardı lms.) He suggested that the lower clastic unit rests unconformably a low-grade metamorphic sequenca (iki-başlı fm.) of an implied Paleozoic age. Bingöl (1977) recognized the anchimetamorphic rocks to the east of Gediz and assigned a Middle to Late Jurassic age on the basis of foraminifera. In the surroundings of Akhisar, Akdeniz et al. (1980) and Akdeniz (1985) subdivided the anchimetamorphic succession into Triassic clastic and carbonate rocks, Jurassic clastic rocks with lenses of meta-volcanics and carbonates, and thickly developed Jurassic to Late Cretaceous carbonates. The basal clastic rocks were said to rest unconformably on the Paleozoic metamorphics. Erdoğan (1990) considered the relevant Mesozoic sequence to be conformably gradational into the underlying low-grade metamorphics of the Menderes massif, and to have an early termination of Maastrichtian age. To the south of Kütahya, Göncüoğlu et al. (1992) recorded a conformable succession of Early Scythian mudrocks and Triassic to Late Cretaceous limestones, in parts probable correlatives of the anchimetamorphic assemblage. They reported that this succession overlies unconformably a Carboniferous to Permian metamorphic basement, and is overlain gradationally by a Late Cretaceous (Middle to Late Maastrichtian) to Early Paleocene sedimentary melange. Okay (1980) considered the relevant areas of anchimetamorphic rocks as being constituted of greenschist-amphibolite facies rocks.

The present report, which is concerned with the upper part of the anchimetamorphic assemblage, (1) revises the stratigraphy and inconclusive Jurassic age proposed by Kaya (1972), in the light of new exposures and fossil findings and recent accumulation of regional data (Kaya, 1992); and, (2) documents new age data on the turbidite-olistostrome unit of the Izmir-Ankara zone, which has a significant bearing on the understanding the structural setting of the anchimetamorphic rocks. Authors have contributed this paper as follows: O.Kaya, field work and text; W. Sadeddin, conod-

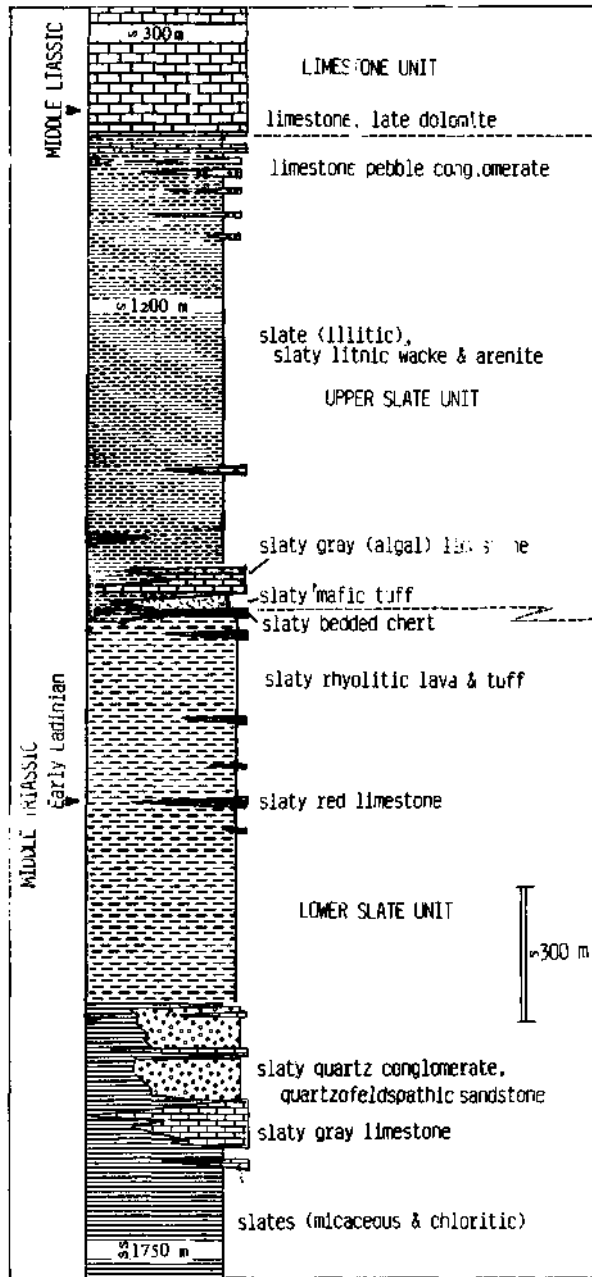
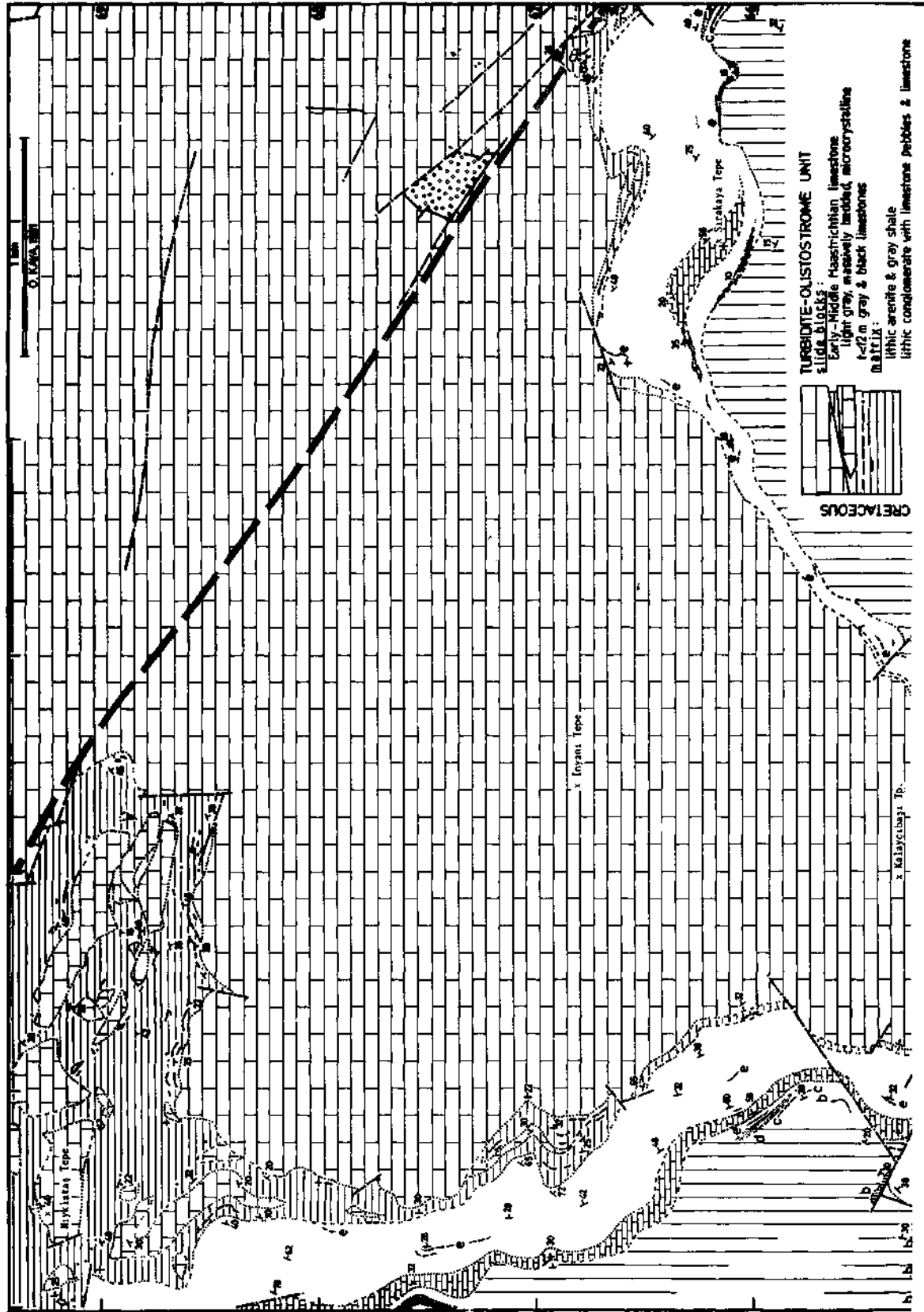


Fig. 3- Generalized order of rock succession of the anchimetamorphic rocks.



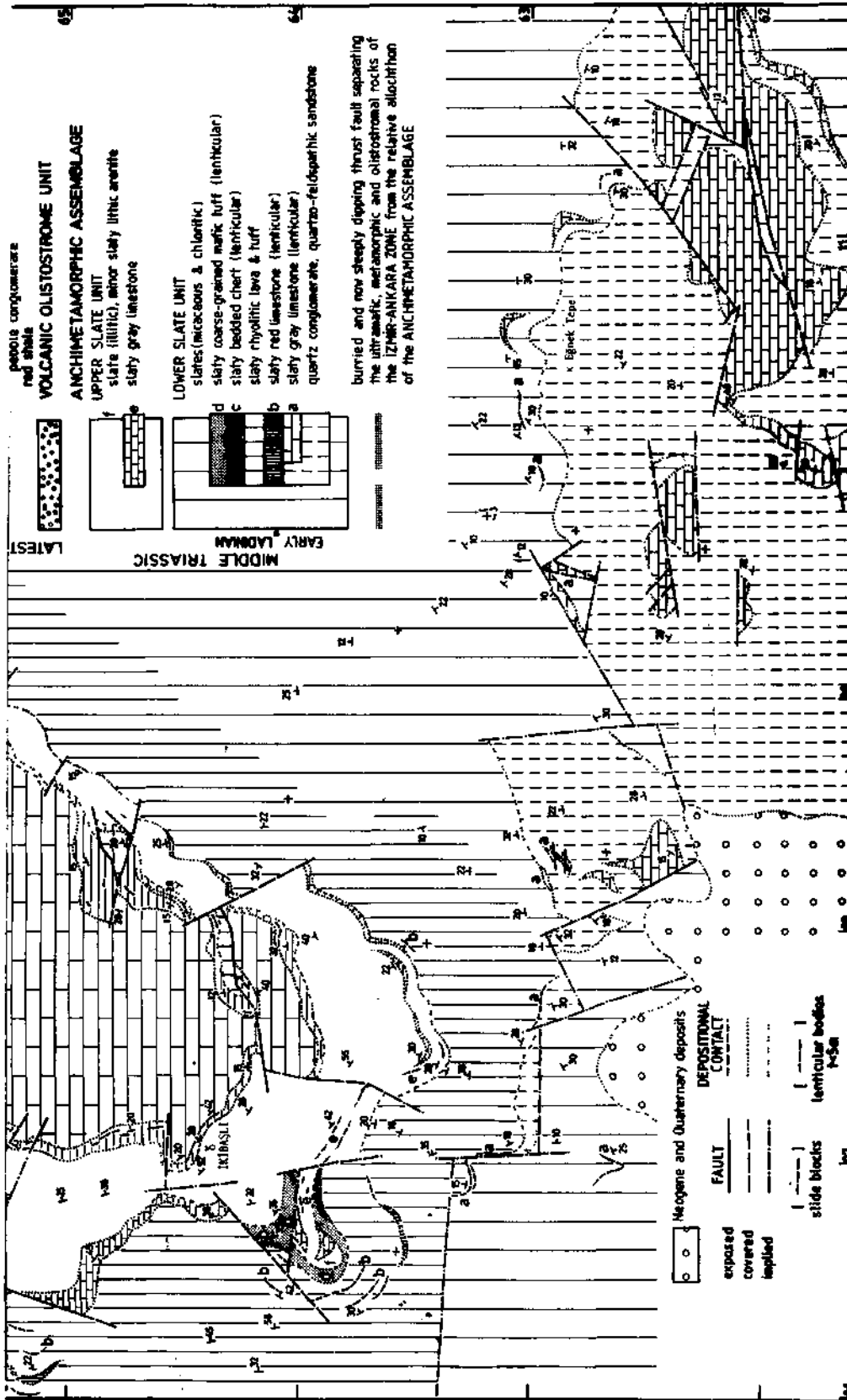


Fig. 4- Distribution of the anchimetamorphic rocks immediately adjoining the Izmir-Ankara zone along a now steeply dipping thrust fault (thrust fault B in Fig. 1). Map area: 35 km SW of Tavşanlı, sheet J22-b2; 'a' in Fig. 1.

onts; D. Altiner, Triassic and Jurassic foraminifers and algae; E. Meriç and İ. Tansel Cretaceous foraminifers; and, A Vural, recovery of conodonts.

#### ANCHIMETAMORPHIC ASSEMBLAGE

##### Lower slate unit

This unit (İkibaşlı fm., Kaya, 1972) consists primarily of volcanogenic slate, and subordinately of volcanic, epiclastic and carbonate rocks all with slaty cleavage. The lower slate unit is divisible into three parts, in ascending order: (1) micaceous slate with sporadic chloritic slate interlayers; (2) quartz conglomerate, quartzofeldspathic sandstone and gray limestone; and, (3) micaceous slate, rhyolitic lava and tuff, red and gray limestones, and bedded chert (Fig.4).

The gray micaceous and greenish gray chloritic slates show affinity, respectively, with silicic and basic fine-grained tuffs. The quartz conglomerates are light gray, massively bedded, and gram and matrix-supported. The clasts are up to 8 cm in size, round to subround and strongly strained in most cases. They include primarily white vein quartz, and in minor amounts silicic volcanic rocks, pink and gray chert and quartzofeldspathic sandstone. The matrix consists of finer-grained versions of the pebbles, and white mica and chlorite. The quartzofeldspathic sandstones are white, thickly bedded and, together with the quartz conglomerates, represent upward-coarsening sequences. The gray limestones, which are lenticular bodies on all scales, are microcrystalline and pervasively recrystallized into sparry patches. The rhyolitic lava and tuff are composed of the mineral assemblage of quartz, albite, minor oligoclase, muscovite (2M), chlorite and minor talc. Quartz and plagioclase which are mostly rotated, occur as stubby crystals up to 5 mm in length and give a knotty appearance to the cleavage plane. Quartz exhibits a moderately undulose extinction and alpha-quartz pseudomorphs after beta-quartz. Plagioclases are mostly euhedral and show overgrowths in pressure shadows. Along the cleavage planes, quartz and plagioclase are thickly sheathed by white mica and chlorite. A late formation of chlorite is associated with widely spaced parallel fractures across S1. The red limestones are up to 3 m in thickness and several

tens of m in lateral extension, and severely recrystallized. The red brown cherts occur at the top of the unit and are laterally discontinuous. They are recrystallized into fine-grained quartz mosaic.

The base of the lower slate unit is not exposed. The quartz conglomerates and quartzofeldspathic sandstones are locally successively channelized into the slates. This channel system, intervened by lenticular limestones, cuts into the lower uniformly micaceous and chloritic slate part of the unit, and defines a very broad SE-NE trend. The rhyolitic lava, which represents the upper part of the unit, rests gradationally on the micaceous slate and shows lateral variations in thickness and texture.

The red limestones contain conodont (Plate I) *Gondolella basisymmetrica* (Budurov and Stefanov), *Paragondolella navicula* (Huckriede), *Gladiogondolella cf. tethydis* (Huckriede), *Prioniodina* (Cypridodella) *muelleri* (Tatge), *P. spengleri* (Huckriede), *P. sp.*, *Prioniodalla sp.*, *Hindeodella suevica* (Tatge), *H. sp.*, *Neospathodus cf. discretus* (Müller), *N. newpassensis* (Mosher), *N. sp.*, *Cornudina sp.*, *Cratognathodus sp.*, *Enantiognathus sp.*, ?Ozarkodina-type unit and *O sp.*, *G. basisymmetrica* places the top strata of the lower slate unit in the early Ladinian (Fassanian)

##### Upper slate unit

This unit (Üyücek fm.; Kaya, 1972) consists primarily of illitic slate and pervasively cleaved lithic wacke, and subordinately of lenticular lithic arenite, limestone, limestone conglomerate, lithic conglomerate and coarse-grained mafic tuff, all with slaty disposition. The unit is essentially gray in color, but pale red to purple gray slates, and lithic sandstones and conglomerates occur increasingly to the top of the unit (Fig. 5).

The slate and lithic wacke, which intergrade, present massive sections, and are locally calcareous. The lithic arenites are thin to thick-bedded, and include micaceous and feldspathic versions. The limestones, which occur mainly in the lower part of the unit as extensive lenses, are algal and crinoidal micrites. They are pervasively recrystallized; and fossils are strongly distorted and variably micritized, or replaced by sparry calcite. The lime-

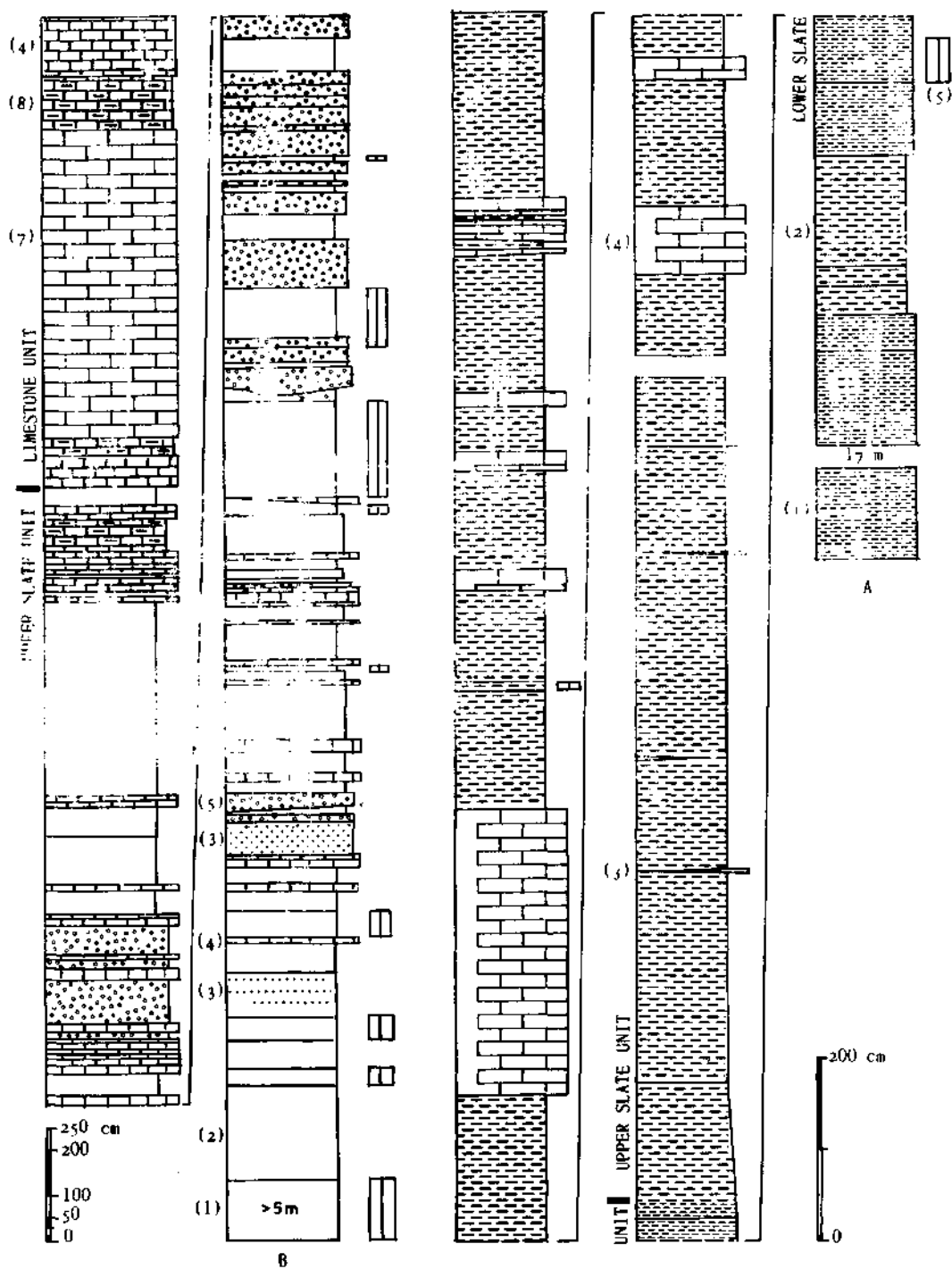


Fig. 5- Contact relationships between the major units of the anchimetamorphic assemblage. A: J22-b2, 12.63:65.79; B, J23-a1, 25.21: 69.28. A1, Gray rhyolitic tuff; A2, gray chloritic slate; A3, gray (grayish yellow weathering) illitic slate; A4, gray limestone; A5, purple gray slate. B1, Purple gray illitic slate; B2, gray (grayish yellow weathering) illitic slate; B3, gray lithic arenite; B4, gray limestone; B5, gray limestone pebble conglomerate; B6, gray limy slate; B7, gray dolomitized limestone; B8, gray clayey limestone.

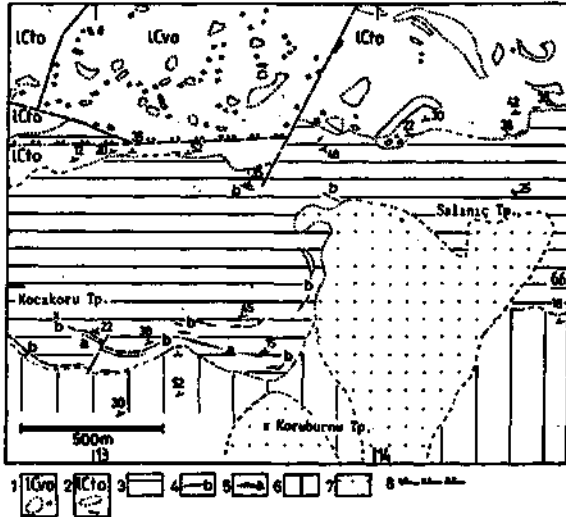


Fig. 6- Bedded chert lenses in the basal part of the upper slate unit suggest an interfingering contact relationship between the lower and upper slate units (Sheet J22-b2). 1- Latest Cretaceous turbidite-olistostrome unit; 2- Latest Cretaceous volcanic olistostrome unit; 3- Upper slate unit; 4- Lenticular gray limestone (upper slate unit); 5- Lenticular bedded chert (upper slate unit); 6- Lower slate unit; 7- Paleo-alluvium; 8- Boundary fault overlain by the Latest Cretaceous turbidite-olistostrome unit, and reactivated.

stone conglomerates occur as thin to medium-thick intercalations in the uppermost part of the unit (Fig. 5). They are composed of fine to medium-sized pebbles of light gray recrystallized limestones, which are slightly strained. The supporting matrix is calcareous mudstone and, less commonly, limestone.- The coarse-grained mafic tuff consists of chlorite, chloritized rock fragments, and minor relic pyroxene, epidote series minerals and white mica. Locally it contains thin interlayers of mafic lava, and interlayers and rows of nodules of marble-like recrystallized limestone.

Both the lower slate and upper slate units exhibit a good diversity of rock types and strong lateral variations near their mutual contacts. However, the contact between the bulk rocks of micaceous slate and illitic slate is conformable and gradational (Fig.5). The presence of the bedded chert in the very base of the upper slate unit (Fig. 6.), several km away from its occurrence at the top of the lower slate unit, may suggest a diachronous contact relationship between the two units.

Lenses of recrystallized algal limestone, at the lowermost part of the upper slate unit have

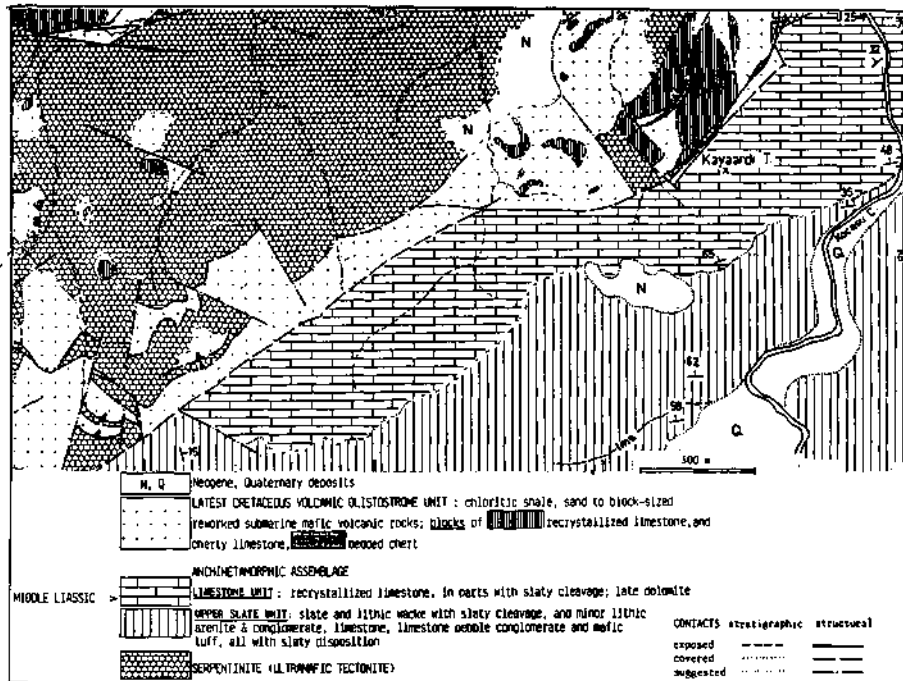


Fig. 7- Exposed Major Fault (Line B in Figs. 1 and 2) which defines the southern boundary of the Izmir-Ankara zone against the anchimetamorphic belt (Sheet J23-a1).

yielded an inconclusive foraminiferal fauna including *Aulotortus* sp. (gr. *sinuosus*), *Ophthalmidium*?, *Auloconus*?, *Duostominidae*, *Galeanellid* foraminifers and *Involutinid*, which may tentatively suggest a Middle to Late Triassic age. The conodonts, which are poorly preserved, include *Prionodina muelleri* (Tatge) and *Hibardella* cf. *magnidentata* (Tatge). *P. muelleri* is Middle Triassic in age and indicates an upper age limit of latest Ladinian. This assigns a Ladinian age to the base of the unit. The upper slate unit should reach as far as Early Liassic, because it is conformably and gradationally overlain by the Middle Liassic limestone unit.

#### Limestone unit

This unit (Kayaardı Limestone: Kaya, 1972) consists primarily of bioclastic limestones, which are white to light gray, medium to thick-bedded and pervasively recrystallized (Fig.7). Widespread dolomitization has obliterated the original texture and stratification. Shearing becomes gradually less distinct to the core of the unit.

The limestone unit lies gradationally on the upper slate unit (Fig.5). The lenticular bodies of limestone conglomerates, in the contact interval seem to be intrabasinal in origin.

In the lower part of the limestone unit recrystallized limestone patches, which locally escaped dolomitization, contain algae *Thaumatoporella parvovesiculifera* Rainer, *Paleodasycladus mediterraneus* (Pia) and *P. elongatulus* (Praturlon), and foraminifers *Lituosepta recoarensis* Cati, *Orbitopsella primaeva* (Henson), *O. praecursor* (Guembel), *Haurania deserta* Henson, *Mayncina termieri* Hottinger, *Pseudocylammina liassica?* Hottinger, *Valvulinasp.*, *Siphovalvulina* sp. and *Ataxophragmiidae*, which indicate as a whole a Middle Liassic age.

#### İZMİR-ANKARA ZONE

The redefined İzmir - Ankara zone (IAZ) is characterized by The Latest Cretaceous volcanic olistostrome unit overlying unconformably an older structural system of ultramafic and low-grade metamorphic (greenschist and blueschist) rocks (Kaya, 1992). The Latest Cretaceous (to Paleocene) turbidite-olistostrome unit which conformably but abruptly overlies the volcanic olistostrome unit, extends

across the boundaries of the IAZ, well into southwest (Bernouilli et al., 1974) and northwest Anatolia (Eroskay, 1965), and consequently is not characteristic for the IAZ (Kaya, 1992).

#### Latest Cretaceous (to Paleocene) turbidite-olistostrome unit

This unit (Karaçalı fm.; Kaya, 1972) consists of turbiditic megasequences of shale and sandstone-shale, pebbly mudrocks of debris-flow origin, and blocks primarily of platform-type limestones, submarine mafic volcanic rocks and pelagic rocks incorporated in olistostromes with a supporting matrix of the above type of strata. In the study area (Fig. 4), for most part the unit is represented by an Early Campanian to Early Maastrichtian platform-type limestone slab (tabular block) more than 7 km long in a S-N direction (the Budağan limestone slab). The matrix rocks underlying the Budağan limestone slab include regularly stratified, gray, thickly bedded to massive, finely pebbly and coarse-grained lithic arenites, gray and red-brown shales, and minor lithic conglomerates. Those overlying the slab are gray lithic arenites and gray shales which exhibit everywhere soft-sediment deformation features to the degree of sandstone-shale melange.

The unit contains Permian, probably Triassic, Jurassic and Early Cretaceous limestone blocks and pebbles. The apparently basal part of the Budağan limestone slab, and many other clasts as well, contain *Orbitoides medius* (d'Archiac), *O. concavatus* Rahaghi, *Pseudosiderolites vidali* (Douville), *Praesiderolites dordoniensis* Wannier, *Lepidorbitoides* cf. *campaniensis* van Gorsel and *Sulcoperculine* sp., as a whole indicating a Late Campanian to Early Maastrichtian age. The pelagic limestone blocks carry *Globotruncana bulloides* Vogler, *G. cf. area* (Cushman), *G. sp. (gr. lapparenti)*, *Globotruncanita* cf. *stuarti* (de Lapparent) and *Abathomphalus?* sp., indicating an Early, to probably Middle Maastrichtian age. A small limestone block of higher stratigraphic position than the Budağan limestone Slab yields a youngest age of Late Maastrichtian. The relevant microfauna consists of *Globotruncanita stuarti* (de Lapparent), *Abathomphalus mayaroensis* Bolli and *Rosita contusa* (Cushman).

In the western parts of Turkey Maastrichtian

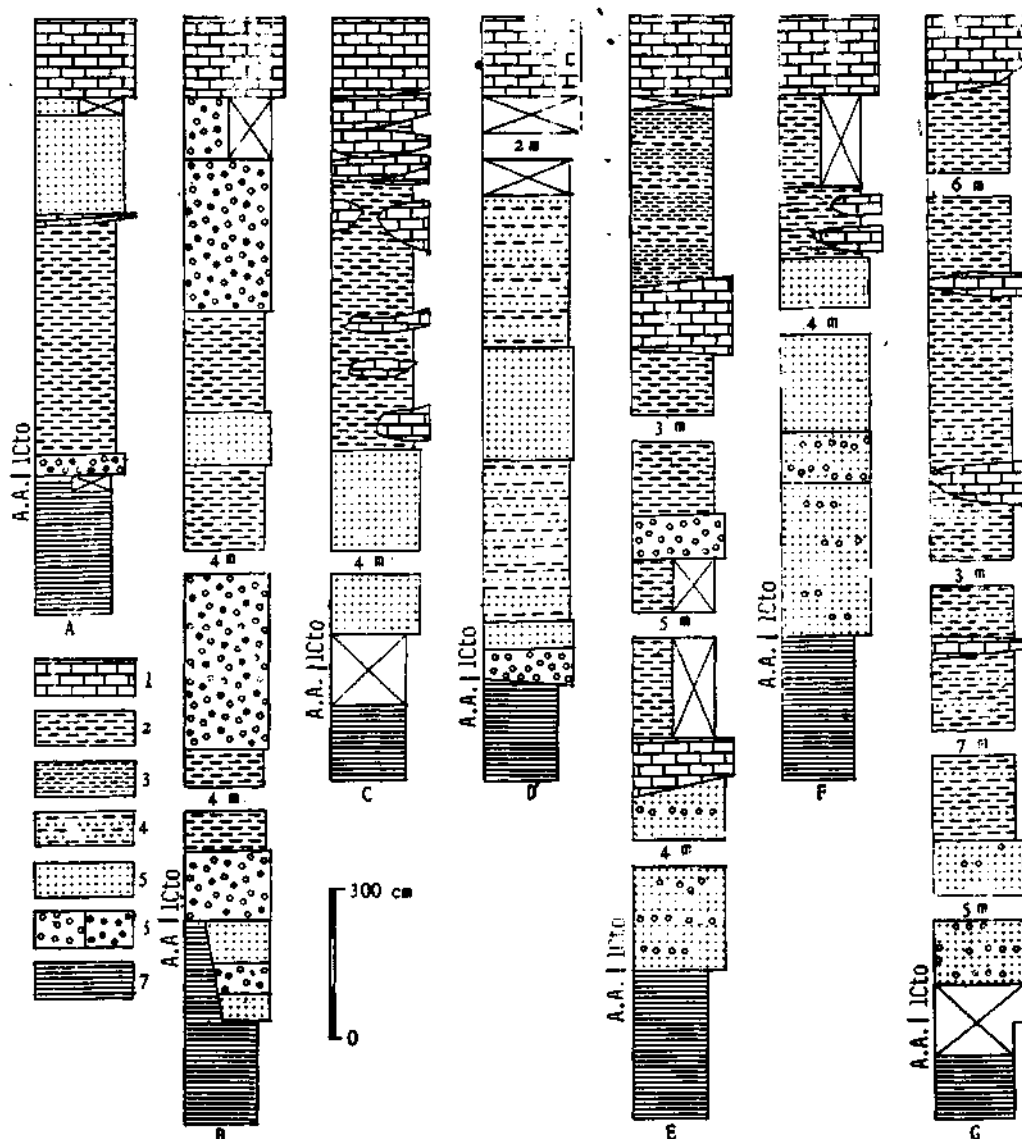


Fig. 8- Unconformity between the Latest Cretaceous turbidite-olistostrome unit (1 Cto) and the upper slate unit of the anchimetamorphic assemblage (A.A.). 1 - Light gray, microcrystalline, medium-bedded to massive limestone block of gigantic proportions; 2- Gray shale with minor thin inter-layers of lithic arenite; 3- Pale red shale; 4- Thin to medium-bedded interstratification of shale and lithic arenite; 5- Gray, thickly bedded to massive, in places, finely pebbly coarse to very coarse-grained lithic arenite; 6- Gray lithic conglomerate with limestone pebbles (left), gray limestone pebble conglomerate (right); 7- Illitic slate and slaty lithic arenite. A, 11.30:66.60; B, 07.77:64.00; C, 07.15:64.36; D, 07.03:64.46; E, 07.12:64.77; F, 07.08:65.10; G, 06.38:68.70.

to Early Paleocene ages (e.g. Eroskay, 1965; Bernouilli et al., 1974; Brinkmann, 1976; Konuk, 1977; Erdoğan, 1990) were assigned to the rock assemblages corresponding to the turbidite-olistostrome unit, in and outside the IAZ. In the report area, the

carbonate clasts indicate a lower age limit of Late Maastnchtian for the seemingly sterile matrix rocks. There, a Latest Cretaceous age can be suggested tentatively for the turbidite-olistostrome unit which is represented by its stratigraphically lowermost part

## STRUCTURAL SETTING OF THE ANCHIMETAMORPHIC ASSEMBLAGE

The Latest Cretaceous (to Paleocene) turbidite-olistostrome unit rests unconformably on the anchimetamorphic rocks (Fig. 8). The basal lithic sandstones contain pebbles derived from the underlying lower slate unit.

The near-vertical boundary fault (Kaya, 1972, 1992) delimits the mutual extent and relative positions of the IAZ and the anchimetamorphic belt (Fig. 1). In places, the fault is exposed between the ultramafics and/or volcanic olistostrome unit of the IAZ and the anchimetamorphic assemblage (Figs. 6 and 7). In Budağan dağ (Fig. 4), the fault passes under the turbidite-olistostrome unit. The buried fault is expressed at the surface by the zones of severe strain recrystallization in the Budağan limestone slab and a fault-bounded block of the volcanic olistostrome pierced through the slab.

The northward underthrust of the anchimetamorphic assemblage is a regional implication (Kaya, 1981, 1992). Biogeographic evidence, such as *Orbitopsella* species in the Middle Liassic limestone unit supports a southern origin (Altiner, 1989). A tectonic transport towards NNW can be suggested tentatively, on the grounds of one-fold structural elements such as strain-related pebble elongation in the quartz conglomerates.

The shearing confined to the basal part of the turbidite-olistostrome unit appears to be related to Tertiary compressional movements in the sense of recurrent northward tectonic transportations.

## CONCLUSIONS

1- The anchimetamorphic assemblage is a coherent structural-stratigraphic entity. Penetrative and polyphase shearing affected the assemblage. However, in most places slaty cleavage is subparallel to the bedding. Recrystallization is confined to new formation of phyllosilicates and extensive overgrowths.

The rock composition of the report and contiguous areas is not compatible with Okay's (1980) "Afyon zone" consisting of greenschist-amphibolite facies rocks.

2- The anchimetamorphic assemblage is divisible, with respect to major rock types, into (i) the lower slate unit consisting of silicic and (minor) mafic volcanogenic rocks, and silicic volcanic rocks; (ii) the upper slate unit consisting of epiclastic rocks; and, (iii) the limestone unit.

An unconformable setting on a so-called low-grade metamorphic basement, as it was implied by Kaya (1972) between the micaceous slates of the lower slate unit and illitic slates of the upper slate unit, is not justified by recent field evidence based on new exposures.

3- The uppermost part of the lower slate unit and the lowermost part of the upper slate unit are Middle Triassic (Ladinian) in age, on the basis of conodont evidence (first introduced in this report). The limestone unit is Middle Liassic in age. A Late Triassic to Early Liassic age can be suggested for the upper part of the upper slate unit, which presents a lithic uniformity and an apparent continuity in succession. As yet no conodont or foraminifer is obtained from the relevant strata.

4- The Latest Cretaceous (to Paleocene) turbidite-olistostrome unit, which is represented by its basal part in the report area, may have a minimum age of Late Maastrichtian. It rests unconformably on the upper slate unit and overlies the boundary fault between the older rocks units of the Izmir-Ankara zone and the anchimetamorphic assemblage.

The Budağan limestone slab and blocks intimately admixed with it are of different Late Cretaceous ages. This invalidates a lithostratigraphic setting accepted by Kaya (1972) and others (e.g. Göncüoğlu et al., 1992) for the Budağan limestone slab.

The suggestion of conformable and gradational contact relationship between the anchimetamorphic rocks (or their correlatives) and the "Late Cretaceous melanges" of the Izmir-Ankara zone, which is widely accepted in previous work (see Introduction), is not tenable.

5- A pre-Latest Cretaceous fault, actually an (under) thrust, separates the Izmir-Ankara zone and the southerly-lying anchimetamorphic belt. The

steepening of the fault, exposure of the anchimeta-morphic rocks and the onlap of the turbidite-olistostrome onto the anchimetamorphics are Latest Cretaceous events.

*Manuscript received October 19. 1996*

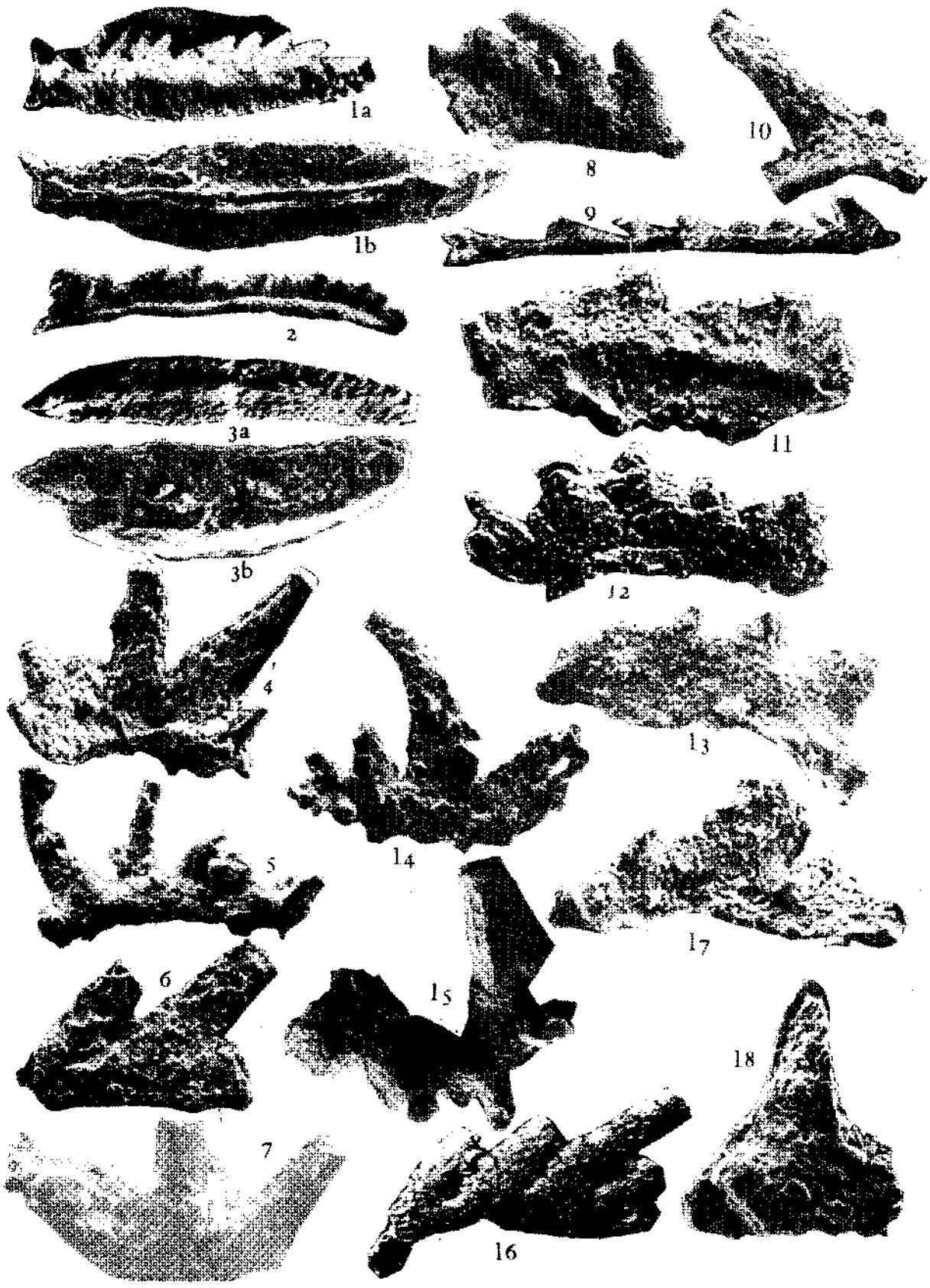
## REFERENCES

- Altınler, D., 1989, An example for the tectonic evolution of the Arabian Platform margin (SE Anatolia) during Mesozoic and some criticisms of the previously suggested models: Şengör, A.M.C., ed., Tectonic Evolution of the Tethyan Region, Kluwer Academic Publishers, Dordrecht, 117-129.
- Akdeniz, N., 1985, Akhisar-Gölmarmara-Gördes-Sındırgı dolayının jeolojisi: Doktora Tezi, İstanbul Üniv., 155 p., (unpublished).
- ; Konak, N. and Armağan, F., 1980, Akhisar (Manisa) güneydoğusunun Alt Mesozoyik kaya birimleri: Türkiye Jeol. Kur. Bull., 2, 77-90.
- Arpat, E. and Norman, T., 1961, Akhisar 70/4 paftasının kapsadığı sahalarda jeolojik incelemeler: MTA Rep., 3458 (unpublished), Ankara.
- Bernouilli, D.; Graciansky, P. Ch. and Monod, D., 1974, The extension of the Lycian nappes (SW Turkey) into the southeastern Aegean islands: Ecl. Geol. Helv. 67, 39-90.
- Bingöl, E., 1977, Muratdağı jeolojisi ve ana kayaç birimlerinin petrolojisi: Türkiye Jeol. Kur. Bull., 20, 13-66.
- Brinkmann, R., 1976, Geology of Turkey. Ferdinand Enke Veriag, Stungart, 158 p.
- Caner, J. and Jaoul, P., 1946, Manisa-Aydın-Kula-Gördes bölgesinin jeolojisi hakkında rapor: MTA Rep., 2068 (unpublished), Ankara.
- Erdoğan, B., 1990, İzmir-Ankara Zonu'nun, İzmir ile Sefehisar arasındaki bölgede stratigrafik özellikleri ve tektonik evrimi: Türkiye Petrol Jed. Der. Bull., 2 (1), 1-20.
- Eroskay, O., 1965, Paşalar Boğazı Gölpazarı sahasının jeolojisi: İstanbul Üniv. Fen Fak. Mecm. Seri B., XXX (3-4), 135-170.
- Göncüoğlu, M.C.; Özcan, A.; Turhan, N. and Işık, A., 1992, Stratigraphy of the Kütahya region: International Symposium on the Geology of the Black Sea Region (ISGB), Guide Book, 3-8, Ankara.
- Kaya, O., 1972, Tavşanlı yöresi ofiyolif sorununun anaçizgileri: Türkiye Jeol. Kur. Bull., 15, 26-108.
- , 1981, Batı Anadolu Altbindirmesi -Ultramafik birimin ve Menderes Masifinin jeolojik konumu: Doğa Bilim Derg., Atatürk Özel Sayısı, 5, 15-37.
- , 1992, Constraints on the age, stratigraphic and structural significance of the ophiolitic and adjoining rocks in the western parts of Turkey -an alternative structural- stratigraphic classification: Savaşçın, Y., and Eronat, H., ed., International Earth Sciences Congress on Aegean Regions (IESCA), Proceedings II, 193-209, İzmir.
- Konuk, T., 1977, Bornova filişinin yaşı hakkında: Ege Üniv. Fen Fak. Derg., Seri B, 1(1), 65-74.
- Okay, A.I., 1980, Mineralogy, petrology and phase relations of glaucophane-lawsonite zone blueschists from the Tavşanlı region: Contrib. Mineral. Petrol., 72, 243-255.

**PLATE**

## PLATE I

- Fig. 1 *Gondolella basisymmetrica* (Budurov ana Stefanov)  
a) Upper view, X100, b) lower view, X130
- Fig. 2- *Paragondolella navicula* (Huckriede), lateral view, X88
- Fig. 3- *Gladigondolella* cf. *tethydis* (Huckriede)  
a) Upper view, X150, b) lower view, X168
- Fig. 4- *Prioniodina* (*Cypridodella*) *muelleri* (Tatge), lateral view, X180
- Fig. 5- *Prioniodina* *spengleri* (Huckriede), lateral view, X84
- Fig. 6- *Prioniodina* sp., lateral view, X180
- Fig. 7- *Prioniodina* sp., lateral view, X148
- Fig. 8- *Prioniodina* sp., lateral view, X119
- Fig. 9- *Hindeodelia suevica* (Tatae), lateral view, X95
- Fig. 10- *Hindeodella* sp., lateral view, X100
- Fig. 11- *Neospathodus* cf. *discretus* (Müller), lateral view, X180
- Fig. 12- *Neospathodus newpasensis* (Mosher), lateral view, X177
- Fig. 13- *Neospathodus* sp., lateral view,
- Fig. 14- *Comudinasp.*, lateral view, X100
- Fig. 15- *Cratognathodus* sp., X117
- Fig. 16- *Enantiognathus* sp., X100
- Fig. 17- ?*Ozarkodina*-type unit, lateral view, X120
- Fig. 18- *Ozarkodina* sp., lateral view, X184



## GENESIS OF THE DİVRİĞİ IRON ORE DEPOSIT, SİVAS, CENTRAL ANATOLIA, TURKEY-AN ORE MICROSCOPY STUDY

Taner ÜNLÜ\*, Henrik STENDAL\*\*; Emil MAKOVICKY" and İ. Sönmez SAYILI\*

**ABSTRACT** - Divriği A-Kafa iron deposit is tectonically located at the contact between serpentinites, and limestones and/or granitic rocks, while Divriği B-Kafa iron deposit lies between serpentinites and limestones. Both deposits were formed during hydrothermal alteration of serpentinites. Magnetite constitutes the dominant ore mineral of A-Kafa with up to 5 vol. % disseminated pyrite. The main ore mineral at B Kafa is a maghemitized and martitized magnetite cross-cut by carbonate and silicate veinlets. Textural relationships of ore minerals indicate that iron is derived from serpentinites. The iron is enriched by serpentinization processes and further concentrated by hydrothermal convective cells caused by the intrusion of the Murmano pluton. These convective cells exert important influence on the shape of the ore bodies. The suggested model implies that the region has potential for future exploration with a good chance for finding additional iron ore reserves.

### INTRODUCTION

The iron ores of the Divriği area of Central Anatolia are the most important in Turkey. Unlu and Stendal (1986, 1989a, 1989b) and Stendal and Ünlü (1988,1991) described the genesis of these iron ores from a geochemical point of view. In this paper the ore mineral textures are studied. Previous field investigations in the area and its close vicinity have been carried out by Koşal (1973), Bayhan (1980), Ozgul et al: (1981) and Gultekin (1993). Detailed geochemical studies of the ore deposits and its surrounding have been described by Gümüş (1979), Stendal and Unlu (1988, 1991), Ünlü and Stendal (1986, 1989a, 1989b), Unlu et al. (1989), Zeck and Ünlü (1987, 1988a, 1988b, 1991), and Unlu (1989). Ore microscopic investigations have been made by Gysin (1938), Klemm (1960), Gümüş (1969), Bozkurt (1974, 1980), Çağatay (1975), Çağatay and Arda (1976), Bayhan (1980), Bayhan and Baysal (1981).

### GEOLOGICAL SETTING

The host and country rocks of Divriği iron deposits are mainly represented by serpentinites tectonically related with Mesozoic limestones, hydrothermally altered serpentinites and granitic rocks. The ore deposits occur in extensively hydrothermally altered serpentinites bordering the contacts to intrusive rocks.

The alteration processes have affected the iron ores at different stages by remobilization of Fe and recrystallization of the iron ore minerals. The main processes are the serpentinization of ultramafic rocks followed by the intrusion of the Murmano granitic pluton. The latest changes of the ore happened during weathering processes.

In this study, the formation of the ore deposit will be discussed, based on the textural relationships between ore minerals in Divriği A-and B-Kafa. Textural features of ore minerals in the Divriği-Güneş-Soğucak region, especially in serpentinites sampled away from the granitic rocks and serpentinites cut by the Murmano pluton (Fig.1) and thus hydrothermally altered, will be discussed as well. Serpentinites of Divriği iron ore deposits are extensively altered by hydrothermal fluids. Both magmatic and meteoric water circulated in a convective system activated by heat from the intrusion of granitic rocks. In this study, the role of two different stages of alteration, the serpentinization and the hydrothermal alteration of the serpentinites will be discussed by means of their reflection in mineral textures.

Lithologies represented by serpentinized ultramafic rocks and mafic rocks of Güneş, ophiolite and Mesozoic aged limestone blocks crop out around Soğucak. Serpentinites are the host rocks of disseminated and vein type mineralizations.

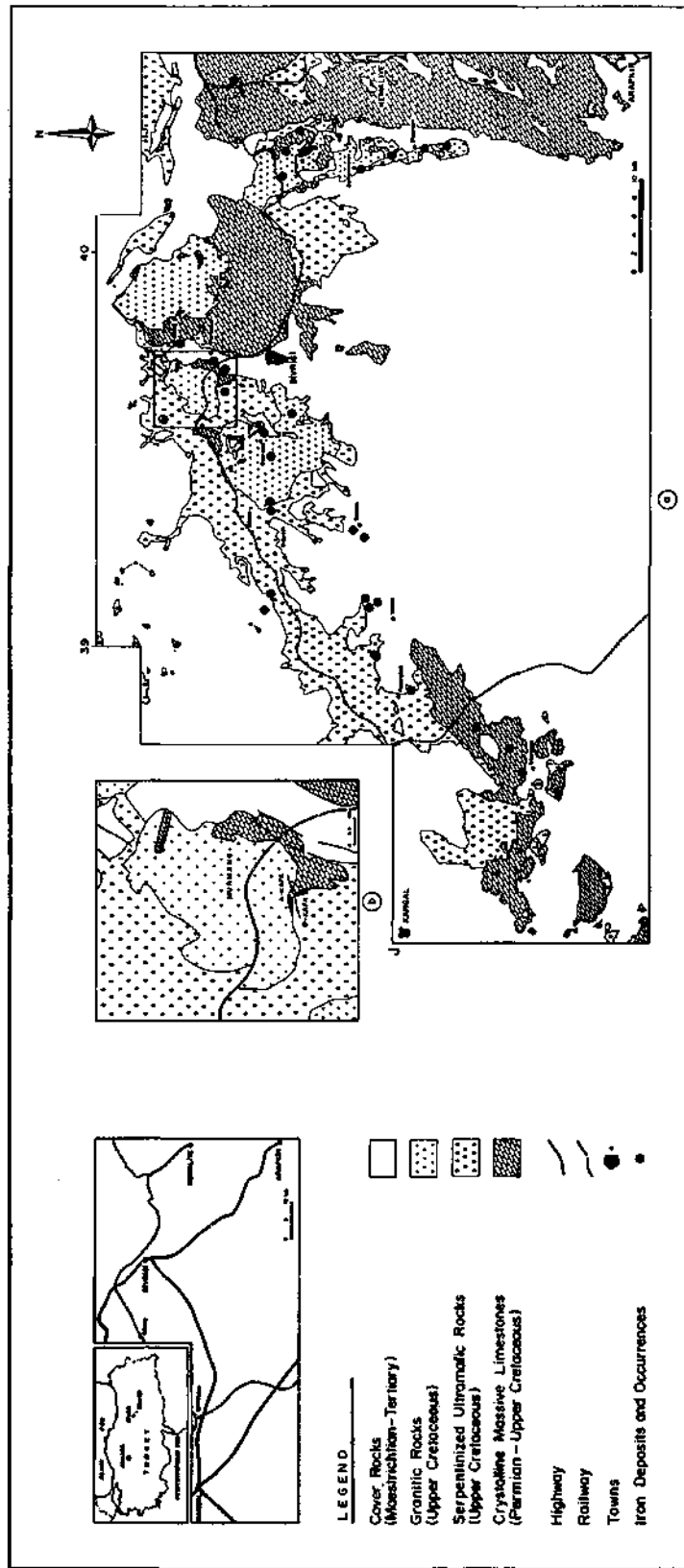


Fig. 1a- Geological map of Sivas-Erzincan iron sub-province (simplified after geological map prepared with the aim of iron exploration studies-registered by 42465 number at MTA archive).

Fig. 1b- Geological map of Divriği A- and B- Kafa iron deposits (simplified after Koşal, 1973).

## ORE PETROGRAPHY

## DĪVRĪĢĪ IRON ORE DEPOSIT

## A- and B-Kafa serpentinites

Serpentinites crop out close to the Divriģi iron ore deposits and are generally derived from peridotites. Pyroxenites are also pervasively serpentinized. Serpentinites contain olivine relics together with lizardite, chrysotile, antigorite, bastite and uralites as well as disseminations and veinlets of opaque minerals. Serpentinites are the host rocks to the Divriģi A- and B-Kafa iron ore deposits.

The dominant opaque mineral in the serpentinites is magnetite. Magnetites with various crystal forms reflect different formation conditions. Massive magnetite contains irregularly scattered, anhedral pyrite and silicate inclusions. The magnetite underwent secondary replacement by goethite and lepidocrocite.

A second magnetite type in the serpentinites occurs as rims of euhedral to subhedral and locally cataclastic chromites (Plate III, fig. 2). A transition zone between magnetite and chromite is illustrated in Plate I, fig. 5-6 and Plate V, fig. 4. In addition, magnetites occur in cracks of the chromites. A third kind of magnetite is apparently localized along the borders between olivine and orthopyroxene relics in the serpentinization texture of the rock.

These magnetite types are formed during serpentinization and are characterized by inclusions of minor amounts of pyrite ( $\pm$  Ni-sulphides) and abundant silicates (Plate III, fig.1). Other forms of magnetite are often observed as ringlike shapes surrounding silicate pseudomorphs. Limonite as another replacement product (Plate II, fig. 1-4) is concentrated in small cracks of above mentioned silicates (Plate IV, fig.4).

Euhedral magnetites without any ore mineral inclusions are younger than the above mentioned magnetites and occur in small amounts in veinlets cross cutting the host rock.

Pyrrhotite is observed occasionally in the serpentinites.

## Hydrothermally altered serpentinites of A-and B-Kafa

Hydrothermally altered serpentinites close to the contact of granitic rocks near the Divriģi iron ore deposit can be distinguished from the unaltered serpentinites by their lighter colour and lesser amounts of disseminated opaque minerals. Breccias in serpentinite and in veinlets are frequently seen in the hydrothermally altered serpentinites and veinlets filled by magnetite with sulphide, silica and carbonate minerals cutting the rock intensively.

Disseminated, fine grained anhedral magnetite occurs together with pyrite and chalcopyrite. Some magnetite is replaced by goethite. Pyrite contains pyrrhotite, magnetite, chalcopyrite and silicate inclusions. Chalcopyrite is accompanied by anhedral millerite and linneite (violarite) minerals.

Magnetite occurs also at the outer rim of euhedral to subhedral and partly cataclastic, rounded chromites like those described in the serpentinites. This type of magnetite surrounds the chromites and is also emplaced in the cracks of chromites (Plate V, fig.3). A transition zone with various colours exists between chromite and surrounding magnetite (Plate V, fig.2). Silicate inclusions are observed in some chromites. Magnetite-chromite occurrences are associated with fine-grained euhedral and disseminated pyrite, chalcopyrite and magnetite. Most of the magnetite is cataclastic and without inclusions.

Another magnetite generation is characterized by transition from magnetite with abundant silicate inclusions to one without any inclusions. This stage indicates the most important feature distinguishing hydrothermally altered serpentinites caused by granitic rocks from the primary serpentinites. Silicate mineral inclusions in magnetite gradually disappear, resulting in a magnetite rim without any inclusions. The pure, recrystallized magnetite is sometimes associated with pyrite without any inclusions, but frequently with coarse grained, angular silicate minerals. Intergrowths between magnetite, pyrite and silicate do exist and magnetite is usually surrounded by silicates.

Veins and veinlets with magnetite contain abundant silicate inclusions. This young generation of magnetite is coarse grained, displays very weak

anisotropy and equilateral quadrant-like sectorial zoning. It should be taken into account that this zoning can be formed as a replacement texture of orthopyroxene by magnetite (Plate VII, fig. 2). This type of magnetite is associated with angular, fine-grained and tabular mica minerals (e.g. phlogopite). Sulphide minerals are absent in this paragenesis, only magnetite and silicates occur together.

Rutile is found in the hydrothermally altered, partly serpentinized and chloritized mafic rocks. Rutile is also found as inclusions in pyrite surrounded by silicates. Rutile is occasionally transformed to sphene. The rutile formation is interpreted as alteration of primary titanomagnetite and ilmenite.

Extensively hydrothermally altered serpentinites have a few late stage veins with sphalerite, chalcopyrite, chalcocite, digenite, tetraedrite-tennantite and galena.

#### A-Kafa ore deposit

Divriği A-Kafa is the largest known ore body in the Divriği region (100 mill. t). It occurs at the contact of granitic rocks and serpentinites and the host rock is hydrothermally altered serpentinite (Fig.1). The contacts between the different rock units are sharp. Extensive crushing and brecciation are observed at the contact of the ore body and the granitic rocks. The magnetite ore includes disseminated pyrite ranging between 1-5 % by volume.

The oldest generation of magnetite in the ore body contains abundant silicate-but rare sulphide inclusions. Most of the sulphide inclusions are dissolved and replaced by limonite. Only a small part of the pyrite exists as relics.

The magnetite ore is cataclastic and the grain size varies from very fine to very coarse (Plate V, fig. 5). Cataclastic grains are zoned more extensively than in the hydrothermally altered serpentinites. The inner part of the grain has more silicate and less sulphide inclusions, whereas the outer part consists of more pure magnetite (Plate V, fig. 6). This pure magnetite is formed as a result of recrystallization of older magnetite. The magnetite occurs generally as angular to subhedral, rounded grains and is located in a matrix of fine-grained silicate and carbonate. Pyrite without silicate inclusions is scattered among these pure magnetite

crystals. This indicates the relationship between iron dissolution from older generation magnetite and the conditions for the precipitation of new minerals. The higher is the oxygen content, the richer is the sample in magnetite. Interplay between the formation of magnetite, pyrite and silicate minerals depends on the oxygen and sulphur fugacities (Plate VI, fig. 1-6). This three component texture constitutes an important part of the crude ore mined from the Divriği A-Kafa iron deposit.

The A-Kafa magnetite is generally fresh but in some places martitization and less maghemitization occur. The youngest generation of magnetite is fracture fillings.

Pyrite with magnetite and silicate inclusions forms droplike, anhedral and very finegrained aggregates. Coarse-grained pyrite without any silicate inclusions is found together with pure magnetite. The coarse-grained pyrite is associated with chalcopyrite and pyrrhotite. Pyrite might contain chalcopyrite and pyrrhotite as inclusions (and/or veinlets) in some places. Chalcopyrite and pyrrhotite are often dissolved, whereas pyrite is more stable. Gold particles are detected very rarely in the youngest pyrites.

Chalcopyrite occurs in pyrite with pyrrhotite as inclusions and veinlets. Coarse-grained chalcopyrite shows lamellar twinning and encloses millerite and linneite (violarite). Cubanite and valleriite exsolutions are seen in coarse-grained chalcopyrite. In addition, anhedral to subhedral chalcopyrite in silicates are accompanied by marcasite and bravoite which replace pyrrhotite and pentlandite, respectively.

Millerite, linneite (violarite) and pentlandite-bravoite occur together with pyrite, chalcopyrite and pyrrhotite. Further, millerite and linneite (violarite) inclusions are observed in chalcopyrite and vice versa. Beyond the alteration phenomena between millerite and violarite, the original textural relationship represents solid solution crystallization.

Subhedral to euhedral pyrrhotite crystals contain frequently chalcopyrite inclusions. Pyrrhotite is replaced by pyrite and marcasite. Inner parts of pyrrhotite are dissolved and hydrogoethite is developed (Plate VII, fig.5). Two constituents represented by marcasite and pyrite are formed as root-

like transitional layers creating bird's eye texture.

The secondary anhedral bravoite originating from pentlandite is observed in pyrrhotite and is further altered to pyrite-marcasite. In the marcasite and pentlandite, mackinawite exsolutions are observed. Angular, euhedral, fine-grained linneites (perhaps carolite ?) are scattered in the silicate and the chalcopyrite.

Lepidocrocite, goethite and sometimes hydrogoethite minerals develop as secondary products at the sites of sulphide minerals. Abundant limonite occurrences as well as covellite are observed in cracks.

Most of the coarse-grained silicates consist of biotite, phlogopite and muscovite. Very fine-grained and unrecognizable, silicate and carbonate minerals are found in the cataclastic magnetite.

#### B-Kafa ore deposit

The B-Kafa ore body is placed at the contact between serpentinite and limestone. The serpentinites are hydrothermally altered and extensively cut by cm to dm thick magnetite veins and in some places by silica and carbonate veins with ore minerals as well. The magnetite is partly maghemitized and martitized. In addition, various sulphide minerals occur.

Two kinds of magnetite can be distinguished in the B-Kafa ore body. One magnetite is pure, without maghemitization and martitization and the other displays these alterations. Different generations of magnetites are found in samples with no alteration. The first generation, anhedral magnetite, contains inclusions of fine-grained sulphide minerals such as pyrite and pyrrhotite and some silicate. A younger generation of pure magnetite occurs together with minor amount of pyrite. Euhedral grains of chalcopyrite occur disseminated and in veinlets with little amounts of pyrrhotite associated with pyrite. Millerite inclusions and very fine-grained sphaerite are observed in chalcopyrite.

Cataclastic magnetite is altered by martitization and accompanying maghemitization (Plate VII, fig. 3). Martitization advanced in two different stages. The first stage envelopes the grains while the younger generation forms needlelike martitization aggregates perpendicular to the grain, developed

at the inner part of the grains and cutting the earlier martitization. Martitization is developed at the edges, cracks and (111) cleavage surfaces i.e. weak zones of the magnetite. Pyrites associated with maghemitized and martitized magnetite contains goethite and lepidocrocite in cracks and are commonly characterized by needle or grain like marcasitization (Plate VII, fig. 4). Sometimes colloform (gellike) goethite is observed. Sulphide minerals are secondarily replaced by lepidocrocite and goethite appearing in boxwork textures in some places.

Fine-grained silicate inclusions occur in older magnetite while younger pure magnetite and pyrite are associated with coarse grained silicates.

#### A-Kafa granitic rocks

Although referred to as granitic rocks in literature, the igneous rocks of the Murmano pluton in contact to the Divriği A-Kafa iron ore deposit vary in composition from quartz syenite to monzonite even diorite. Dominant rock type of this complex pluton is characterized by monzonite (Zeck and Ünlü 1987; 1988a; 1988b).

Tabular hematite and ilmenite grains and euhedral to subhedral magnetite occur among the silicates of the monzonite. The magnetite is martitized along cleavages. Sphene and rutile occur as well. The minerals are associated with coarse-grained ilmenite with fine hematite exsolutions. Magnetite is partly replaced by goethite and/or goethite occur occasionally after pyrite in magnetite. Some hydrogoethites contain pyrite relics.

Widespread martitization observed in most of the coarse-grained magnetite is developed both in cracks, and parallel to (111) surfaces, of the magnetite. Martitization is also seen at the border of euhedral ilmenite grains occurring in magnetite.

Sulphide minerals are generally replaced by limonites.

Two types of magnetite occur in diorites of the Murmano pluton located a little further from the A-Kafa iron ore. The first type is represented by coarse-grained magnetite of primary origin and exhibits penetrating martitization and maghemitization. The second type of magnetite tends to form

during reactions between the silicate minerals and is concentrated at the edges of the silicates as tiny magnetite crystals. Small amounts of ilmenite, rutile, sphene and hematite are also observed in diorites.

#### Soğucak (Güneş) region serpentinites

Serpentinite crops out between Divriği and Çetinkaya and is derived from peridotites. Pyroxenite is also serpentinized. Serpentinite contains olivine relics together with serpentine group minerals represented by lizardite, antigorite and chrysotile and uralites in addition to large amount of opaque minerals. Serpentinized peridotite and pyroxenite are the host rocks for disseminated mineralizations of Ni-, Co-, Cu-, and Fe- sulphides and magnetite and chromite. Magnetite-bearing veins in fractures and cracks of the Serpentinite vary from millimeter to several dm in thickness.

Disseminated, fine-grained euhedral to subhedral magnetite usually contains pyrite and silicate mineral inclusions and pyrite in veinlets. Pyrite is generally droplike. Euhedral to subhedral pyrrhotite is often associated with magnetite, including pentlandite exsolutions frequently replaced by violarite. Mackinawite exhibits wormlike figures in pentlandite. Cubanite lamellas in chalcopyrite occur together with disseminated pyrrhotite and pentlandite. Magnetite surrounds the chromite like a zone, a transition zone between magnetite and chromite is observed in almost every grain (Plate I, fig. 1-4).

Typical magmatic corrosion features are observed along the edges of some euhedral chromites (Plate III, fig. 4) but in others this feature is missing (Plate III, fig. 5-6). In the chromite, magnetite is preceded by a transition zone to pure magnetite surrounding the chromite like a haloe. Euhedral pyrite and silicate inclusions are observed in this magnetite (Plate III, fig. 3). Silicate inclusions also occur in the chromite. Magnetite separated out due to the serpentinization process postdates the chromites (Plate IV, fig. 5). Two kinds of textural relation appear at the contact between silicate and chromite surrounded by magnetite. One part of the chromite represents almost angular and regular contact relation, another part of the chromite shows irregular, dissolution-like contact relations with sili-

cates (Plate IV, fig. 6). Serpentinization is common in the latter type of texture. Some chromite grains contain both types of relationship (Plate V, fig. 1).

Magnetite formed by serpentinization is located as pseudomorphs after olivine and orthopyroxenes (Plate II, fig. 5). Common silicate inclusions and pyrite occurrences are observed in this kind of magnetite. Flowerlike growths of magnetite observed besides finegrained, irregularly distributed magnetite and euhedral and/or subhedral magnetite grains are thought to be related with serpentinization. Additionally, fine-grained secondary magnetite is often situated along the cleavage and cracks of silicate minerals (Plate II, fig. 6) (Plate IV, fig. 1-3). In the Serpentinite pyrrhotite is intensively altered to pyrite and magnetite (Plate VII, fig. 6) and rarely to marcasite with bird eye texture. Magnetite is magnetized and martitized. The youngest magnetite occurs in veinlets and in the cracks and fractures of the serpentinites (see also Bozkurt, 1974; Bayhan, 1980; Bayhan and Baysal, 1981).

#### DISCUSSION

As a result of textural studies, three, main stages and one transition stage are recognized in the ore, host and country rocks of Divriği and Soğucak regions by ore microscopical investigations. In general, the first stage is characterized by primary minerals, second stage by serpentinization, the transition stage by intensive cataclasis and the third stage by intrusion of granitic rocks (Fig. 2).

##### Stage I: Primary minerals

Primary minerals formed during upper mantle conditions are illustrated in Plate I.

##### Stage II: Serpentinization

Sequential events of emplacement into continental crust by obduction of oceanic lithosphere and intrusion of granitic rocks are emphasized at this stage (Plate II-IV).

##### Transition Stage: Intensive Cataclasis

Additional intensive deformation developed during serpentinization and at early stages of granitic intrusion is described at this stage (Plate V).

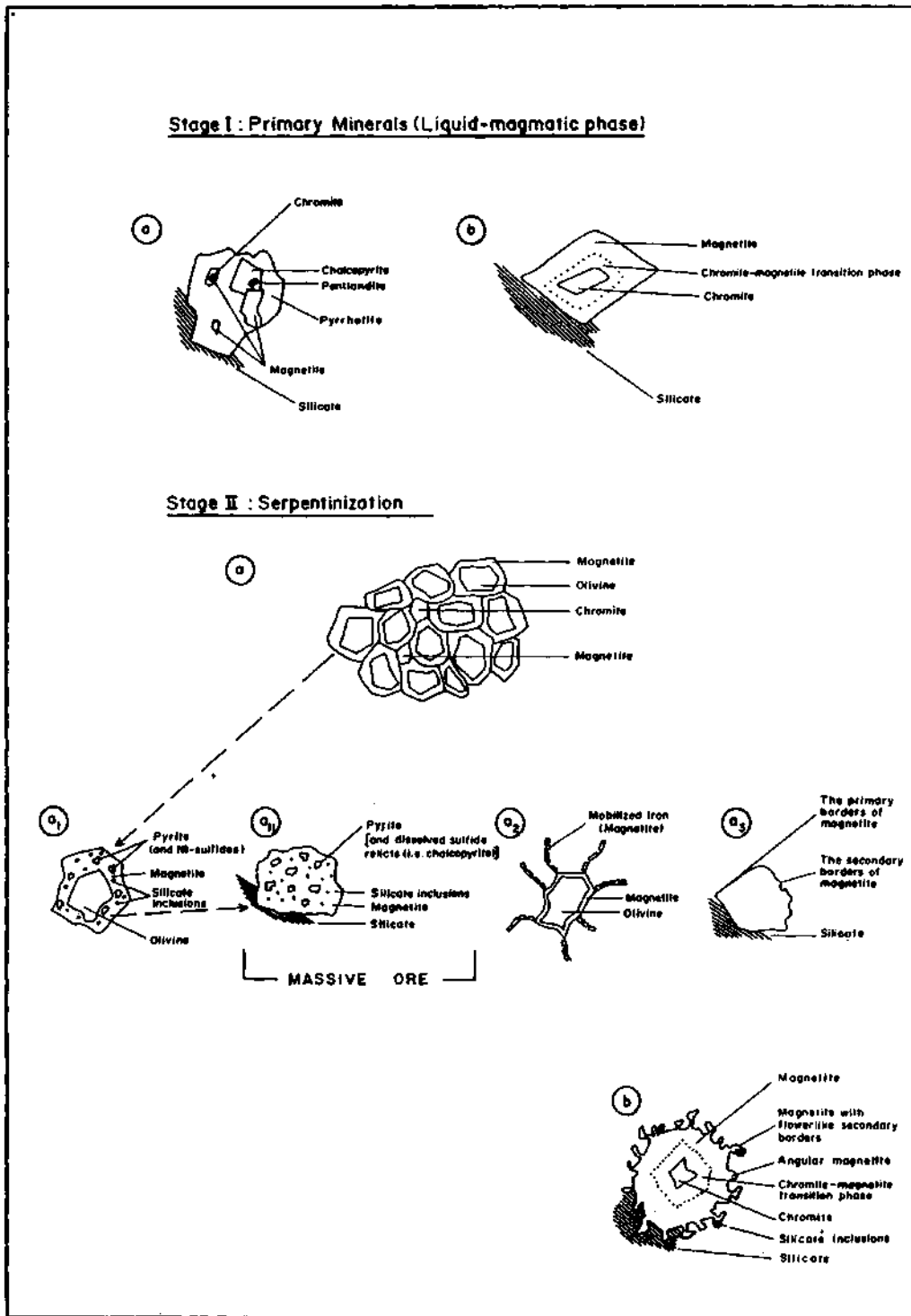


Fig. 2

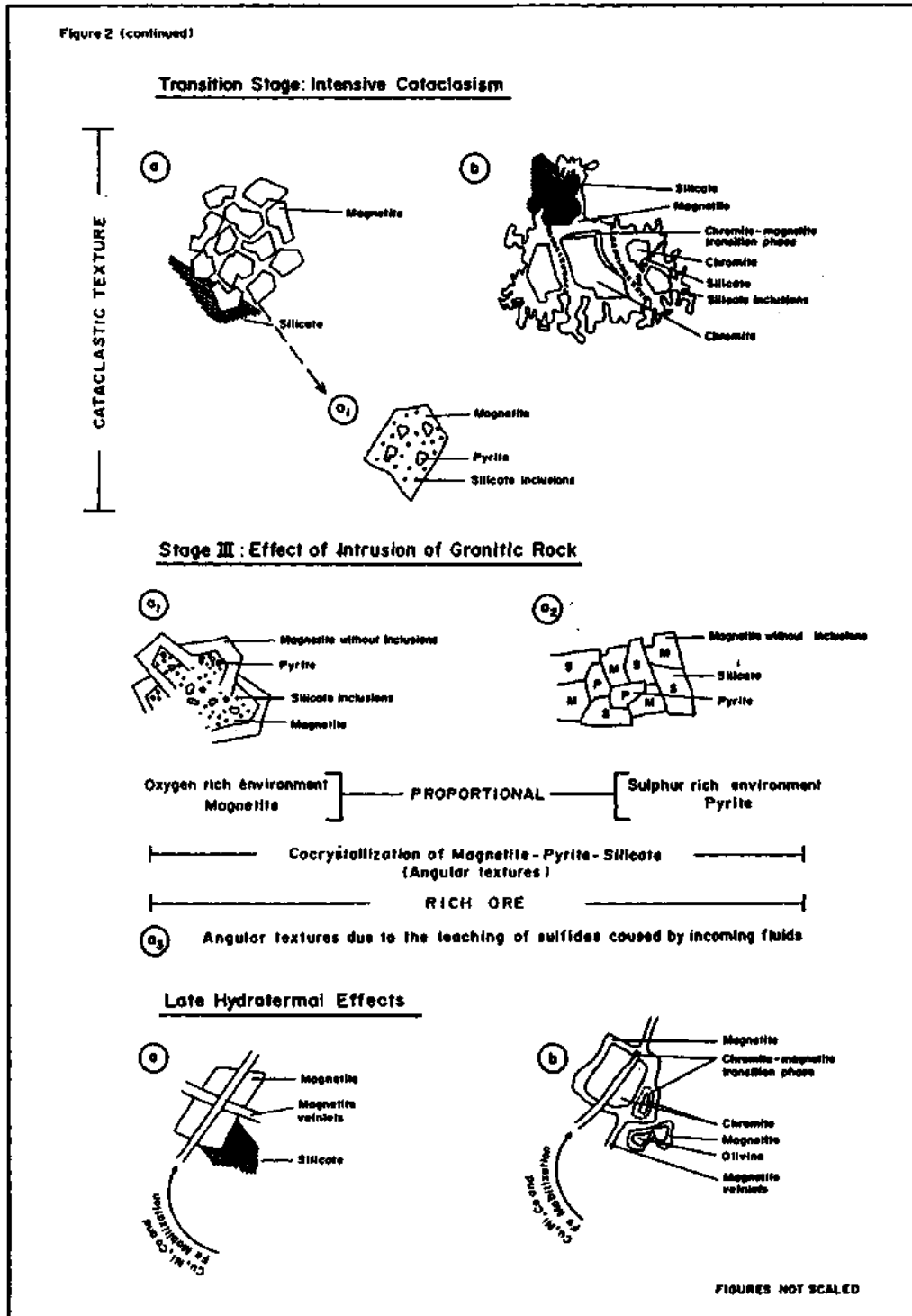


Fig. 2- Textural characteristics of different mineralization stages from older to younger (Stage II and Transition Stage silicate minerals are mainly serpentinite minerals like chrysotile, antigorite etc. Stage III silicate minerals are mainly chlorite, biotite, phlogopite and/or muscovite. No cataclasis have been observed on mica minerals. Very fine-grained, anisotropic silicate and/or carbonate minerals are also observed in the Transition Stage a).

Stage III: Granitic Rock Effects

The hydrothermal alteration events developed by hydrothermal convective cells in the serpentine are the main process in this stage (Plate VI-VII).

It is possible to characterize the genetic interpretation of the Divriği iron ore deposit as a sequence of metamorphic + hydrothermal alteration processes beginning with metamorphism under upper mantle conditions, continuing at various metamorphic conditions contemporaneous with the emplacement of the obducted oceanic crust upon the continental crust imposing hydrothermal alteration processes and finally weathering (Table 1).

Genetic Features

Genesis of the ore from the Divriği and Soğucak areas is outlined in Table 1. A very general synthesis is suggested for the Divriği and Soğucak ore deposits based on the comparison of textural features of ore minerals from the two areas.

The liquid magmatic phase with primary ore minerals (e.g. chromite) is more characteristic for Soğucak than Divriği. This reflects relative intensity

of hydrothermal alteration in the two areas. The auto-hydration developed at early stages is similar for both Divriği and Soğucak areas.

Magnetite formed by serpentinization and associated with chromites is well known from Soğucak while the magnetite, pyrite and silicate association is more common at Divriği. The iron mobilization followed by formation of veinlet type magnetite is less pronounced in the Soğucak area than in Divriği area. The concentration of veinlets with magnetite is proportional with the abundance of hydrothermal fluids.

Tectonic events such as deformation and cataclasis of chromite and magnetite are more pronounced from the Divriği than the Soğucak region. This also confirms the direct or indirect effect of the granitic intrusion. The intrusion of the "granitic" rock mobilized the iron and developed magnetite, pyrite and silicate to the Divriği iron ore type.

Alteration processes like maghemitization, martitization and marcasitization are more common at Divriği than at Soğucak, also due to processes generated by hydrothermal convection. The youngest veinlets cut all structures and this hydrothermal event is similar in both regions.

Table 1- Mineralization stages and genetic features determined after ore microscopical studies

GEOLOGIC PROCESSES	PHOTOGRAPHIC PLATES	MINERALIZATION STAGES	EXPLANATIONS	
Effect of Intrusion of Granitic Rock	Primary Mineralization	PLATE I	Liquid-magmatic phase	Chromite, magnetite and sulfide association
		PLATE II	Serpentinization	Auto-hydration
	PLATE III	Magnetite, pyrite, silicate occurrences and chromite association as a product of serpentinization		
	PLATE IV	Mobilization of iron		
	PLATE V	Tectonic deformation (intensive cataclasis)	Mechanical deformation in chromite and magnetite	
	PLATE VI	Early hydrothermal effects of granitic rocks	Cocrystallization of magnetite, pyrite and silicate (angular textures)	
	PLATE VII	Late hydrothermal effects	The youngest veinlets intersecting the structure and maghemitization, martitization and marcasitization	

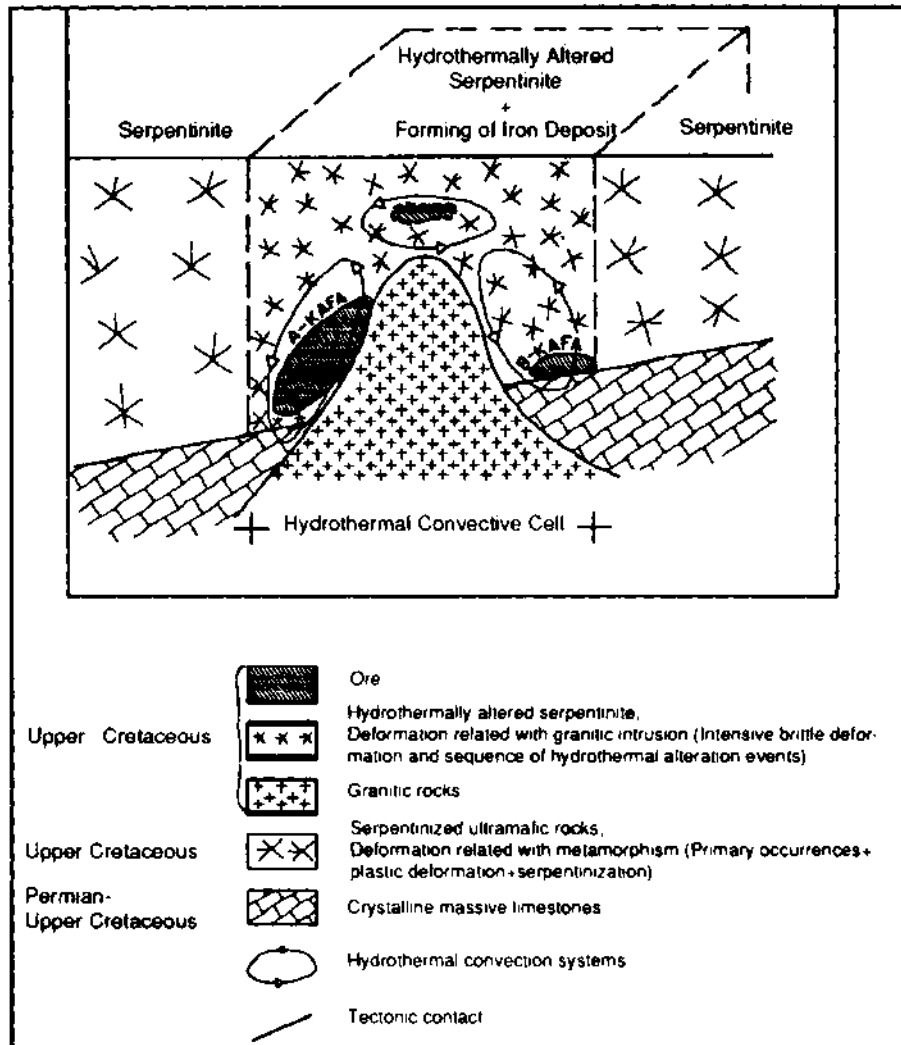


Fig. 3- Schematized formation model of Divriği A- and B- Kafa iron deposits (non scaled).

## CONCLUSIONS

### Mobilization and genesis

Most of the iron deposits in the Divriği region is found in serpentinized ultramafic rocks. Granitic rocks intrude these rocks. Thus, the serpentinite is hydrothermally altered.

The serpentinization stage is the most important stage at the formation of the studied iron deposits. It follows from the following model reactions: [Engin and Hirst, 1970;  $7(\text{Mg}_{0.9}\text{Fe}_{0.1})_2\text{SiO}_4$  (forsteritic olivine) +  $3(\text{Mg}_{0.9}\text{Fe}_{0.1})\text{SiO}_3$  (enstatitic pyroxene) +  $10.57 \text{H}_2\text{O}$  -  $5\text{H}_4\text{Mg}_3\text{Si}_2\text{O}_9$  (serpentine) +  $0.57$

$\text{Fe}_3\text{O}_4$  (magnetite) +  $0.3 \text{MgO}$  +  $0.57 \text{H}_2$ ; Spooner and Fyfe, 1973;  $11\text{Fe}_2\text{SiO}_4$  (fayalite) +  $2\text{SO}_4^{2-} + 4\text{H}^+$

$7\text{Fe}_3\text{O}_4$  (magnetite) +  $\text{FeS}_2$  (pyrite) +  $11 \text{SiO}_2$  (quartz) +  $2\text{H}_2\text{O}$ , Pallister and Hopson, 1981]. The iron bearing silicates of primary origin are the basis for the formation of iron deposits and therefore yield a generally low grade iron ore.

Second stage is characterized by leaching. Hydrothermal fluids circulate in convective cells generated by the heat from the intrusion of granitic rocks and mobilize iron from the serpentinite, but the iron is quickly precipitated again in the serpentinite and in this way concentrated to a high grade iron ore deposit (Fig. 3). The high-grade iron ore is

formed as a result of repeated mobilization and precipitation of iron.

### Exploration

According to previous mining geological studies, Divriği iron ore deposit and the other iron ore deposits of the Divriği region were desented evaluated as skarn type related with granitic rocks (Gysin, 1938; Klemm, 1960; Koşal, 1973; Petrascheck and Pohl, 1982 and Gümüş, 1989). Gümüş, 1979 has interpreted the Divriği iron ore deposit as formed by processes of pyro-mobile metasomatism. High interest in skarn formation caused that exploration by drilling was undertaken on the contact of the granitic rocks.

Recent studies (Stendal and Ünlü, 1991) and the follow-up by magnetic anomalies over the hydrothermally altered serpentinites led to the discovery of 40 million tons of high grade iron ore in the serpentinites.

According to world standards (Bottke, 1981) Divriği iron deposit is a medium grade iron deposit with 100 million ton reserve with 55 % Fe grade. Since 1939 and with the discovery of new reserves the Divriği deposit new reaches 140 million tons. But with the ongoing exploration studies the size of the deposit can still increase in the future.

### ACKNOWLEDGEMENTS

The authors thank Dr. Ahmet Çağatay, Prof. Dr. Ayhan Eler, Assoc. Prof. Dr. Okan Tekeli and Prof. Dr. Hasan Bayhan for the constructive criticism of the paper and also acknowledge the financial contributions of the University of Copenhagen to the laboratory studies. Polished sections of ores and rock samples referred in this paper are in the custody of the Geological Institute, University of Copenhagen. The authors acknowledge the financial support of the NATO FELLOWSHIP PROGRAMME of Denmark (Nos. 29/86 and 38/87) and of MTA and TDCI., Ankara for the field work.

*Manuscript received April 18, 1995*

### REFERENCES

Bayhan, H., 1980, Güneş-Soğucak (Divriği/Sivas) yöresinin jeolojik, mineralojik, petrografik-petrolojik ve

metalojenik incelenmesi: Ph. D. thesis, Hacettepe University, 188 p., (unpublished), Ankara.

Bayhan, H. and Baysal, O., 1981, Güneş-Soğucak (Divriği-Sivas) yöresindeki sülfür cevherleşmelerinin mineralojik ve jenetik incelenmesi: Hacettepe University Yerbilimleri 8, 41-52.

Bottke, H., 1981, Lagerstättenkunde des Eisens: Verlag Glückauf GmbH, Essen, 202p.

Bozkurt, R., 1974, Dumluca Köyü (Sivas) Ni-Co-Bi mineralizasyonunun metalojenik ve yakın yöresinin petrografik etüdü: Ph. D. thesis, Black Sea Technical University, 144 p., (unpublished), Trabzon.

———, 1980, Divriği demir madenleri cevher minerallerinin incelenişi ve oluşumu: Qualification thesis for Assoc. Prof., 59 p., (unpublished), Trabzon.

Çağatay, A., 1975, Erzmikroskopische Untersuchung der mackinavüfuhrenden Kernproben von Kangal-Yellice: MTA Bull., 84, 61-72.

———, and Arda, O., 1976, Sivas'ın Divriği-Güneş Köy-Ağpınar deresi mntıkasında, wilkeit ile birlikte bulunan enteresan maden minerallerinin etüdü: MTA Bull.,86, 105-112.

Engin, T. and Hirst, D.M., 1970, Serpantinization of harzburgites from the Alpine peridotite belt of southwest Turkey: Chem. Geol., 6, 281-295.

Gültekin, A.S., 1993, Alacahan-Çetinkaya-Divriği (Sivas ili) arasında kalan alanın jeolojisi: Ph. D. thesis, 183 p., (unpublished), Istanbul.

Gümüş, A., 1969, Pınargözü-Davutoğlu (Kangal-Sivas) hematit yatağı jeolojisi and jönezi: Qualification thesis for Assoc. Prof., 41 p., (unpublished), Trabzon.

———,1979, Nouvelles observations sur la genese du gisement de Per de Divriği (Sivas, Turquie): Verh. Geol. B-A, 3, 347-355.

———,1989, Metalik Maden Yatakları: Bilim Ofset, 528 p. İzmir.

Gysin, M., 1938, L ere impression sur la geologie de la region de Divrik, sur la structure et sur l'origine du gisement de fer: MTA Rep., 700 (unpublished), Ankara.

- Klemm, D.D., 1960, Die Eisenerzvorkommen von Divriç (Anatolien) als Beispiel tektonisch angelegter pneumatolytisch-metasomatischer Lagerstättenbildungen: N. Jb. Min., 94, 591-607.
- Koşal, C., 1973, Divriçi A-B-C demir yataklarının jeolojisi ve oluşumu üzerine çalışmalar: MTA Bull., 81, 1-22.
- Özgül, N.; Turşucu, A., Özyardımcı, N., Şenol, M., Bingöl, İ. and Uysal, S., 1981, Munzur Dağlarının jeolojisi: MTA Rep., 6995 (unpublished), Ankara.
- Pallister, J.S. and Hopson, C.A., 1981, Samail ophiolite plutonic suite: Field relations, phase variation, cryptic variation and layering, and a model of a spreading ridge magma chamber: J. Geophys. Res., 86, 2593-2644.
- Petrascheck, W. and Pohl, W., 1982, Lagerstättenlehre: E.S.V.H., Stuttgart, 341 p.
- Spooner, E.T.C. and Fyfe, W.S., 1973, Sub-sea-floor metamorphism, heat and mass transfer: Contr. Mineral, and Petrol., 42, 287-304.
- Stendal, H. and Ünlü, T., 1988, An example to evaluation of geochemical data by multivariate geostatistical analyses: Divriçi region iron deposits, Central Anatolia: Commun. Fac. Sci. Univ. Ank. Series C, 6, 361-379.
- and ———, 1991, Rock geochemistry of an iron ore field in the Divriçi region, Central Anatolia, Turkey. A new exploration model for iron ores in Turkey: Journal of Geochemical Exploration, 40, 281-289.
- Ünlü, T., 1989, Türkiye demir yatakları arama çalışmalarında 1. derecede ağırlıklı hedef saha seçimi ve maden jeolojisi araştırmaları ile ilgili proje teklifi: MTA Rep. No. 8593 (unpublished), Ankara.
- Unlu, T. and Stendal, H., 1986, Divriçi bölgesi demir yataklarının element korelasyonu ve jeokimyası (Orta Anadolu-Türkiye): Jeol. Müh., 28, 5-19.
- and ———, 1989a, Divriçi bölgesi demir cevheri yataklarının nadir toprak element (REE) jeokimyası; Orta Anadolu, Türkiye: Türkiye Geol. Bull., 32, 1-2,21-38.
- and ———, 1989b, Jeokimya verilerinin çok değişkenli jeostatistik analizlerle değerlendirilmesi bir örnek, Divriçi bölgesi demir yatakları, Orta Anadolu: MTA Bull., 109, 127-140.
- ; Yıldızeli, N., Yıldırım, A., Yurt, Z., Adıgüzel, O., Özcan, H., Avcı, N. and Çubuk, Y., 1989, Divriçi (Sivas) yöresi granitik kayaç-yan kayaç ilişkilerine yönelik jeoloji raporu: MTA Rep., 8914, (unpublished), Ankara.
- Zeck, H.P. and Ünlü, T., 1987, Parallel whole rock isochrons from a composite, monzonitic pluton, Alpine belt, Central Anatolia, Turkey: N. Jb. Min. Mh., 5, 193-204.
- and ———, 1988a, Alpine ophiolite obduction before 110±5 Ma ago, Taurus Belt, eastern central Turkey: Tectonophysics, 145, 55-62.
- and ———, 1988b, Murmano Plütununun yaşı ve ofiyolitle olan ilişkisi (Divriçi/Sivas): MTA Bull., 108,82-97.
- and ———, 1991, Shoshonitic, monzonitic pluton near Murmano, eastern central Turkey-A preliminary note: MTA Bull., 112, 47-58.

## PLATES

## PLATE-I

Fig. 1- Deformed pyrrhotite (light grey) in serpentinite.

Euhedral chromite (dark grey) surrounded by magnetite (grey) are at the central and right-hand portions of the lower edge of the grain. Mackinawite inclusions-bearing pentlandite grains (white) are at the center of the upper edge of pyrrhotite. At right chalcopyrite (white) with cubanite lamellae (Soğucak N-83, in air, parallel nicol=P.N.)

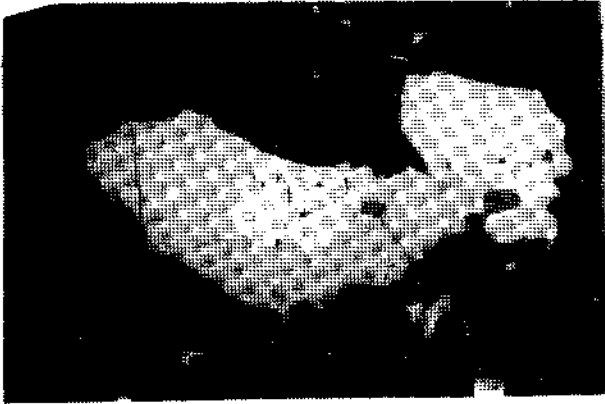
Fig. 2- Mackinawite inclusions in pentlandite cleavages in the same sample as Figure 1 (Soğucak N-83, in air, P.N.).

Fig. 3- Euhedral chromite (dark grey in the centre) with magnetite envelopes (grey) and euhedral chalcopyrite with cubanite lamellae. Tongue-like pentlandite (light grey) with tiny mackinawite inclusions lies at the contact of magnetite and chalcopyrite in chalcopyrite. This figure represents the right edge of Figure 1 (Soğucak N-83, in air, P.N.).

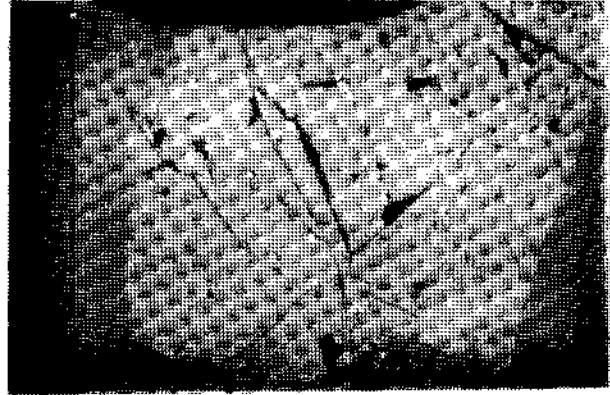
Fig. 4- Pyrrhotite (light grey) cracked along its cleavages in serpentinite. Euhedral magnetite (grey) and chromites (dark grey) at the core of pyrrhotite. Mackinawite-bearing pentlandite (very light grey) between magnetite and pyrrhotite (Soğucak N-83, in air, P.N.).

Fig. 5- Magnetite (white) crystals with chromite relics (light grey) in serpentinite. Chromite-magnetite transition phase in very light grey (Divriği CS 1-12, in air, P.N.).

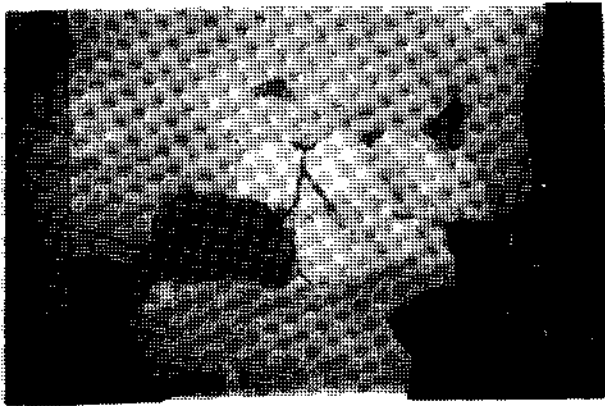
Fig. 6- Chromite relic (in core, dark grey), surrounded by a chromite-magnetite transition phase (grey) and magnetite (light grey). Euhedral magnetite crystal (white) in the centre of the figure (Divriği CS 1-12, in oil, P.N.).



1



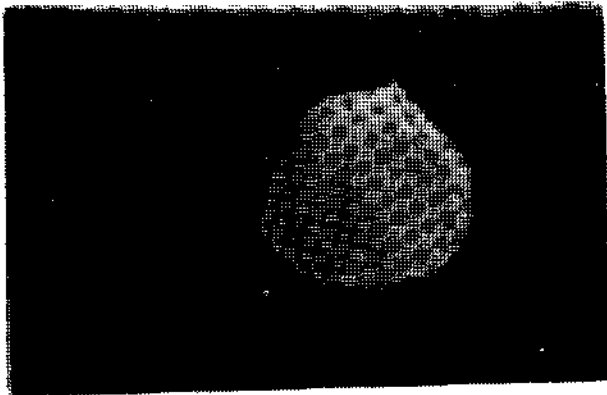
2



3



4



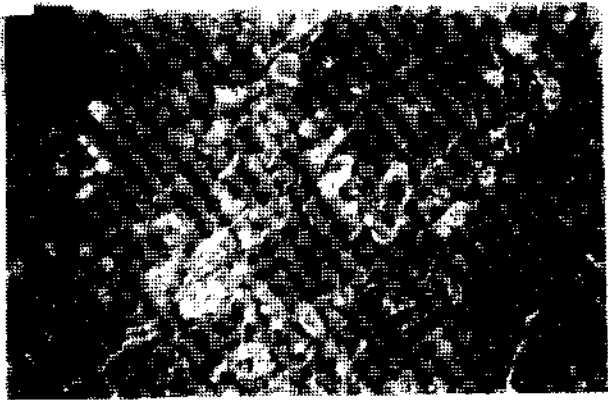
5



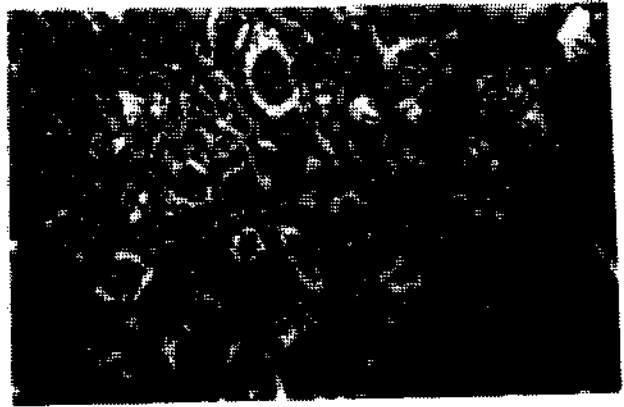
6

## PLATE-II

- Fig. 1- Ringlike magnetite (white) around anhedral olivine relics and tiny veinlets of magnetite between divines in serpentinite (Divriği CS 1-12, in air, P.M.).
- Fig. 2- Hydrogoethite (grey) and towards the core magnetite (white) in anhedral olivine relics (skeletal, white at its edges) (Divriği CS 1-12, in oil, P.N.).
- Fig. 3- Hydrogoethite (grey-light grey) in the centre and around it magnetites (white). Ringlike magnetite (light grey) at the outer part of oval shaped olivine relic in serpentinite (Divriği CS 1-12, in oil, P.N.).
- Fig. 4- Magnetite aggregates (grey) with pyrite (white) inclusions formed around and over olivine relics (light grey) in serpentinite, in the right-hand and middle upper part of figure (Divriği CS 1-12, in oil, P.N.).
- Fig. 5- Magnetite (white anhedral skeletal crystals) formed after serpentinization in serpentinite (Soğucak G-120, in air, P.M.).
- Fig. 6- Mesh texture showing small magnetite grains (white) in serpentinite (Soğucak G-48, in air, P.N.).



1



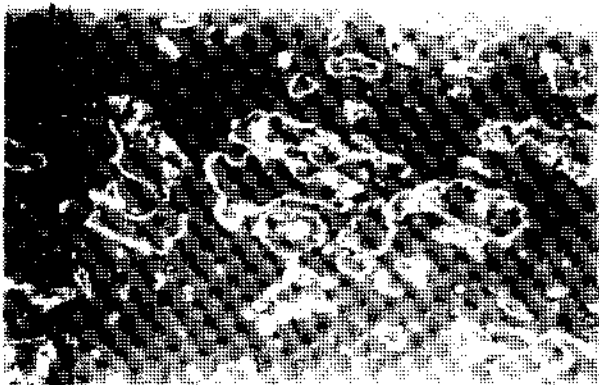
2



3



4



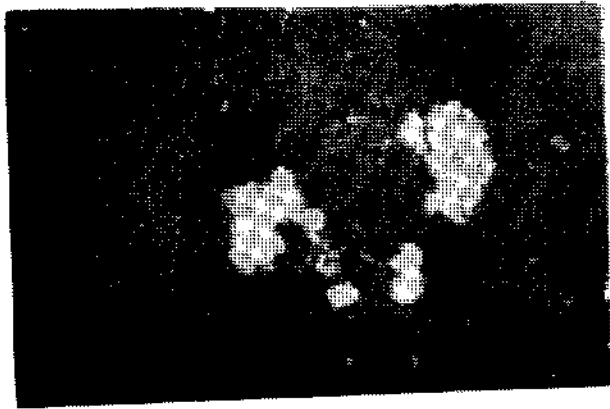
5



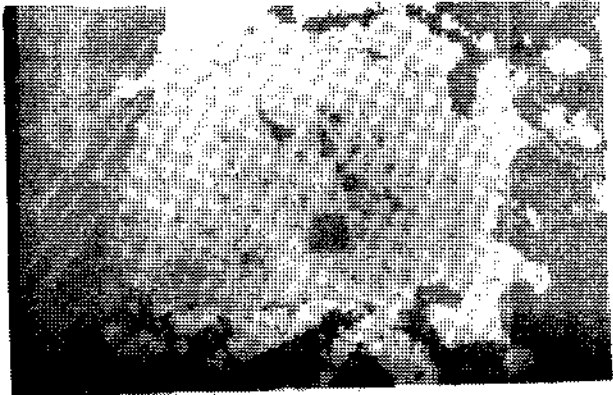
6

### PLATE -III

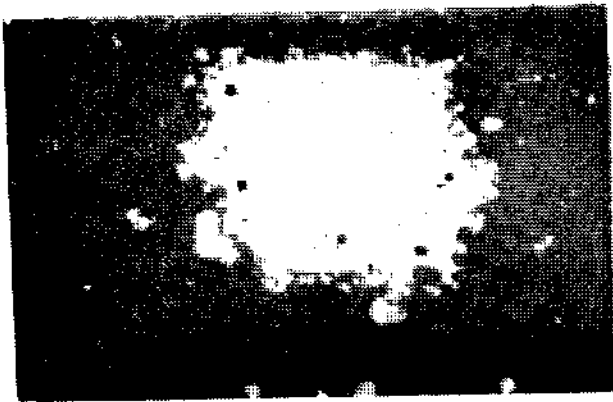
- Fig. 1- Magnetite (light grey) with pyrite inclusions (white) and silicate inclusions (dark grey) in serpentinized olivines. Secondary magnetite crystals grow on euhedral magnetite in lower right-hand portions (Divriği CS 1-12, in air, P.N.).
- Fig. 2- Magnetite (white) crystals around chromite (light grey) core in serpentinite. Primary silicate inclusions (dark grey) in chromite (Divriği CS 1 - 12, in air, P.M.).
- Fig. 3- Euhedral chromite (grey) surrounded by magnetite (white). Secondary magnetites (white) at the outer parts of the complex crystal in serpentinite. Partly dissolved small pyrite inclusions (light grey) and small silicate inclusions in chromite and magnetite (Soğucak G-48, in air, P.N.).
- Fig. 4- Magnetite (white) around euhedral chromite core (light grey) in serpentinite. Pyrite (light white) at lower right parts and uppermost parts of the right-hand crystal. Magmatic corrosion suggested by lines of small black dots in the outermost parts of chromite cores and by silicate inclusions in magnetite zone (Soğucak G-119, in air, P.N.).
- Fig. 5\* Small magnetite grains (white) and magnetite zones (white) around euhedral chromite cores in serpentinite. Triangular magnetite grain in chromite at the left. Silicate inclusions (dark grey) in the magnetite zone of the right-hand crystal. The outermost shell is secondary magnetite with baylike outlines (Soğucak G-120, in air, P.N.).
- Fig. 6- Chromite (grey) cores surrounded by a chromite-magnetite transition phase (light grey). A very small pyrite crystal (light white) occurs in transition phase at right lower part of figure; magnetite (white) surrounds the transition phase. At the outermost parts secondary magnetites break the primary outlines. Fine grained, angular silicate inclusions (dark grey) in the crystal (Soğucak G-162, in air, P.M.).



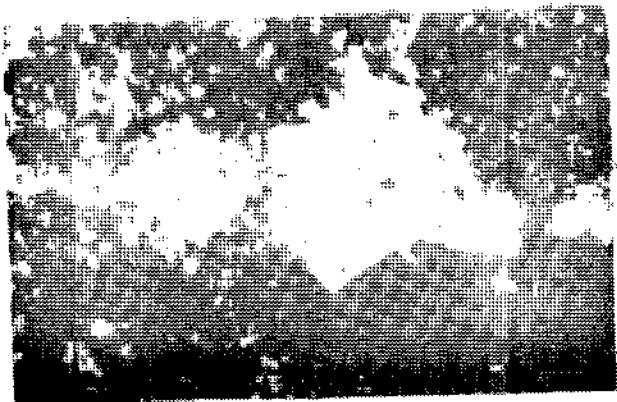
1



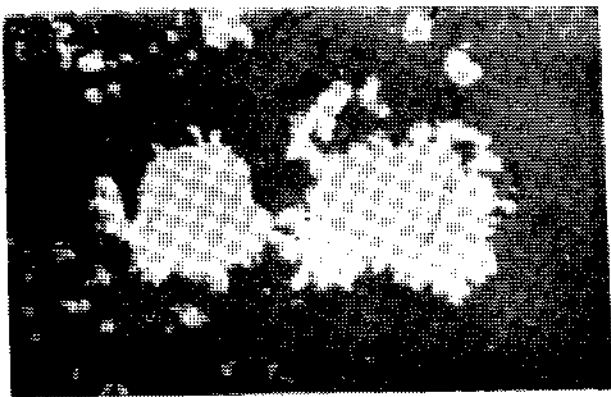
2



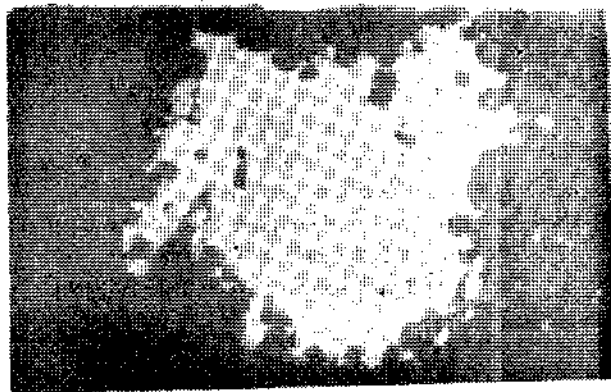
3



4



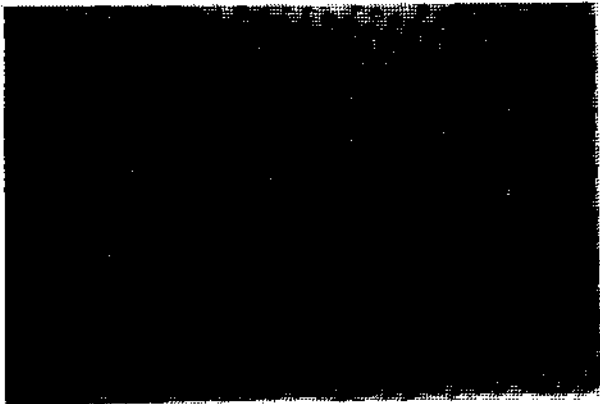
5



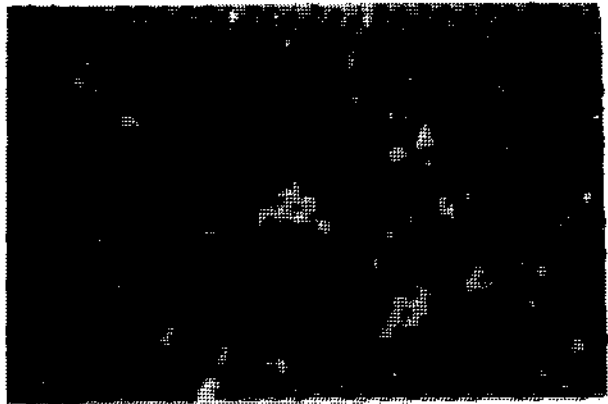
6

PLATE -IV

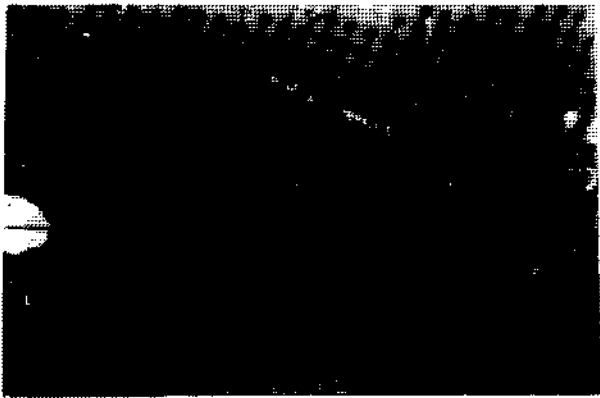
- Fig. 1- Magnetite (white) as a result of iron mobilization among anhedral olivine relics (dark grey) in serpentinite (grey) (Soğucak N-83, in air, P.N.).
- Fig. 2- Coarse-grained, euhedral magnetite (white) with porous magnetite rims (light grey) and secondary magnetite (light grey) in the cracks in serpentinite (Soğucak N-83, in air, P.N.).
- Fig. 3- Pyrrhotite (white) and pentlandite (white) intergrown at the center of the left-hand edge of the figure in serpentinite and magnetite (white) formed after mobilization in cracks (Soğucak N-83, in air, P.N.).
- Fig. 4- Anhedral magnetites (white, oval skeletons) formed by serpentinization processes and veinletlike, mobilized magnetites (white) in serpentinite (Divriği CS 1-12, in air, P.N.).
- Fig. 5- Magnetite (very light grey), anhedral chromite relics (grey) at its core and transition phases (light grey) between those minerals. Primary silicates (black) at the middle lower part of magnetite. Secondary magnetites (white) disturb the primary grain contacts at lower right-hand part of the same mineral (Soğucak G-162, in air, P.N.).
- Fig. 6- Chromite (grey) core, the chromite-magnetite transition phase (light grey) around it and magnetite (white) in the outer parts of the oxide aggregate. Secondary magnetites disturb and overprint the baylike primary outlines outermost parts of the crystal. Colloform magnetite at the right part (Soğucak G-119, in air, P.N.).



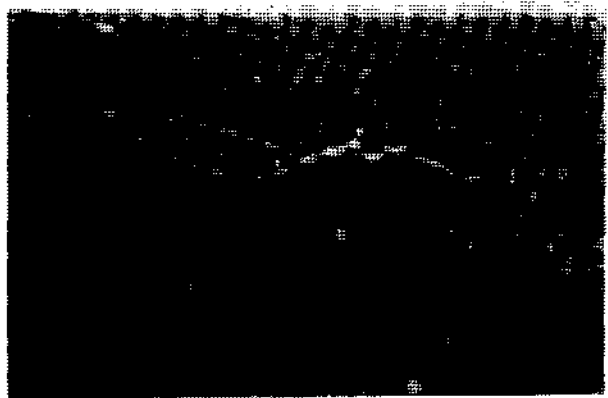
1



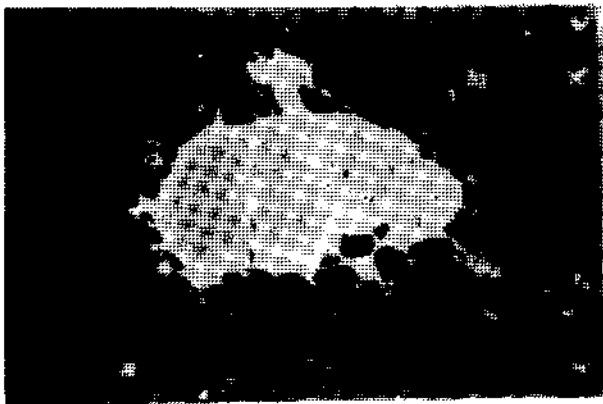
2



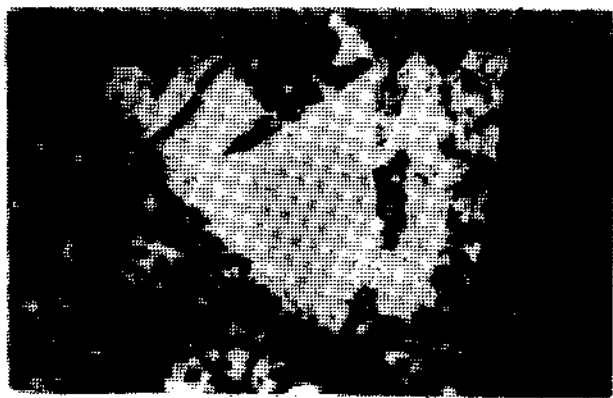
3



4



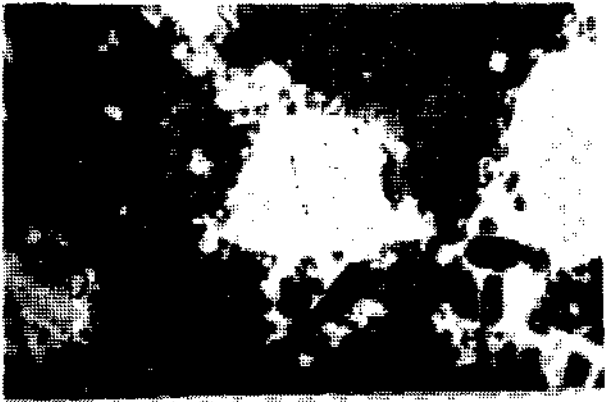
5



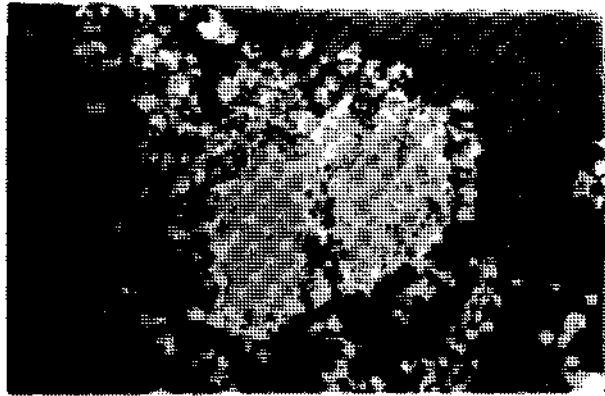
6

## PLATE -V

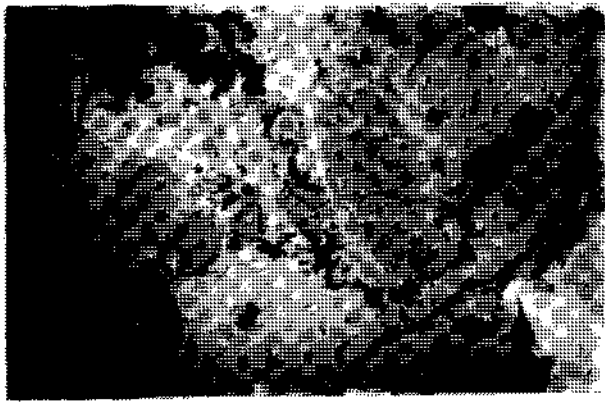
- Fig. 1- Cataclastic chromite (grey) in the middle of the crystal aggregates surrounded by the magnetite transition phase (light grey) and magnetite (white). Silicate inclusions (dark grey) and secondary magnetite towards the outer zones of magnetite (Soğucak G-162, in air, P.N.).
- Fig. 2- Cataclastic chromite (grey) at the core and the surrounding chromite-magnetite transition phase (dark-light grey) in magnetites (light grey) in serpentinite. Silicate fillings (dark grey) of the open spaces (Divriği AS 1-12, in air, P.N.).
- Fig. 3- Cataclastic chromite (grey) in magnetite (white), cross-cut by veinlike magnetite. Fine-grained magnetites (white) in serpentinite (Divriği AS 1-12, in oil, P.M.).
- Fig. 4- Zoned replacement of chromite (grey, relics in the core), a narrow zone of chromite-magnetite transition phase (light grey) and around them a crystal aggregate of magnetite (white), Point-like hydrogoethite at the lower left-hand parts (Divriği CS 1-12, in oil, P.M.).
- Fig. 5- Cataclastic magnetite in serpentinite (Divriği AS 1-2, in air, P.M.).
- Fig. 6- Cataclastic zoned magnetite (grey). Silicate inclusions (dark grey) are in the centre, pure magnetite without inclusions on periphery (Divriği AC 1 -2, in air, crossed nicols = C.N.).



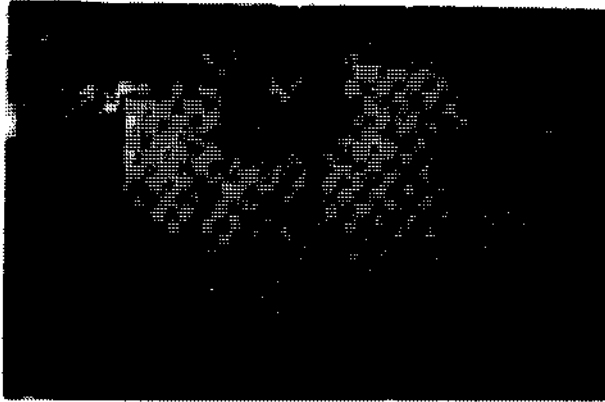
1



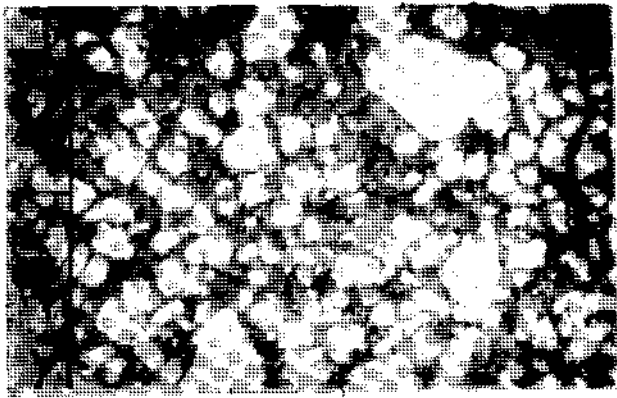
2



3



4



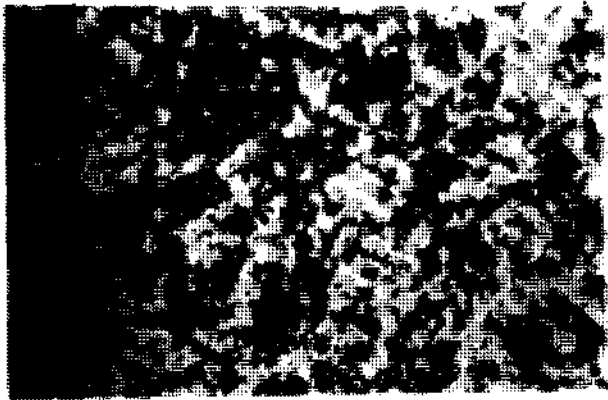
5



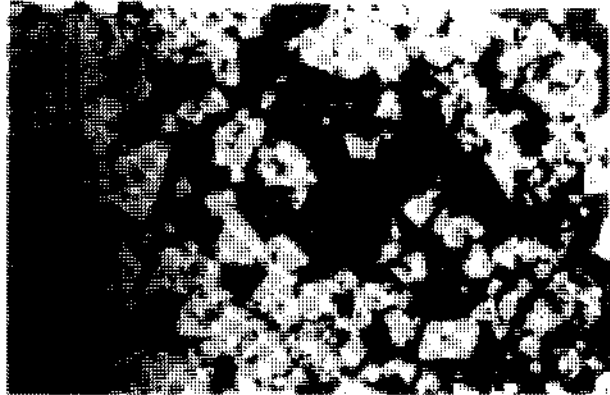
6

PLATE -VI

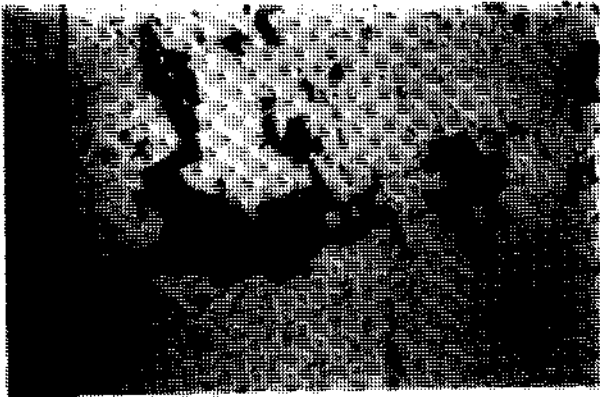
- Fig. 1- Magnetite (white) and silicate (grey) minerals with open spaces (black) left after dissolution of sulphide minerals. Angular silicate inclusions (grey) in magnetites (Divriği AC 2-6, in air, P.N.).
- Fig. 2- Angular magnetite (white) intergrown with silicate minerals (grey) (Divriği AC 3-15, in air, P.N.).
- Fig. 3- Dissolved sulphide areas (dark grey) among angular magnetite crystals (light grey). Silicate inclusions in magnetite. A very fine-grained pyrite (white) in the middle upper portions (Divriği AC 2-1, in air, P.N.).
- Fig. 4- Euhedral pyrite (white) in angular, pure magnetites (grey) without inclusions. Small silicate inclusions (black) in the middle part of magnetites. Silicate minerals in the dark grey areas among magnetite (Divriği AC 3-2, in air, P.N.).
- Fig. 5- Coarse-grained, angular magnetite (grey). Small but abundant silicate inclusions (black) in the magnetite cores. Subhedral pyrite (white) at left lower part. Silicate fillings (dark grey) between euhedral magnetite and pyrite (Divriği AC 1-6, in air, P.N.).
- Fig. 6- Angular, pure magnetite crystals (grey) without inclusions and euhedral pyrite crystals (white) around silicate inclusions bearing magnetite. Silicate minerals (black) in open spaces (Divriği AC 3-15, in air, P.N.).



1



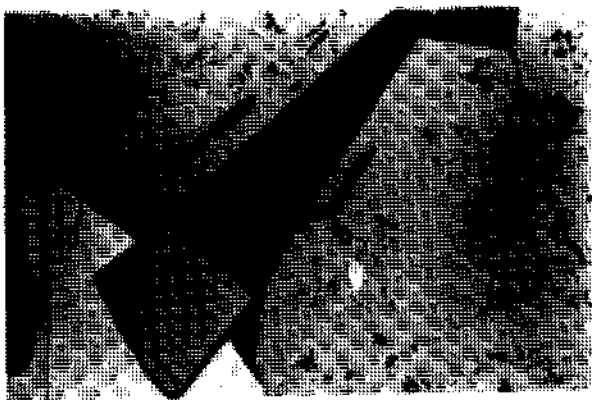
2



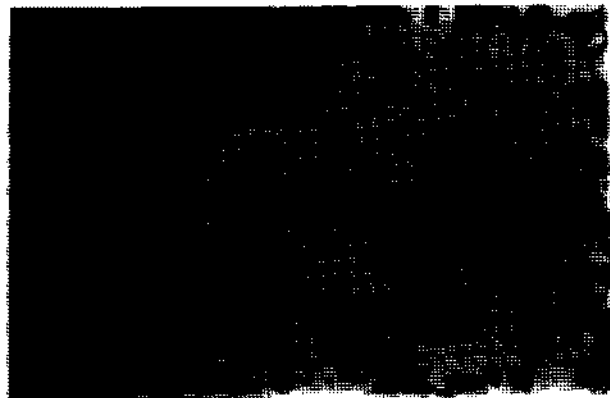
3



4



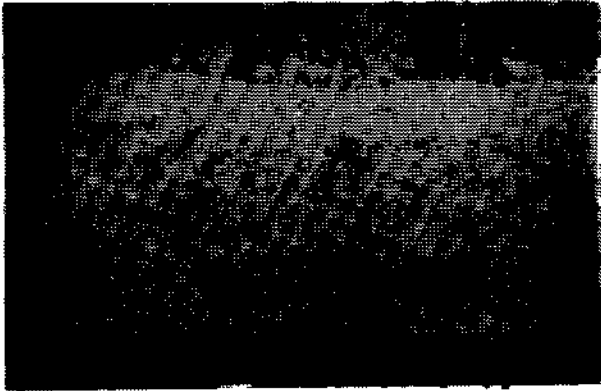
5



6

## PLATE -VII

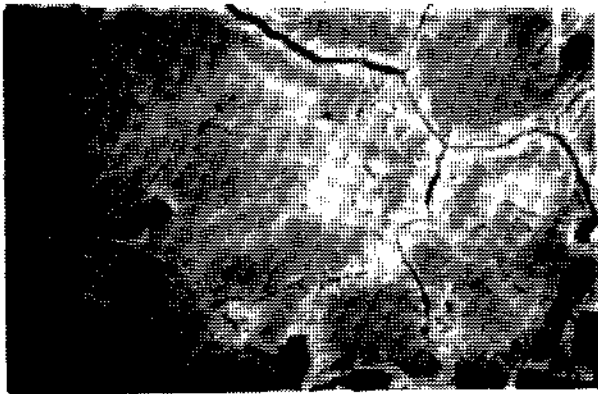
- Fig. 1- Silicate inclusions (black) bearing magnetite in pure magnetite without inclusions. Young magnetite (grey) with small pyrite crystals (white) developed at a crack in the upper part of figure (Divriği AC 2-16, in air, P.N.).
- Fig. 2- Magnetite crystals (light grey and grey) showing sectoral zoning in a veinlet (Divriği AS 1-2, in air, P N.).
- Fig. 3- Magnetite (grey) maghemitized (light grey) in the central parts and martitized in a needle-like form (white) at the outer parts (Divriği BC 2-24, in oil, P.M.).
- Fig. 4- Veinletlike maghemitization (light grey) of magnetite (grey) at lower and right edges of figure. Marcasitization (light grey) at outer zones of pyrite crystal (white) at the left side. Silicate (black) at upper left corner and lowermost part (Divriği BC 2-3, in air, P.N.).
- Fig. 5- Dirty white coloured, layered, needle-like marcasite (white) replacing pyrrhotite at the upper side of figure and coarse-grained pyrite crystals (white). Above pyrite hydrogoethite (grey) occurrences in open spaces (Divriği AC 3-6, in oil, P.M.).
- Fig. 6- Chromite in the core (dark grey), around the chromite-magnetite transition phase (grey) and surrounding them magnetite rim (light grey) in the centre of the figure. Most of the figure is covered by pyrite (white) and magnetite (light grey) obtained from pyrrhotite. Silicate minerals (black) at the left-hand side of the figure (Soğucak G-49, in air, P.N.).



1



2



3



4



5



6

## GEOLOGICAL CHARACTERISTICS OF THE AŞIKÖY-TOYKONDU (Küre-Kastamonu) MASSIVE SULFIDE DEPOSITS

Üner ÇAKIR\*

**ABSTRACT.-** Massive sulfide deposits of Küre occur in a basaltic sequence, the uppermost unit of the Küre ophiolite. This unit is massive at the bottom and passes into the pillow lavas and hyaloclastites towards the top. Geochemical analyses indicate an origin of oceanic ridge basalt. The basalts are overlain by a detritic sedimentary sequence represented essentially by shales at the base and shale-sandstone alternations at the upper levels. Beneath the shale, the ore is generally massive and has a high grade, and towards the lower levels of the basalts it becomes stockworked and disseminated. Structurally, the Aşıköy ore deposit has a form of ridge with a general direction of N45 W. The average grade of the ore is 1.96 % Cu and 35 % S. Main ore minerals are chalcopyrite and pyrite. Cobalt minerals like linneite, bravoite and native gold minerals are also present. Ore mineralization is mainly thought to be the result of submarine volcanism and hydrothermal processes occurred during the Lias. It probably developed near a spreading axis of a narrow and short-lived back-arc marginal basin and remobilized later due to granitic intrusions of Dogger age.

### INTRODUCTION

Aşıköy-Toykondur massive sulfide deposits are situated in the western part of the Küre district of the Kastamonu province (Fig.1.) The orebody is extracted at present by open pit methods. The preparations for underground mining are in progress.

Early detailed geological investigations of Küre mining area was carried out by Kovenko for the MTA General Directorate. He prepared a geological map of the Küre area with a scale of 1:5000 and discovered the Aşıköy-Toykondur deposits from the gossan (Kovenko, 1944).

In 1966, a Cento team aiming to train geologists in geological mapping techniques under the management of MTA, made a general geological map of the Küre district with a scale of 1:5000 and a detailed geological map of the Aşıköy pit with a scale of 1:1000. They however misinterpreted the repetition of the basalt-shale alternation related to the thrusting ascribing incorrectly to two horizons. They proposed that the ore mineralization was formed by the hydrothermal solutions flowing along the old faults much after deposition of the shale and the intrusion of the grafiites.

Güner (1980) remapped the Küre area with a scale of 1:10 000. His major and trace element analyses revealed that, the basalts had an oceanic

ridge basalt character. The relative ages of different units determined from his paleo-magnetic data, are very questionable. His suggestion that the shale-sandstone unit is older than the basalts and peridotites are younger than the dacite dykes contradicts the field observations made in this study. It is clearly observed that the shale sandstone unit covers the basalts and the dacite dykes cut all the ophiolitic units.

Demirbaş (1984) calculated by the cross-section method, that the proven+probable reserves of Aşıköy is 15.24 million tons with an average grade of 1.69 % Cu and 36.73 % S.

MTA with an objective to discover new ore deposits and enlarge the known ones prepared a geological map of an area of 850 km<sup>2</sup> with a scale of 1:25 000 and prospected an area of 100 km<sup>2</sup> between 1976-1978. As a part of this project, the area including Aşıköy, Toykondur, Bakibaba and Kızılsu ore deposits was also mapped with a scale of 1:5000 and 1: 2000, and the Aşıköy pit with a scale of 1: 1000 (Pehlivanoğlu, 1985).

In another study conducted by the cooperation of Etibank with the Japan international Cooperation Agency (JICA) and Metal Mining Agency (MMAJ), a semi-detailed geological and detailed geophysical prospection of the Aşıköy, Toykondur, Bakibaba and Kızılsu mine districts were carried out (JICA and MMAJ, 1992).

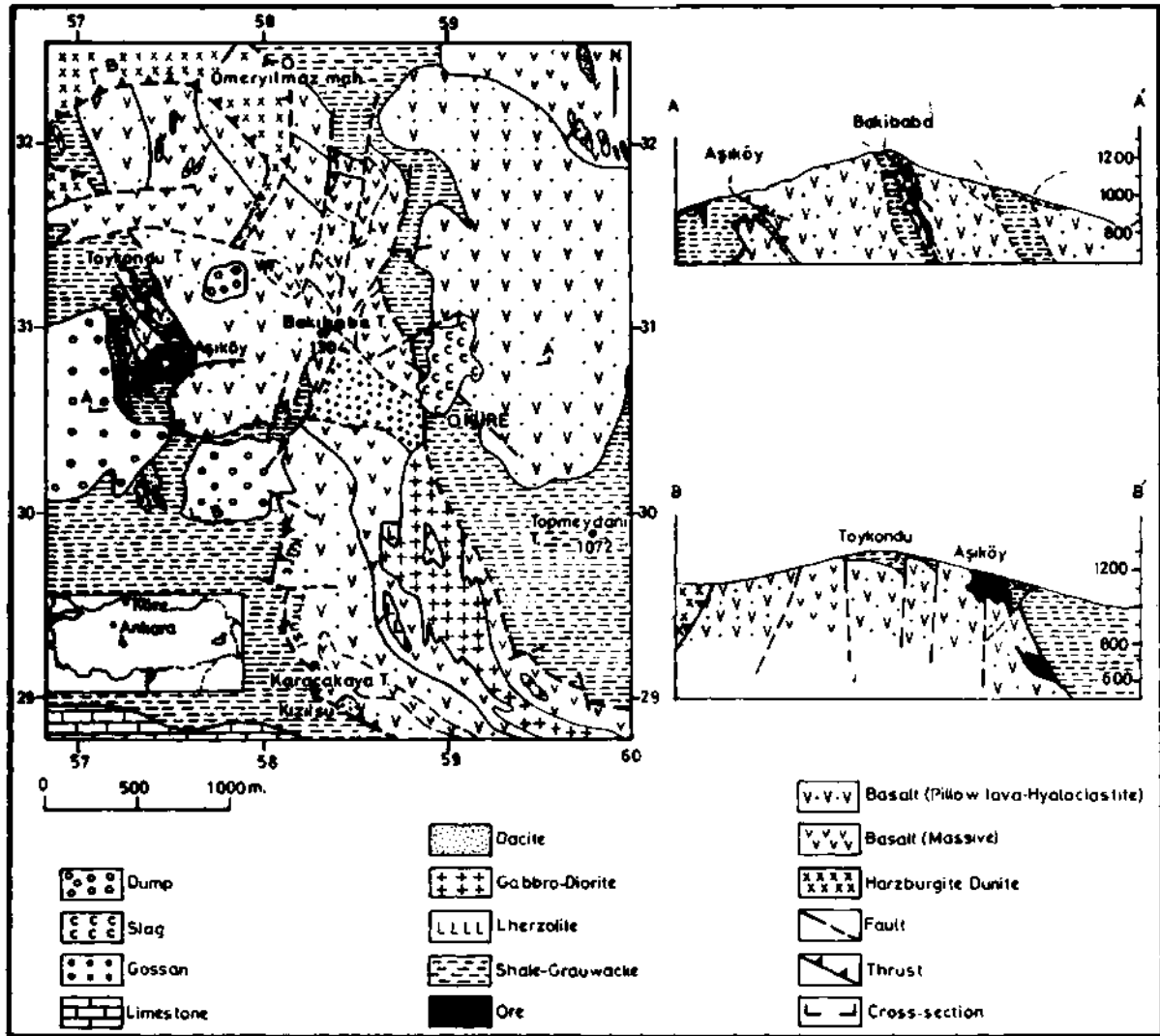


Fig. 1- Geological map and cross-sections of Küre area. Based on Pehlivanoğlu (1985), JICA and MMAJ (1992) with the exception of the mine areas of Aşıköy, Toykondü and Bakibaba.

Recently, Ustaömer and Robertson (1994) studied the petrological characters of the different lithological units of the Küre area and by evaluating their chemical compositions concluded that the ophiolite of Küre represents the slices of a marginal back-arc basin.

This paper is prepared from the results of the detailed geological study of the Aşıköy, Toykondü and Bakibaba ore deposits within the Aşıköy underground mining project signed between Etibank and Teknomad in 1986.

The objective of the work was to determine

the geological characteristics of the ore deposits and to calculate the proven reserves. To update the geological data with the progress of the mining operation the detailed surface geological maps of the Aşıköy, Toykondü and Bakibaba areas and underground geological maps of Bakibaba underground mine and Eti gallery were prepared with a scale of 1:1000 (Teknomad, 1988). The logs of the 164 drills from surface and 69 drills from drifts obtained by Etibank in the Aşıköy, Toykondü and Bakibaba areas between 1965-1986 were classified and standardized. The cores of some important drill-holes was re-examined.

Based on the geological maps and drill-hole data, 70 vertical geological cross-sections with 20 m interval and 43 horizontal geological cross-sections with 12 m intervals were prepared for the Aşıköy deposit. Similarly for the Bakibaba deposit 24 vertical and 23 horizontal geological cross-sections and for the Toykondur deposit 20 vertical geological cross-sections were drawn with a scale of 1:1000.

The proven reserves were estimated from the vertical geological cross-sections. The ore tonnage of each grade and structure type were separately calculated for each horizontal slice of the deposit with 12 m of thickness. The results of all the data are summarised in this paper so as to present the general characteristics of Aşıköy-Toykondur massive sulfide deposits.

#### GEOLOGY OF THE SURROUNDING ROCKS

Küre massive sulfide deposits are situated within the basalts forming the upper unit of the Küre ophiolite (Teknomad, 1988). The Küre ophiolite is formed by harzburgite and dunite tectonite, intrusive gabbro-diorite and lherzolite, basaltic volcanics and detritic sedimentary rocks. The primary successions of the different ophiolitic units generally disappeared as a result of strong tectonic activity. The harzburgites forming the lower unit in a normal ophiolitic massive occur on the volcanic and sedimentary unit as tectonic slices. The basalts are generally overthrust onto their cover, the shale sandstone unit (Fig. 1).

The basalts, enclosing rocks, are represented by massive lavas at the bottom and pillow lavas and hyaloclastites at the upper levels. The ore lies essentially in the hyaloclastites. The pillow lavas have ellipsoidal form of which long axis varies between 5-10 cm and 2-3 m. Their interstices are filled generally by calcite, argiles and chloritised volcanic glass. They have some separation planes having onion skin form parallel to their external surfaces and millimetric radial tension cracks filled by ore minerals.

Hyaloclastites, are formed by angular elements of basaltic lavas millimetric to decimetric in size. They are cemented generally by basaltic glass. Some pieces of red jasper can also be seen. The rock has greenish color and is cut by the veins of various thickness, filled by calcite, quartz and ore minerals.

The microscopic examination indicate that the basalts are formed principally by microlites of albitised, sensitised and epidotised plagioclase and by ouralited and chloritised interstitial augites. Some skeletal augites can also be observed.

The major and trace element analyses of the basalts show that they have oceanic ridge basalt character (Güner, 1980; JICA and MMAJ, 1992; Ustaömer and Robertson, 1994). Basaltic unit is cut by diabasic dykes having centimetric chilled margins and a general strike of NW-SE. Their thickness varies between 20 cm and 10 m. They crop out generally in the eastern part of the Aşıköy open pit. They have ophitic texture and are formed essentially by albitised plagioclase and ouralited augite. Some chlorite, sericite, quartz, magnetite, pyrite, chalcopyrite and ilmenite can be seen. Ustaömer and Robertson (1994) pointed out the existence of some sheeted dykes at the eastern flank of the Bakibaba pit. The lower levels of the basalts are also cut by gabbroic and lherzolitic intrusive rocks. The gabbros crop out in dyke and batholithic form at the south of Küre. In thin section they represent granular texture and constituted essentially by labrador, augite and hornblende. Some minerals such as olivine, sphene, magnetite are also observed.

The lherzolites are found as two small intrusions at south of Küre. The first one is enveloped by gabbros and has a triangle form with hectometric dimension. Its contacts are covered. The second intrusion is observed further south than the first one in the basalts. It is in ellips form striking N37W, with 400 m length and 75-100 m thickness. Near the contacts it is brecciated and, some traces of high temperature metamorphism are observed along a zone of about one meter thickness from the contact within the basalts. In thin section the lherzolites are fresh and have poikilitic texture. Subeuhedral and rounded olivines are included in large pyroxenes. The principal mineralogical constituents of the rock are olivine (augite, orthopyroxene ( $En_{62-67}$ ), brown titanian-magnesian-hastingsitic hornblende and kaersutite garnet, rare plagioclase and phlogopite. The secondary formation of the hornblende, garnet and some phlogopite from the pyroxenes and olivines is interpreted as the metasomatism of the peridotite by an alkaline and hydrous melt. The lherzolites represent probably the partial-

ly melted and uplifted upper mantle and metasomatised later at depth. The origin of the metasomatising melt is questionable. But nevertheless it may be related to a subducted slab (Çakır and Genç, 1995).

The basalts are covered by a detritic sedimentary unit represented by shale at the bottom and shale-sandstone alternations towards the top. Shale is dark grey or black in color and characterised by the much less strength relative to the basalts. It is foliated in the fault zones parallel to the fault planes. It is often folded. Along the fold axis the recrystallization of the quartz makes this part harder. It is formed principally by illite, quartz, chlorite and muscovite. The other minerals, such as pyrite, chalcopyrite, chromite, hematite and ilmenite are rarely observed (Güner, 1980). In the Aşıköy open pit, at the basal parts of the sedimentary unit, near the contacts with the basalts, some blocks of basalts are found. On the drill hole cores the basalt-shale alternations are often seen. Pehlivanoğlu (1985), investigating a much wider area, pointed out the existence of the basaltic lava layers in the lower levels of the shale. In the Elekdağ ordered ophiolite, situated at the south-east of Küre and thought to be a continuation of the Küre massif, the basalts lies in alternation with similar sedimentary rocks towards the top (Tüysüz, 1985). This finding is important because it shows that the upper parts of the basalts and lower parts of the shale are formed at the same time and in the same geological environment. The shale-sandstone unit named Akgöl (Ketin and Gümüş, 1962) or Börümce formation (Yılmaz, 1979) lies conformably on the Kayabaşı Upper-Triassic platform limestones at the south of Abana (Önder et al., 1987) and covered unconformably by conglomerates and limestones of Dogger-Malm age at south of Küre (Pehlivanoğlu, 1985). The fossils found in this formation are generally indicative of Lias (Kovenko, 1944, Ketin, 1962) or Upper Trias-Lias (Aydın et al., 1986) in age. The pollens of Upper Carboniferous-Lower Permian age found in this formation (Kutluk and Bozdoğan, 1981) are supposed to be transported from the continent because of the considerable age difference between them and conformable geological situation of this unit on Upper-Triassic limestones. Its general detritic character and the occurrence of some elements of metamorphic rocks in the sand-

stone unit (Pehlivanoğlu, 1985) show that the shale-sandstone formation was formed in a basin near a continental margin. From these data, it may be suggested that the volcanic and sedimentary unit representing the upper unit of the Küre ophiolite was formed in an oceanic ridge environment not far from the continental margin in Lias and obducted on the continent in Dogger. In this scheme, it seems that the Küre ophiolite represents the fragments of a narrow and short-lived oceanic lithosphere. For this reason without obtaining systematic geochronological data, the interpretation of Küre ophiolite as a fragments of the Paleo-tethyan oceanic lithosphere (Şengör et al., 1980; Tüysüz, 1985) must be taken with precaution.

The volcanic and sedimentary unit, surrounding rocks of the Küre massive sulfide deposits, are cut by the dacitic and rhyodacitic dykes (Fig.2). In the Aşıköy and Toykundu areas they have a general direction of NW-SE. Their length varies between 150-500 m and thickness between 10-60 m. They contain some blocks of shale which are baked at the contact zones. They are composed of corroded semieuhedral quartz, sericitised plagioclase and chloritised biotite. It is supposed that the dacites and rhyodacites are the dyke form prolongation of the granites and granodiorites cropping out northwest of Küre. Yılmaz and Boztuğ (1986) give a Dogger age for the granitoides of the Daday-Devrekani area having similar geological characteristics and interpret them as the products of northward subduction of the Paleo-Tethyan oceanic lithosphere.

In this case, the oceanisation giving birth to the Küre ophiolite may be interpreted as the result of the same subduction process and that the Küre massif represents the fragments of a back-arc marginal basin. The reaching to the same conclusion from the major and trace elements analyses of different units of Küre area (Ustaömer and Robertson, 1994) fortifies this hypothesis.

## STRUCTURAL GEOLOGY

The volcanic and sedimentary unit represented by basalts at the bottom and shale-sandstone at the top is divided into two tectonic units by the Küre thrust (Fig.1). The basalts thrust onto their own cover, i.e. shale-sandstone unit,

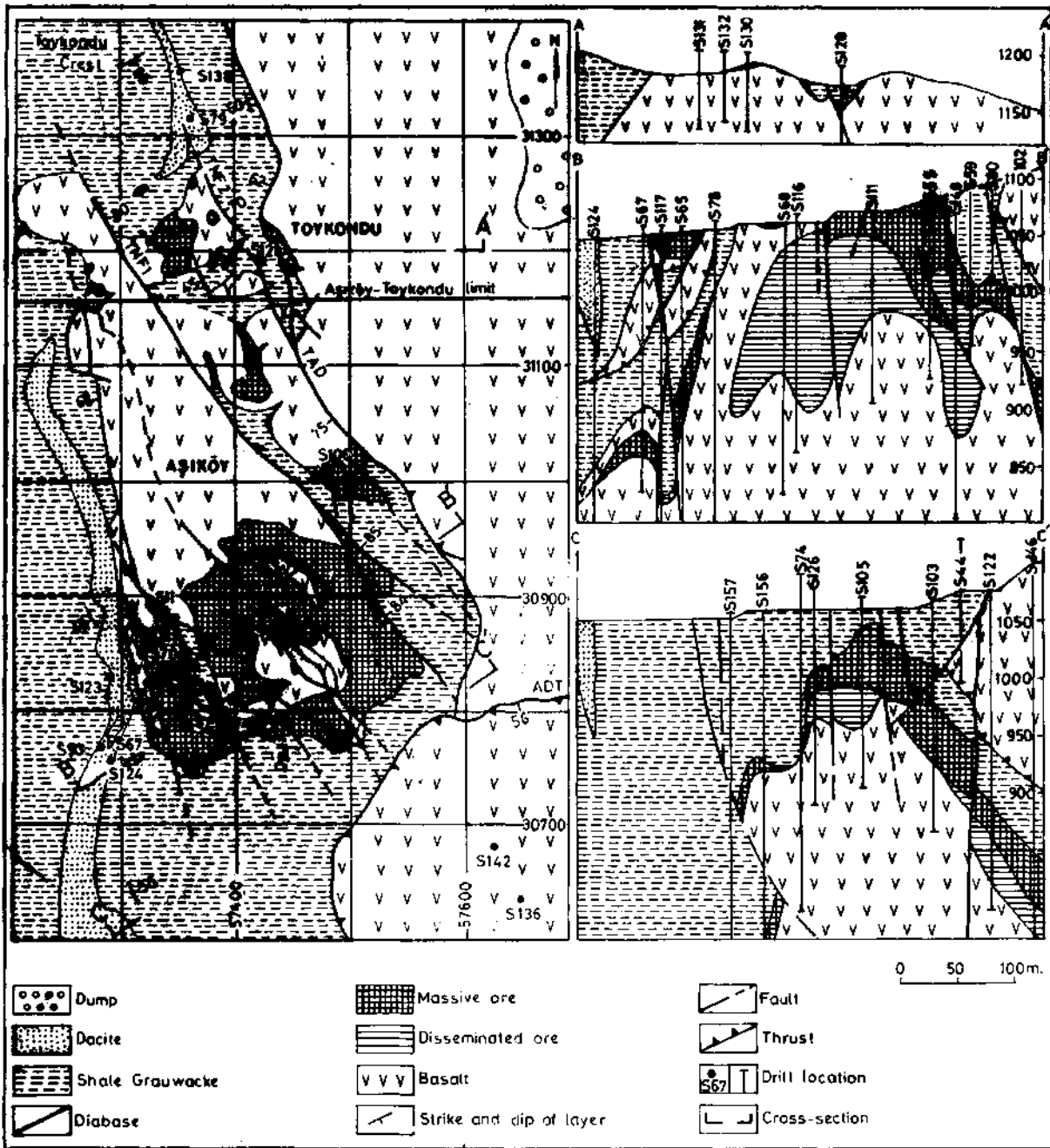


Fig. 2- Geological map and cross-sections of Aşıköy-Toykondü massive sulfide deposits.

along the Aşıköy and Kızılsu line. The western part of the upper slice has generally been eroded. However it is important to observe in places that the shale shows long continuation through the basalts. The shale on the Bakibaba crest having 40 m of thickness can be followed at least 375 m along the dip, with a degree of 65. On the surface and in

Bakibaba drift the observation of some non-faulted contacts between the basalt and shale give the impression that this situation could be the result of the initial structural setting. The lower tectonic unit is bordered by TAD fault in the east of the Aşıköy area (Fig.2). This fault begins south of Toykondü pit as a strike slip fault and turns into the reverse

strike-slip fault towards the southeast. In Toykundu area its general strike and dip is N30W/73 SW and the lineation measured on the upper mirror is N13W/24SE. It is followed 850 m. In the southeast end, the TAD fault disappears under the ADT fault. The latter with a brecciated zone of approximately of 15 m thickness is a reverse fault with a sinistral oblique slip. Its strike and dip measured at the intersection zone with TAD fault is N76W/56SW and the lineation is N83E/24SW.

The lower tectonic unit including the Aşıköy ore deposit has a ridge form with a general direction of N45W. It is generally fractured by normal faults usually parallel to the axial plane. The Aşıköy massive appears to have been rotated around a NE-SW oriented axis. The elevated northwest part has been eroded and the lower levels of the basalts crops out. The southeastern part formed by basalt, ore and shale plunges under the basalts of the upper tectonic unit. The general direction and dip of the NE flank of the Aşıköy ridge is N4W/60NE, and that of the SW flank is N87E/62SE (Fig.3). The upper tectonic unit is also fractured by reverse and strike slip faults oriented generally NE-SW direc-

tion-Trie latter is important because of their roles of principal guidance for the mineralization in the Bakı-baba area.

- It is interesting to point out that various structural elements observed in the volcanic and sedimentary unit of the Aşıköy massive are parallel to each other and show a general direction of NW-SE. Especially the parallel orientation of diabase dykes, gabbroic and Iherzolithic intrusions to the Aşıköy ridge axis give the impression that this ridge form represents a primary structure formed in an oceanic environment. Consequently the contradictory situation of the normal faults being parallel to the ridge axis and creating a horst graben system becomes explainable. Bailey et al. (1967) suggests that these faults were formed before the mineralization and created the channels for the mineralising solutions.

In the Aşıköy and Toykundu areas the parallel orientation of the dacitic dykes to the primary structures give the impression that these rocks were injected into the fractures formed during the extensive phase of the Küre ophiolite and represents the product of the same mechanism.

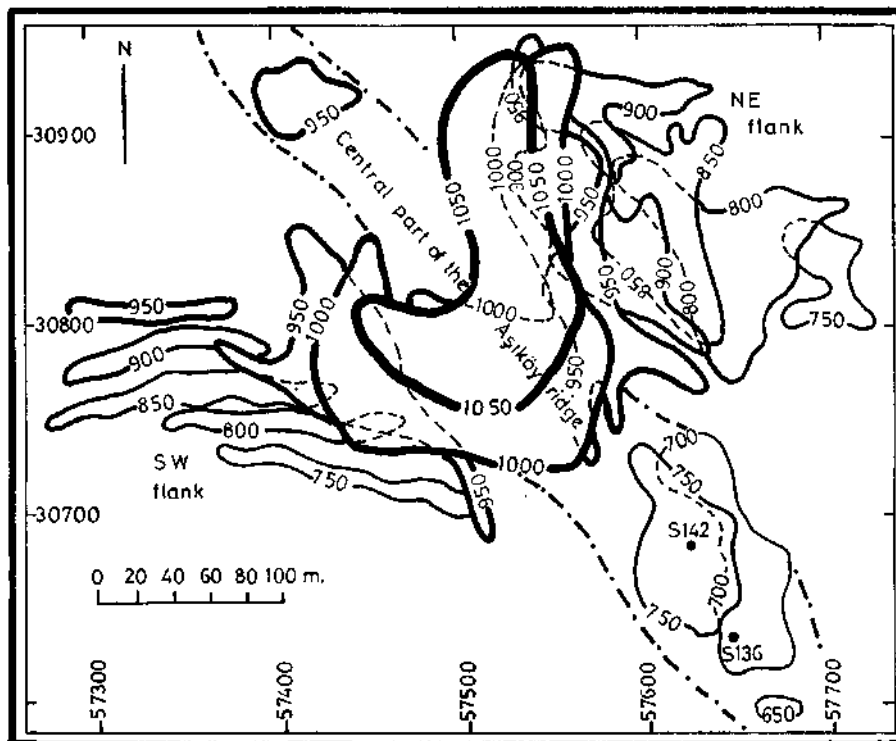


Fig. 3- Isophase map of Aşıköy massive sulfide deposit.

## GEOLOGY OF THE ORE DEPOSITS

The ore deposits in Aşıköy and Toykondum are as occur:

1- As lenses of different dimensions in the upper levels of the basalts. Right under the shale, the ore has a massive structure and the axial planes of the lenses are parallel to the basalt-shale contact plane. Towards the lower levels, it becomes partially stockworked and disseminated.

2- As the discontinuous and non-determined shaped mass at the top of the secondary anticline between basalt and shale. The structure of the ore has the same properties. The ore deposits at the south of Toykondum are the characteristic examples of this type.

The Aşıköy ore deposit is the most important mineralization of Küre. It forms the upper parts of the Aşıköy ridge of which the axis has a general direction of N45W and dip of 38-60 SE (Fig.2). In the southwest it plunges with a dip of 55 degrees. The northwest flank, the most important part of the deposit, continues under the shales and the basalts of the upper tectonic unit. The southwest flank lies under a thick shale unit.

The central part of the Aşıköy deposit is bounded by a shale observed along the S11, S70, S78 at the Southwest (Fig. 2). The ore block at the west of this shale is interpreted as a thin slice because of the presence of two levels of ore and basalt along the drill of S65, S67, and S117. The two orebodies, i.e. the one drilled by S106 and the other situated 100 m away from the former, form discontinuous mass of a thickness of maximum 25 m at the roof of the secondary anticlines.

An important orebody which does not crop out is discovered by the drill holes of S136 and S142. It shows that the main mineralization of Aşıköy follows the ridge axis along N45W/55SE and forms thick ore lenses in places.

The Toykondum ore deposit is situated at the northwest of the Aşıköy open pit (Fig.2). The orebodies between the faults TNF1 and TNF2 occupy the roof of the secondary anticline. Their\* axial orientation is N85E/62SW and they have an average thickness of 5 m.

The orebody at the east of S128 forms a lense having 50 m of length, 10 m of width and 5 m of thickness. The direction and dip of its axial plane is N25W/65SW. The drill-holes S79, S128 and S138 indicated that its thickness reaches 13 m between the depths of 50 m-75 m.

In the upper levels of the basalts at the west of the TNF1 fault small orebodies could be seen in places. This mineralization zone has a N-S general direction and a dip of 50-70 to the west. The cutting of some ore levels by the drill-holes of S93, S123 and S124 shows that this zone continues at least 360 m towards the south and forms massif ore lenses in places.

## MINERALOGY

The ore deposits of Toykondum and Aşıköy have very similar mineralogical characteristics. The principal ore minerals are chalcopyrite and pyrite. Some marcasite, sphalerite, covellite and neodigenite are also observed. The rare minerals are bravoite, linneite, tetrahedrite, goethite, hematite, chromite, rutile, anatase, chalcocite, tenorite, magnetite, pyrrhotite, bornite and native gold. The gangue is represented by calcite, siderite and quartz. The microscopical characteristics of the main ore minerals were described in detail by Çağatay et al., (1980), Güner (1980) and Pehlivanoğlu (1985). They may be summarised as follows:

Pyrite constitutes the major party of the ore. It is idiomorphic and generally smaller than 1 mm in size. Some melnicovite having colloform structure can also be seen. The cracks of the idiomorphic pyrite are filled by chalcopyrite, melnicovite and gangue minerals, showing that it is the mineral formed first. It is replaced by chalcopyrite along the cleavages and its borders are corroded. Economically, chalcopyrite is the most important mineral. It is generally interstitial between the pyrites and fills the cracks of the pyrites. Along its cleavages and cracks it is replaced by neodigenite and covellite (Çağatay et al., 1980; Güner, 1980; Pehlivanoğlu, 1985).

Bravoites and pyrites form some zoned structures having a thickness of 5-30 microns.

Linneite is the most important cobalt mineral observed in the Küre massive sulfide deposits. It occurs as idiomorphic and semi-idiomorphic minerals smaller than 200 micron in chalcopyrite and chalcopyrite rich sections.

Native gold occurs as very fine grains smaller than 30 micron generally along the contacts between chalcopyrite, idiomorphe pyrite, bornit and along the cracks in these minerals.

#### RESERVES AND GRADE VARIATIONS

The proven reserves of the Aşıköy and Toykondü deposits were calculated by the prism method from the cross-sections perpendicular to the direction of the Aşıköy ridge at intervals of 20 m. The ore tonnages and grades variations of different structural units of the deposit for each mine levels were determined separately. The ore is classified into six types according to their Cu and S grades. The grade ranges for open pit and underground mine are presented on Table 1.

**Table 1- Classification of ore types in the Aşıköy and Toykondü Deposits.**

Ore type	Open pit mine		Underground mine		
	Symbol	Grade(g)		Grade(g)	
		Cu%	S%	Cu%	S%
Massive high grade	MH	$g \geq 2$	$g \geq 34$	$g \geq 3$	$g \geq 34$
Massive medium grade	MM	$1.5 \leq g < 2$	$g \geq 34$	$1.5 \leq g < 3$	$g \geq 34$
Massive low grade	ML	$0.5 \leq g < 1$	$g \geq 34$	$0.5 \leq g < 1.5$	$g \geq 34$
Disseminated high grade	DH	$g \geq 2$	$g < 34$	$g \geq 3$	$g < 34$
Disseminated medium grade	DM	$1.5 \leq g < 2$	$g < 34$	$1.5 \leq g < 3$	$g < 34$
Disseminated low grade	DL	$0.5 \leq g < 1$	$g < 34$	$0.5 \leq g < 1.5$	$g < 34$

The density of different type of ore is approximated from the relationship obtained from grade-density measurements. The results are presented

on Tables 2,3 and 4 separately for the different parts of the deposit, types of ore and mining levels.

The Aşıköy ore deposit is planned to be extracted by open pit method till it reaches 936 m level and by underground method between 936 m and 756 m. The present lowest level in the open pit is 1140. m. The preparation for underground mining is in progress.

It can be seen from the tables that the north-east flank represents the most important reserves of the Aşıköy ore deposit in terms of quantity and grade.

In the Toykondü area the grade is high, but the reserve is very low. The maximum depth of the ore is 90 m. It is to be extracted by open pit method.

The Küre massive sulfide deposits also contain gold and cobalt. Çağatay et al. (1980) estimated that the average grades of cobalt and gold of Küre deposit are 0,3 % and 2,48 g/t respectively. In Toykondü area, the average grades of cobalt and gold calculated from 12 m of massive ore cores obtained in 1993, were 0,016 % and 1,55 g/t respectively. Although these grades appears to be low in the massive ore, it is expected that the grades of the gold in the desulphurated alteration zones will be as high as it can be, to be considered as a gold deposit.

#### DISCUSSION ON MINERALIZATION

Aşıköy-Toykondü massive sulfide deposits are interpreted as being formed during a submarine volcanism in Lias and subsequent hydrothermal process. All the deposits occurs at the upper levels of the basalts. However in the lower parts of the shale covering the basalts some thin levels of pyrite can be seen. Especially the occurrence of some breccia formed by angular pieces of pyrite and cemented by shale and pyrite (Kamitani and Çamaşircioğlu, 1976) shows that the mineralization continued during the sedimentation of the first levels of the shale.

In the south of Toykondü pit, it is observed that the pillow lavas forming the upper levels of the basalts are entirely replaced by the ore. This proves that the mineralization taking place after the volcanism includes a replacement process.

**Table 2- Proven Reserves of the Aşıköy Open Pit Mine (surface-936 m).**

Part of Deposit	Ore Type	Average Cu%	Grade S%	Density	Reserve (tonne)
N F	MH	3,79	44,30	4,5	119001
c l	MM	1,61	40,93	4,4	674080
r a	ML	0,71	43,08	4,3	469904
t n					
h k	DH	2,69	29,24	3,7	28415
e	DM	1,76	26,42	3,6	44928
a	DL	0,66	17,01	3,3	452534
s					
t	Total	2,23	35,33		2859874
C P	MH	2,94	45,72	4,5	346869
e a	MM	1,30	44,45	4,3	985043
n r	ML	0,17	40,31	4,1	574615
t t					
r	DL	0,86	20,15	3,2	797620
a					
l	Total	1,14	36,56		2704147
S P	MH	2,67	41,74	4,4	360800
o a	MM	0,76	45,89	4,5	157500
u r					
t t	DH	2,48	27,05	3,7	2620
h	DL	0,81	26,05	3,5	948500
w					
e					
s					
t	Total	1,26	32,03		1469420
Grand Total		1,61	35,11		7033441

**Table 3- Proven Reserves of the Aşıköy Underground Mine (936m-756 m).**

Part of Deposit	Ore Type	Average Cu%	Grade S%	Density	Reserve (tonne)
N F	MH	6,29	44,22	4,6	857440
o l	MM	1,94	44,17	4,4	254144
r a	ML	0,65	43,20	4,3	536124
t n					
h k	DH	3,69	27,48	3,8	234992
e	DM	1,66	19,11	3,4	6664
a	DL	0,75	13,18	3,1	447659
s					
t	Total	3,18	36,27		2337023
C P					
e a	DL	0,89	21,28	3,2	129138
n r					
t t					
r	Total	0,89	21,28	3,2	129138
a					
l					
S F	MH	3,35	42,72	4,5	26100
o l	MM	2,38	42,81	4,3	283628
u a	ML	0,88	40,02	4,2	122808
t n					
h k	DH	3,15	28,08	3,8	44785
e	DL	0,60	17,72	3,3	250272
a					
s	Total	1,60	32,80		727593
t					
Grand Total		2,73	34,88		3193754

Part of Deposit	Ore Type	Average Cu%	Grade S%	Density	Reserve (tonne)
N P	MH	6,04	42,83	4,5	101700
o a	ML	0,32	39,17	4,2	28560
r r					
t t	DL	0,55	23,87	3,5	10780
h	Total	4,47	40,64		141040
S P	MH	2,59	35,76	4,3	17974
o a	MM	1,84	45,60	4,4	16940
u r					
t t	Total	2,26	40,53		34914
h					
Grand Total		4,03	40,62		175954

**Table 4- Proven Reserves of the Toykondü Open Pit Mine**

The orebody does not contain any high temperature minerals. Some high temperature minerals such as magnetite, ilmenite and chromite rarely observed in the basalts are believed to be contemporaneous with these rocks. The minerals such as melnicovite, chalcopyrite and gangue form colloform structure indicating a low temperature formation. From these data it may be suggested that the mineralization comprised of hydrothermal and sedimentary process. Thereby the Aşıköy and Toykondur deposits can be considered analogues to that at the modern oceanic spreading centres. An especially well observed example lies along the axial ridge of the Galapagos spreading center in the East Pacific rise (Corlis et al., 1979; Haymon and Kastner, 1981).

As it is cited from Koski (1983), "This mineralization results from large scale circulation of sea-water through basaltic basement along the fracture zones near the technically active axis of spreading. The high geothermal gradient above 1 to 2 km-deep magma chambers emplaced below the ridge axis drives the convective circulation cell. Cold oxidizing sea-water penetrating the crust becomes heated and evolves into a highly reduced somewhat acidic hydrothermal solvent during interaction with basaltic wall-rock. Depending on the temperature and water/rock ratio, this fluid is capable of leaching and transporting the ore metals. Dissolved sea-water sulphate is reduced to sulfide. Consequently metal sulfides are precipitated along channelways and replaced the wall-rock from ascending fluid. Vigorous fluid flow results in venting of reduced fluid at the sea-floor/sea-water interface and deposition of ore minerals."

In Küre deposits following data indicating the remobilization of ore posterior to the principal mineralization is observed:

1 - In Toykondur area some of the orebodies occur along the axis of the secondary anticlines oblique to the primary structures. They were probably formed during or after the obduction of the Küre ophiolite.

2- The ore right under the shale is generally massive and Cu rich, and becomes stockworked and disseminated downwards.

3- In Bakibaba area the mineralization also occurs as discontinuous veins in the fracture zones.

4- The cracks of idiomorphic pyrites, the first mineral in paragenesis, are filled by chalcopyrite.

The results obtained by Pehlivanoğlu (1985) indicate that some of the sulfide mineralizations is associated with the granitic intrusions of Dogger age. It appears that the granitic intrusions increases the temperature of the environment and causes the remobilization of some mobile elements. They consequently formed the secondary mineralization by precipitation and replacement mainly under the shale which did not allow the mineralising solutions to penetrate.

## CONCLUSIONS

The Küre massive sulfide deposits constitute a typical-example for a mineralization in ophiolitic volcanic rocks. They probably occurred near the spreading axis of a narrow and short-lived back-arc marginal basin at Lias and obducted on continent at Dogger.

Aşıköy ore deposit occurs at the upper levels of the Aşıköy ridge. As proven reserves, it contains 10,2 millions tons of ore with average grade of 1,96 % Cu and 35 % S.

Toykondur deposit is smaller with 176 000 tons of proven reserves and average grade 4% Cu and 40,6 %S.

Küre massive sulfide deposits also contain cobalt and gold. Their grade distribution within the deposit is not well known because of insufficient number of assays obtained from drill cores. Therefore it will be very useful to investigate especially gold distribution in Küre area by assaying the old core samples and the samples taken systematically from the atmospheric alteration zones.

## ACKNOWLEDGEMENTS

This paper is based on the study carried out as a part of the project signed between Teknomad and Etibank. I would like to thank the management of Etibank Küre Mine, Project Implementation and Mineral Research Departments of Etibank for their support for the project. I also thank Hacı Karakuş,

geologist, who collaborated with me on the field and office, Assoc. Prof. Taylan Lünel and his team who started the project and obtained the first results.

*Manuscript received May 9, 1994*

## REFERENCES

- Aydın, M.; Şahintürk, O.; Serdar, H.S.; Özçelik, Y.; Akarsu, İ.; Üngör, A.; Çokuğraş, R. and Kasar, S., 1986, Ballıdağ-Çangaldağı (Kastamonu) arasındaki bölgenin jeolojisi. Geol. Bull. of Turkey, 29, 1-16.
- Bailey, E.H.; Barnes, J.W. and Kupfer, D.H., 1967, Geology and ore deposits of the Küre District, Kastamonu Province, Turkey: Shields, L.L. (Ed.) CENTO summer training program in geological mapping techniques Küre, Turkey, part II, CENTO, 17-75, Ankara.
- Corliss, J.B.; Dymond, J.; Gordon, L.I.; Edmond, J.M.; vanHerzen, P.P.; Ballard, R.D.; Green, K.; Williams, D.; Bambridge, A.; Crane, K. and vanAndel, T.H., 1979, Submarine thermal springs on the Galapagos Rift: Science, 203, 1073-1082.
- Çağatay, A.; Pehlivanoğlu, H. and Altun, Y., 1980, Küre piritli bakır yataklarının kobalt-altın mineralleri ve yatakların bu metaller açısından ekonomik değeri: MTA Bull., 93/94, 110-117, Ankara, Turkey.
- Çakır, Ü. and Genç, Y., 1995, Küre ofiyolitinde flogopitli and granatlı lerzolit intruzyonları: 30th. Ann. Sym. of the Geol. Dept. at KTÜ, Abstracts, 23, Trabzon.
- Demirbaş, T.T., 1984, Aşıköy rezerv hesabı raporu: Etibank Rep., Maden Arama Dairesi Başkanlığı (unpublished), Ankara.
- Güner, M., 1980, Küre civarının masif sülfid yatakları ve jeolojisi, Pontidler (Kuzey Türkiye): MTA Bull., 93/94, 65-109, Ankara, Turkey.
- Haymon, R.M. and Kastner, M., 1981, Hot spring deposits on the East Pacific Rise at 21°N: preliminary description of mineralogy and genesis: Earth Plan. Sci. Lett., 53, 363-381.
- J.I.C.A. and M.M.A.J., 1992, The Republic of Turkey report on the mineral exploration of Küre area: Etibank Rep., Etibank Genel Müdürlüğü (unpublished), Ankara.
- Kamitani, M. and Çamasırcıoğlu, A., 1976, Kastamonu-Küre'nin batı kısımlarındaki cevherleşme ve jeolojisi: MTA Rep., 1335 (unpublished), Ankara.
- Ketin, I. 1962, 1:500 000 ölçekli jeolojik harita ve izahnamesi (Sinop): MTA Yayl., Ankara, Turkey.
- and Gümüş, Ö., 1962, Sinop, Ayancık ve güneyinde, III. bölgeye dahil sahaların jeolojisi hakkında rapor: TPAO Rep. No. 288 (unpublished), Ankara, Turkey.
- Kovenko, V., 1944, Küre'deki eski bakır yatağı ile yeni keşfedilen Aşıköy yatağının ve Karadeniz Orta ve Doğu kesimleri sahil bölgesinin metallojenisi: MTA Bull., 2/32, 180-211, Ankara.
- Kutluk, H. and Bozdoğan, N., 1981, IV. Bölge Üst Paleozoyik-Alt Mesozoyik çökelleri palinoloji ön raporu: TPAO Rep., 1545 (unpublished), Ankara, Turkey.
- Önder, F.; Boztuğ, D. and Yılmaz, O., 1987, Batı Pontidlerdeki Göynükdağı-Kastamonu yöresi Alt Mesozoik kayalarında yeni paleontolojik (Konodont) bulgular: Melih Tokay Geol. Symp., 87, Abstracts, 127-128, Ankara.
- Pehlivanoğlu, H., 1985, Kastamonu-Küre piritli bakır yatakları (Bakibaba-Aşıköy) ve çevresinin jeoloji raporu: MTA Rep., 1744: (unpublished), Ankara, Turkey.
- Şengör, A.M.C.; Yılmaz, Y. and Ketin, İ., 1980, Remnants of a pre-Late Jurassic ocean in northern Turkey: Fragments of Permian-Triassic Paleo-Tethys?. Geol. Soc. Am. Bull. Part 1, v. 91, 599-609.
- Teknomad, 1986, Etibank-Küre masif sülfid yatakları (Aşıköy-Toykond-Bakibaba) Jeoloji ve rezerv-kalite raporu: Etibank Rep. (unpublished), Ankara, Turkey.
- , 1988, Aşıköy-Toykond-Bakibaba masif sülfid yatakları cevherleşmenin oluşum modeli ve arama programı raporu: Etibank Rep. (unpublished), Ankara, Turkey.
- , 1991, Etibank-Küre Aşıköy yeraltı işletme projesi, cevher yatağı modellemesi ve rezerv hesapları revizyonu raporu: Etibank Rep. (unpublished), Ankara.
- Tüysüz, O., 1986, Kuzey Anadolu'da iki farklı ofiyolit topluluğu: Eski ve Yeni Tetisin artıkları: Doğa Tr. Müh. and Çev., 10, 2, 172-179.
- Ustaömer, T. and Robertson, A.H.F., 1994, Late Palaeozoic marginal basin and subduction-accretion: The Palaeotethyan Küre Complex, Central Pontides, northern Turkey: Jour. Geo. Soc., 151, 291-305, London.

Yılmaz, O., 1979, Daday-Devrekani masifi kuzeydoğu kesimi metamorfik petrolojisi: Doçentlik Tezi, Hacettepe Üniversitesi, Jeo. Müh. B61.176 p. Ankara.

Yılmaz, \*O. and Boztuğ, D., 1986, Kastamonu granitoid belt of northern Turkey: First arc plutonism product related to the subduction of the paleo-Tethys. *Geology*, 14, 179-183.

GEOLOGY, GEOCHEMISTRY AND GEOTECTONIC SETTING OF VOLCANICS COMPRISING KÜRE (KASTAMONU) ORE MINERALIZATION

Şükrü KOÇ\*; Ahmet ÜNSAL\*\* and Yusuf Kaan KADIOĞLU\*

ABSTRACT.- The rock formations cropping out in the area have the following stratigraphic sequence: The basement rocks are commonly serpentinized peridotite of pre-Jurassic age associated with occasional pyroxenite and dunite. This is overlain by the Küre formation of pre-Lias/Lias age composed of basaltic volcanics at the lower section and a thick sedimentary portion at the upper part. Next is the Karadana formation of Upper Dogger-Lower Malm age consisting of reef limestones with interlayers of sandstone. In addition, gabbro, diorite, dacite, and basaltic dikes intruding these formations are also observed. Küre volcanics are determined as tholeiitic basalts based on their petro-chemical properties. These rocks are island-arc type volcanics produced from the mixture of continental crust and magma originated from mantle. The pyritic copper deposits are of the Kieslager-type mineralizations which were determined as Cyprus-type in the earlier studies. This new and important finding was obtained after a detailed study on the geotectonic setting, host rock types, geochemical properties, and paragenesis of the ore mineralization.

## FEATURES OF THE TERTIARY VOLCANIZM OBSERVED AT BİGA PENINSULA AND GÖKÇEADA, TAVŞAN ISLANDS

Tuncay ERCAN\*\*\*; Muharrem SATIR\*\*\*\*; Gideon STEINITZ\*\*\*\*\*; Ayşin DORA\*\*\*\*\*; Ender SARIFAKIOĞLU\*\*\*\*\*; Christoph ADIS\*\*\*\*; Hans-Jürgen WALTER\*\*\*\* and Talat YILDIRIM . . . . .

ABSTRACT.- Six main volcanic rock groups that formed at different stages between Eocene to late Upper Miocene were differentiated in the area, depending on the field and laboratory studies, namely "Balıklıçeşme volcanics" of Eocene age, "Çan volcanics" of Oligocene age, "Kirazlı volcanics" of Upper Oligocene age, "Behram volcanics" of Lower to Middle Miocene age, "Hüseyinfakı volcanics" of Middle Miocene age and "Ezine volcanics" of Upper Miocene age. Together with petrographic and geochemical studies, K/Ar dating and Stronbium/Neodium isotope ratio measurements ( $87\text{Sr}/86\text{Sr}$  and  $143\text{Nd}/144\text{Nd}$ ) were done on the rocks. Volcanic rocks formed between Eocene and Middle Miocene were found to be of calc-alkaline, whereas only that formed during Upper Miocene were of alkaline type. Geochemical and isotopic studies show that the magma formed the calc-alkaline volcanism have undergone intense contamination and got a hybrid character whereas the source of alcali volcanism is different and formed by partial melting of a heterogeneous mantle material. The rocks are related with tectonic regime of the area; calc-alkaline volcanics have been formed under a compressional regime, but alkaline rocks have been formed under a tensional regime, contrarily.

DEPOSITIONAL CONDITIONS OF PLEISTOCENE ALLUVIAL FAN DEPOSITES IN THE GÜZELYURT BASIN (TURKISH REPUBLIC OF THE NORTHERN CYPRUS)

Engin OLGUN\*\*\*\*\*

ABSTRACT.- The alluvial fan deposits are widely distributed in the Güzelyurt basin. In the southern pan of the Güzelyurt basin, these deposits unconformably overlie the units of Middle-Late Cretaceous Troodos massive, Late Miocene-Early Pliocene Myrtou Marls and Late Pliocene Athalassa formation. Towards the north, they are unconformably overlain by recent alluvium deposits. The fan deposits are deposited by high-viscosity debris flows and braided streams dominated by sheet-flood events. Six different lithofacies are recognized; (A) Clast supported conglomerates are hyper-concentrated debris flow deposits, (B) Matrix supported conglomerates represent mud flow deposits, (C) Thick bedded sandy conglomerates represent sheet-flood and braided-stream deposits, (D) Clast supported, thick bedded conglomerates with interbedded sandstones are suggested as a braided-stream deposits, (E) Thin bedded sandstones and conglomerates represent sheet-flood deposits by very shallow migrating channels on a broad, planar surface during upper-flow regime, (F) Caliche bearing mudstones represent distal sheet-flood deposits in semiarid climates. At the end of the Late Pliocene, due to the rapidly uplifting of the Troodos massive, the coarse-very coarse pebbles of alluvial sediments are deposited as the inner fan deposits over the Pliocene sediments. As from Middle Pleistocene, the other alluvial fan facies are deposited together with relatively the coarse facies. The depositional conditions and the caliche concentrations in the alluvial fan deposits indicate a semi-arid climate.

## MICRO-TEXTURAL FEATURES OF THE SANDSTONES IN THE ÜZÜMDERE FORMATION (NORTH OF AKSEKİ, ANTALYA)

Turhan AYYILDIZ\*; Erdoğan TEKİN\*; Nurettin SONEL\* and Mehmet BÜLBÜL\*

**ABSTRACT.**- Üzümdere formation, Liassic aged is the oldest unit of the paraautochthonous sequence in the region and located within the Anamas-Akseki carbonate platform. Lithological units consist of sandstones and limestone, claystone, and conglomerates. The Üzümdere sandstones are claret-green in color, medium-thick bedded, well sorted, and highly fractured. The unit is petrographically described as quartz arenite-quartz wacke and sublitharenite based on the classification of Folk (1968). X-ray diffractometry studies have revealed that illite, kaolinite, and montmorillonite are the main clay minerals in the sandstones. Scanning electron microscope (SEM) and x-ray micro analyses (EDS) performed on some samples indicated that the development of cement in these rocks are of calcite, dolomite (?), iron oxide, chlorite and kaolinite. Moreover, calcite and iron-oxide are developed as filling the pores within the fractures. The unit, in which authigenic clay occurrences and quartz overgrowths are observed, has a poor porosity.

### INTRODUCTION

Sandstones of the Üzümdere formation, Liassic aged are exposed on the core of Akseki anticline at the north of Akseki (Antalya) (Fig. 1). The studies carried out in the investigated area so far are based on the petroleum geology (Demirtaşlı, 1979, 1987; Ayyıldız, 1992). These studies revealed the presence of a unit as the source rock in the region. In addition, it has been stated that sandstone levels in the Üzümdere formation are of importance as reservoir rock (Demirtaşlı, 1979).

conditions which they gain and preserve under some events they subjected. However, authigenic clays and other minerals developed in the structures of this type of rocks can worsen the reservoir conditions and lower porosity and permeability. Therefore, micro-textural features of this type of clastic sediments should be determined.

That is why, in this study, permeability and porosity properties of the sandstones of Üzümdere formation have been determined based on the examinations of their petrographic, mineralogic, and micro-textural parameters.

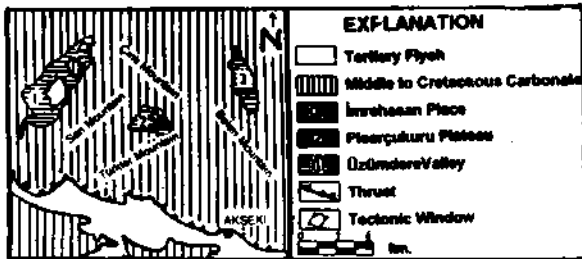


Fig. 1- Location map showing exposures of the Üzümdere formation in the study area.

As it is known, sandstones can form important hydrocarbon reservoirs depending on their depositional facies and, permeability and porosity

During these studies, petrographical descriptions of the sandstones and evaluations based on mineralogic and micro-textural features were made in accordance to Folk (1968) and McDonald (1979a, b), respectively. A number of 30 samples was collected from the sandstones of the Üzümdere formation and their petrographic description was made on thin sections. Mineralogic descriptions (whole rock day) x-ray diffractometry method with a Rigaku Geigerflex D/Max-Q/Q WC model diffractometer. Scanning electron microscope (SEM) studies for micro-textural features (grain-grain, grain-cement and grain-porosity relations) and x-ray micro analyses (EDS) studies were performed with Jeol JSM 840 A and Tracer TN 5502 ma-

chines, respectively. In addition, in order to determine the pore surfaces and their percentages, blue dyed epoxy was performed in the thin sections of all samples. With the aid of a Swift model point counter, modal analyses technique was also applied to determine the quantitative mineralogic composition of some selected samples. Furthermore, in order to determine the type of secondary iron oxide fillings within the fractures, polished samples was prepared and they were examined under the Nikon model ore microscope.

#### DESCRIPTION OF ÜZÜMDERE FORMATION

Formation was first named by Martin (1969) and later was described in detail by the studies of Monod (1977) and Demirtaşlı (1979, 1987). The basement of the unit under investigation has a tectonic contact and it is concordant with the Pisarçukuru formation in Dogger-aged above. The dominant lithologic assemblage of the Üzümdere formation is claret-green in color sandstone, limestone, claystone, and conglomerate. Its real thickness can not be determined due to the tectonic contact at the basement. However, in the measured stratigraphic sections of the Üzümdere valley (M.S.S. 1), Pisarçukuru plateau (M.S.S. 2) and Imrehasan places (M.S.S. 3) the thicknesses of 250, 450, and 400 m were measured, respectively.

In the Üzümdere M.S.S. 1, formation starts with limestones at the basement and continues with well sorted, medium to thick bedded, highly fractured sandstone and claystone alternations. Alternating sandstone levels are claret-green in color whereas claystone levels are red in color. Above these units in the Üzümdere village is the conglomerate levels (Plate 1, photo 1). The lower and upper levels of conglomerates of petromictic character, whose lateral transition is limited, are grain and matrix supported, respectively. The basement of conglomerates are erosional and imbricated are developed in them. In the upper most part, sandstone-claystone and dolomitic time-stones in places are found. The stratigraphic sequence observed in M.S.S. 1 is also traced in M.S.S. 2 and M.S.S. 3. The sandstone in M.S.S. 2, however, contains significant amount of iron oxide concretions (Plate 1, photo 2). On the contrary, at the basement of M.S.S. 3, bituminous bearing levels are observed.

#### PETROGRAPHIC ANALYSES

Petrographic studies indicate that the constituents of sandstones in the Üzümdere formation are composed mostly of quartz, calcite, muscovite, magmatic-metamorphic rock fragments and little amounts of feldspar and opaque minerals. The cement of the sandstones is dominantly calcite and iron oxide, but clay in some samples. They are described as quartz arenite, quartz wacke and sublit arenite.

Under the microscope, quartz grains are mostly monocrystalline, but in some samples polycrystalline grains are also observed. It was also observed that quartz grains are generally highly fractured, angular, but are sub-rounded and oval in some samples. Most of fractured quartzs are filled by secondary calcite and partly by iron oxide (Plate II, photo 3). Muscovite inclusions were also observed in quartzs. Iron oxide interferences are detected as filling the rock Assures (Plate II, photo 4). It was also determined polycrystalline quartz grains are schistose structured metamorphic quartzites. Due to the tectonic activity, calcite grains in places shown pressure twin growths. Calcite grains are medium to coarse grained, partly rounded and have well developed cleavages. Calcite is observed as both a fixing agent and secondary pore filling, while feldspars appear to have been subjected to alteration and are transformed to cericite. Textural studies reveal that grains are well sorted and they show point, concave, and convex contacts with each other, and that they have a medium degree maturity. The results of modal analyses conducted on selected sample are given in Table 1. The results are obtained from an average counting of 1650.

**Table 1- Average composition of sandstone determined by the modal analyses method**

Sample No	Quartz	Feldspar	Calcite	Rock Fragment
ÜZ-4	1863	15	363	205
ÜZ-7	391	17	770	152
ÜZ-9	546	31	231	286
ÜZ-11	987	57	195	513

### X-RAY DIFFRACTOMETRY ANALYSES (XRD)

XRD studies for the mineralogic descriptions of the sandstones of the Üzümdere formation were realized as whole rock and clay analyses (analyses with no treatment, with ethylene glycol and with treatment of HCl). Of these, the main minerals of samples, examined by the whole rock analyses, are quartz, muscovite, chlorite, calcite, feldspar (K-feldspar-plagioclase) and lesser amounts of dolomite (Fig. 2 a-b-c).

First the analyses with no treatment was done for the clay analyses of these samples (Fig. 3 a-b). In order to differentiate the clays in the rock, then the analyses were repeated with the treatment of ethylene glycol (Fig. 2 d). Finally, to test kaolinite and chlorite minerals detected, analyses were made with treatment of HCl. During this experiment, samples were boiled 1 hour in a mixture consisting of 1 mol HCl and 1 mol pure water. After samples were washed out with the remnant pure water and dried, the analyses were repeated. Chlorite peaks became extinct at the end of this analyses. This results confirms the presence of chlorite within the-rock. Different amounts of muscovite, kaolinite, chlorite and montmorillonite were determined by the analyses. The presence of a little amount of illite was also detected as coinciding with the peaks of muscovite.

### MICRO-TEXTURE STUDIES (SEM-EDS)

As a result of SEM-EDS studies on some selected sandstone samples, detailed information were obtained for some features, such as cementing, porosity, clay neomorphism and the relations of grain-grain and grain-cement. There is almost no porosity in all the examined samples, and authigenic clay occurrences together with the compaction of sandstones are well developed. In addition, quartz overgrowths of authigenic origin and radial developments are well distinguished (Plate III, photo 5). On the other hand, calcite crystals have partly a zoning structure and dissolution pores in places are detected on their surfaces (Plate III, photo 6). Microporosity and cave occurrences in places are observed in calcite cement (Plate IV, photo 7). It was also detected in some samples that chlorite cement fills the pores between grains (Plate IV, photo 8).and

that microporosity fields (Fig. 4a) are widespread in the iron-chlorites which were particularly detected with EDS studies. In some samples of the Üzümdere sandstone having a cement of kaolinite it was observed that smectites together with kaolinite completely fill pore fields as semi-booklets (Plate V, photo 9, 10; Fig. 4b).

Dissolution and alteration effects are typical for feldspar (Plate VI, photo 11). Secondary fracture fields are filled with calcite and iron oxide (Plate VI, photo 11,12; Fig. 4c). Filling of fractures negatively affects the porosity (Ayyıldız, 1992; 1994). These secondary iron oxide fillings have been determined as "hematite" based on the field observations by Martin (1969) and Demirtaşlı (1979). However, ore microscopy and x-ray diffractometry studies reveal that this iron oxide filling is limonite (goethite and lepidocrocite) rather than hematite. Pyrite occurrences were also detected along the fractures.

### DISCUSSION

The events observed in the sandstones of the Üzümdere formation are in the order of; calcite and iron oxide cementing, compaction, secondary dissolution of calcites, quartz overgrowth, alteration of feldspar, authigenic clay occurrences, development of secondary fracture systems, and filling of these fractures by calcite, limonite (goethite and lepidocrocite) and pyrite.

Of these, carbonate cement was formed by the neoformation of possible primary micritic cement depending on the compaction. Based on blue dyed epoxy test and SEM studies it is believed that secondary dissolution and dissolvments observed in the calcite cement were formed by the expelling CO<sub>2</sub> during the development of kerogen in the organic material-bearing levels of the Üzümdere formation. Similar statements are also found in the study of Schmidt and McDonals.(1979a). Iron oxide developments in the sandstones of the Üzümdere formation are observed as both cement and secondary fracture filling. Iron oxide in a cement character must have been probably brought to the basin by been absorbed on the detritic clay minerals (Greenland, 1975) or by mixing with humic acid (Picard and Felbeck, 1976). The source of secon-

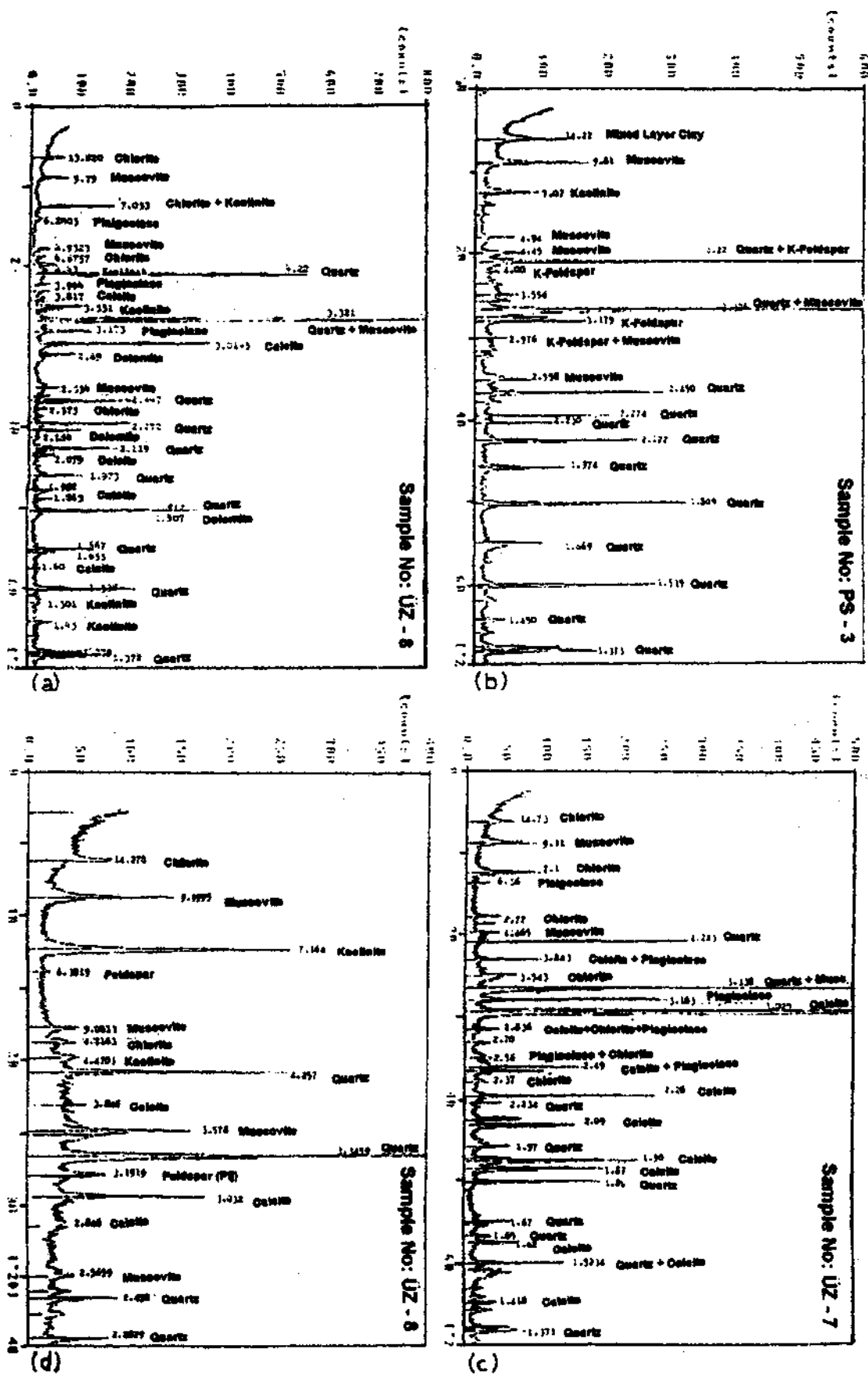


Fig. 2- X-ray diffractometry diagrams of whole rock and clayey units upon treatment with ethylene glycol.

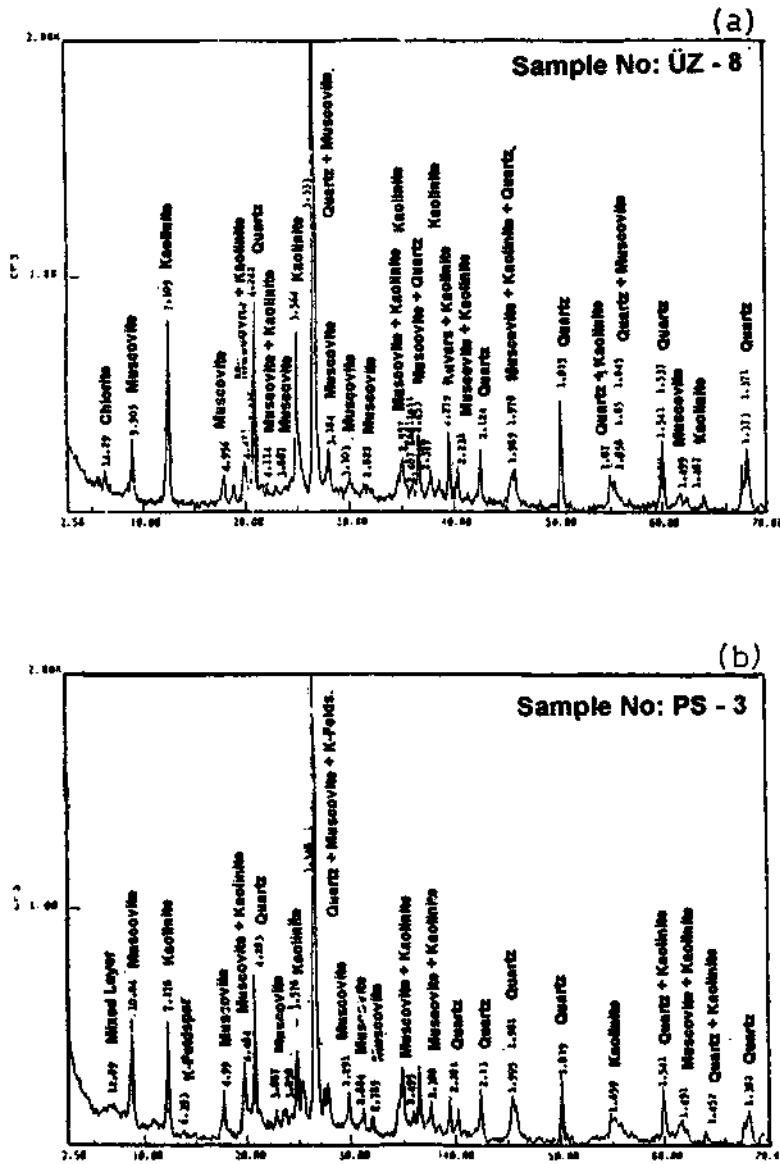


Fig. 3- X-ray diffractometry diagrams of clayey units.

source of secondary-fracture-filling iron oxide may be flushing in the atmospheric conditions as stated by Thomas (1974). Because, microporous iron-chlorites were observed on the edges of iron oxide zonings filling the fractures. These microporous developments give rise to the opinion that iron-chlorites are subjected to flushing time to time and,

hence, are the source of iron in the environment. However, if it is assumed that chlorites are formed as the last product, speculation given above fails. Alteration of mafic minerals such as pyroxene, amphibole, and hornblende, detected in the heavy mineral analyses carried out for the investigation of source rock (Ayyıldız, 1992), may be the source of

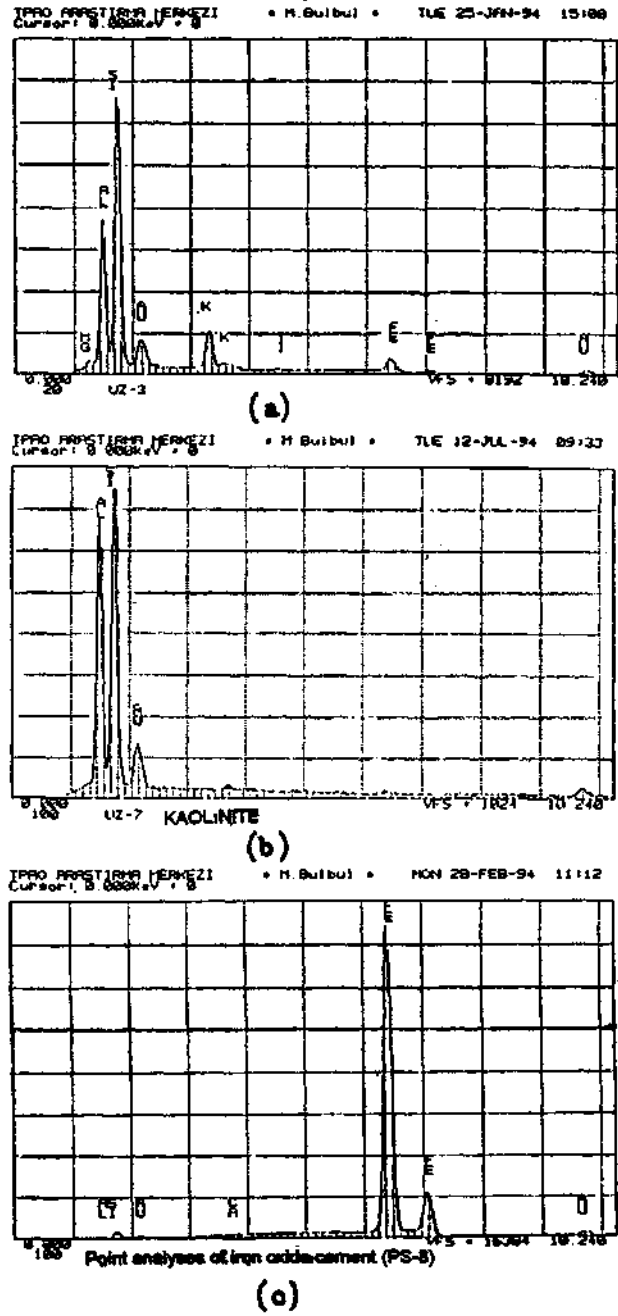


Fig. 4- Semi-quantitative EDS diagrams of components determined by SEM studies.

authigenic iron oxide minerals. Similar results were also given in the study of Sayın (1984). Quartz overgrowth detected in the quartz grains by SEM studies are formed by  $Si^{+2}$  concentrations yielding from the dissolution of partly amorph unstable aluminosilicate minerals through the reaction with the fresh waters in the pores that are come to exist due to lowering of PH by the intense bicarbonate formation of aerobic bacteria. Similar formation mechanism are also presented in the studies of Garrets and Christ (1965) and Curtis (1978).  $Al^{+2}$  expelled from the some mechanism is thought to be consumed in the formation of kaolinite. Kaolinite may also be formed as a result of alteration of K-feldspar. According Curtis and Spears (1971), both formation type are possible to occur.

In addition, the possible source of authigenic chlorites, which were observed as grain bounding and pore filling during the SEM studies, could be the reaction of kaolinite with  $Fe^{+2}$  ve  $Mg^{+2}$  which are supplied to the system. The study of Boles and Franks (1979) gives information on this manner.

## RESULTS

Calcite, iron oxide, silica, and clay cement detected in the sandstones of the Üzümdere formation have negatively affected the porosity and permeability properties of the unit.

Development of silica and clay cement may decrease the secondary porosity.

Fracture systems developed after the unit was exposed have been destroyed by the secondary calcite and iron oxide fillings.

## ACKNOWLEDGEMENTS

Authors are grateful to A. Sarı, L. Karadenizli, A.Acar. and A.O. Doğan (AÜFF) for their help during the field studies. Appreciation is extended to V.Ş. Ediger (TPAO) for performing SEM analyses and resinous coloring. Thanks go to S. Gürsü of MTA for making x-ray analyses of clay minerals. A.U. Doğan (AUFF) and Ş.A. Sayın (MTA) are also thanked for reviewing the manuscript.

**Manuscript received November, 11, 1994**

## REFERENCES

- Ayyıldız, T.. 1992. Üzümdere-Akkuyu (Akseki-ANTALYA) Civarının petrol olanakları: Y. Lisans Tezi, A.Ü. Fen Bilimleri Enstitüsü., 196 8. (unpublished), Ankara.
- , 1994, Üzümdere formasyonu (Akseki Kuzeybatısı) kumtaşlarının diyajenetik gelişimi ve rezervuar karakteri (Antalya-TÜRKİYE): Çukurova Üniversitesi 15. Yıl Simpozyumu Bildiri Özleri.
- Boles, J.R. and Franks, S.G., 1979, Clay mineral diagenesis in Wilcox of south-west Texas: Implications of smectite diagenesis in sandstone cementation. J. Sedim. Petrol, 49. 55-70.
- Curtis, C.O. and Spears, D.A.. 1971, Oiaegenetic development of kaolinite: Clays and Clay Miner., 19, 219-227.
- , 1978, Possible links between sandstone diagenesis and depth related geochemical reactions occurring in enclosing mudstones: J. Geol. Soc. London, 135. 107-117.
- Demirtaşlı. E., 1979, Batı Toros kusağının (Akseki Kuzeybatısı) petrol potansiyeli: 1. Bilimsel ve Teknik Kongresi, Ankara, 187-190.
- , 1987, Akseki-Manavgat-Köprülü bölgesinin temel jeoloji incelemesi: MTA Rap., 3292 (unpublished), Ankara.
- Folk. R.L., 1968, Petrology of Sedimentary Rocks: Hemphills Bookstore. Austin, Texas.
- Garrets, R.M. and Christ, G.L, 1965, Solution, Minerals and Equilibria: Herper and Row, New York.
- Greenland, D.J., 1975, Charge characteristics of some kaolinite-iron hydroxide complexes: Clay Miner. 10,407-416.
- Martin, C., 1969, Akseki kuzeyindeki bir kısım Toroslarn stratkjrafik ve tektonik incelemesi: MTA Derg., 72, 158-175.
- Monod, O., 1977, Recherches geologiques dans les Taurus occidental au sud de Beyşehir: These Erasente a l'Universite de Paris sud Centre d'Orsa.
- Picard, G.L. and Pel beck, (Jr), G.T., 1976, The oomplexation of iron by marine humic acid: Geochim. Cosmochim. Acta, 40, 1347-1350.

- Sayın, Ş.A., 1984, The geology, mineralogy, geochemistry and origin of Yeniçağa kaolinite deposits and other similar deposits in western Turkey: Ph. D. Thesis., London. 77-85 (unpublished).
- Schmidt. V. and McDonalds, D.A., 1979a, The role of secondary porosity in the course of sandstone diagenesis: In: Aspects of Diagenesis (Ed by P.A. Scholle and P.R. Schluger) Spec. Publ. Soc. Econ. Paleont. Miner., Tulsa, 26, 175-207.
- Schmidt, V. and McDonalds, D.A., 1979b. Texture and recognition of secondary porosity in sandstones: In: Aspects of Diagenesis (Ed by P.A. Scholle and P.R. Schluger) Spec. Publ. Soc. Econ. Paleont. Miner, Tulsa, 26, 209-225.
- Thomas, M.F., 1974, Tropical Geomorphology, A study of Weathering and Landform Development in Warm Climates: Mac Millan Press, London.

## PLATES

**PLATE-I**

Photo 1- A view of conglomerate and sandstones belonging to the Üzümdere formation (NW of Üzümdere village. View direction is from SE to NW).

Photo 2- A view of iron oxide concretion-bearing sandstones of Üzümdere formation (Pisarçukuru plateau. View direction is from SE to NW).

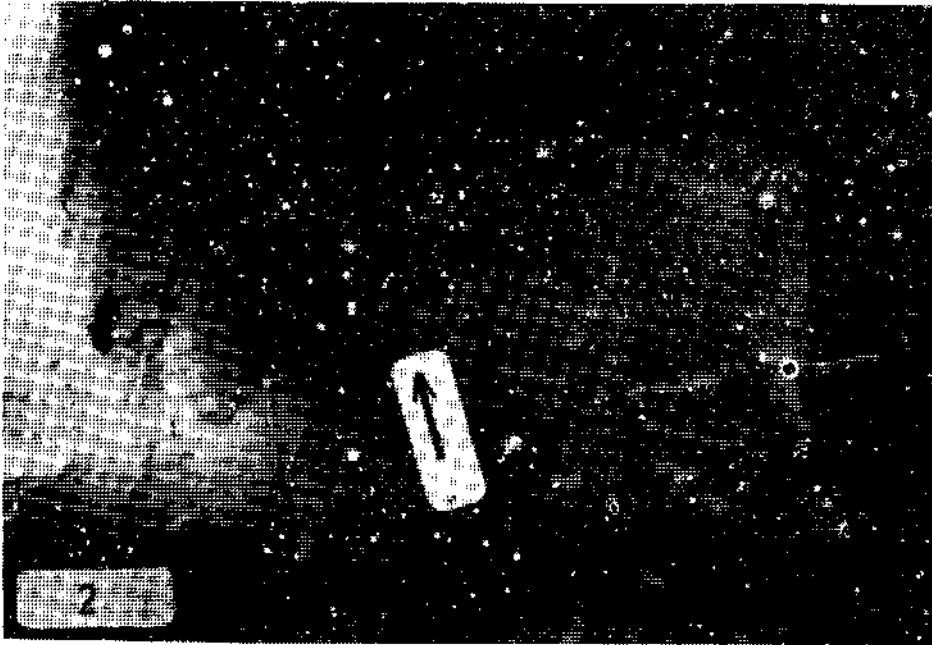


## **PLATE-II**

Photo 3- Photomicrographic view of carbonate fillings in the fractures of iron oxide and clay cement-bearing quartz arenites and quartzs observed in the Üzümdere formation (Quartz (Q); Calcite (kls) and chert (çrt); crossed nicole: X63).

Photo 4- Photomicrographic view of iron oxide filling in the rock fracture (Quartz (Q); iron oxide (dmr); Pısarçukuru Pletau, PS-8, plane light; X63).

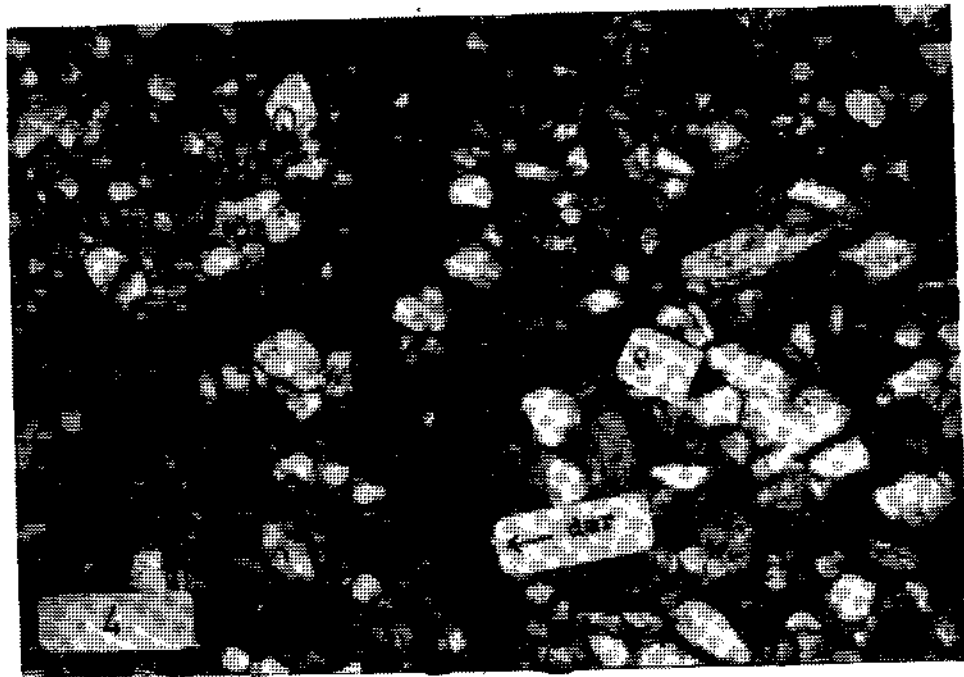
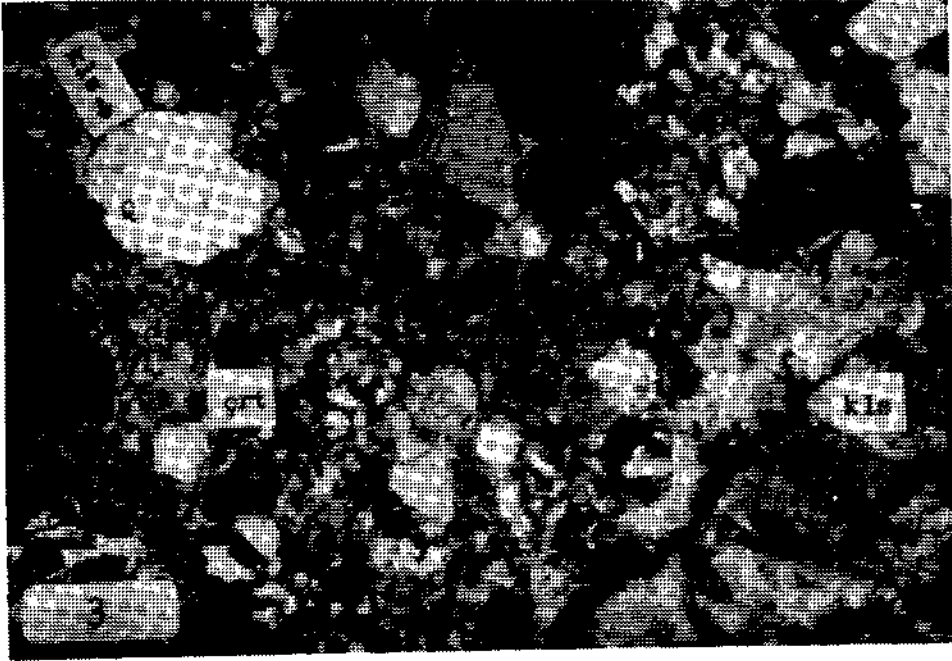


**PLATE -III**

Photo 5- SEM image of secondary quartz overgrowths and calcite fracture fillings (calcite (kls)).

Photo 6- SEM image of zonal growing calcite and feldspars altered on the margins.

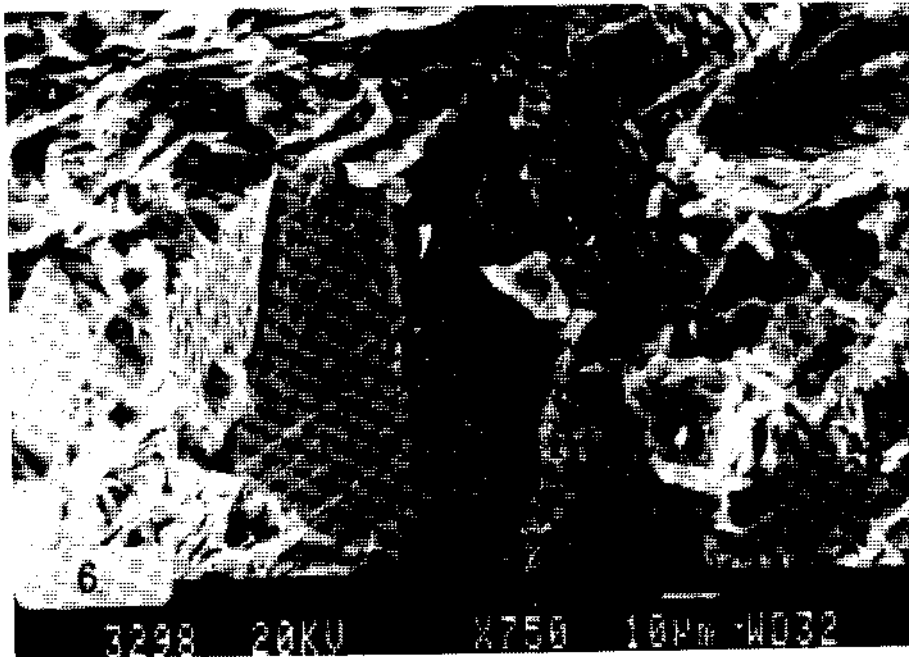
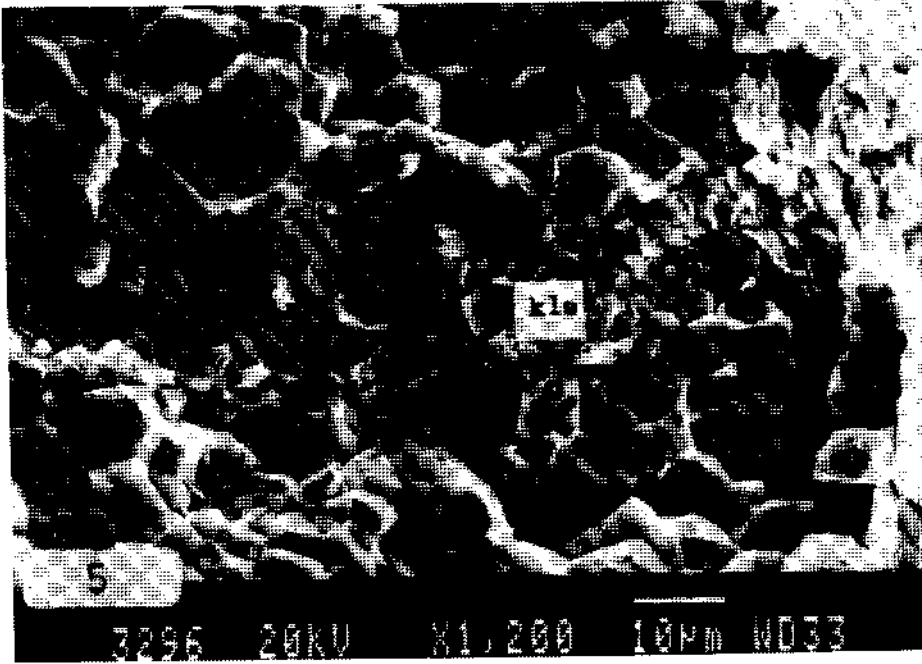


**PLATE -IV**

Photo 7- SEM image of microporosity and microform porosity between the calcite grains.

Photo 8- SEM image of chlorites developed in micropores.

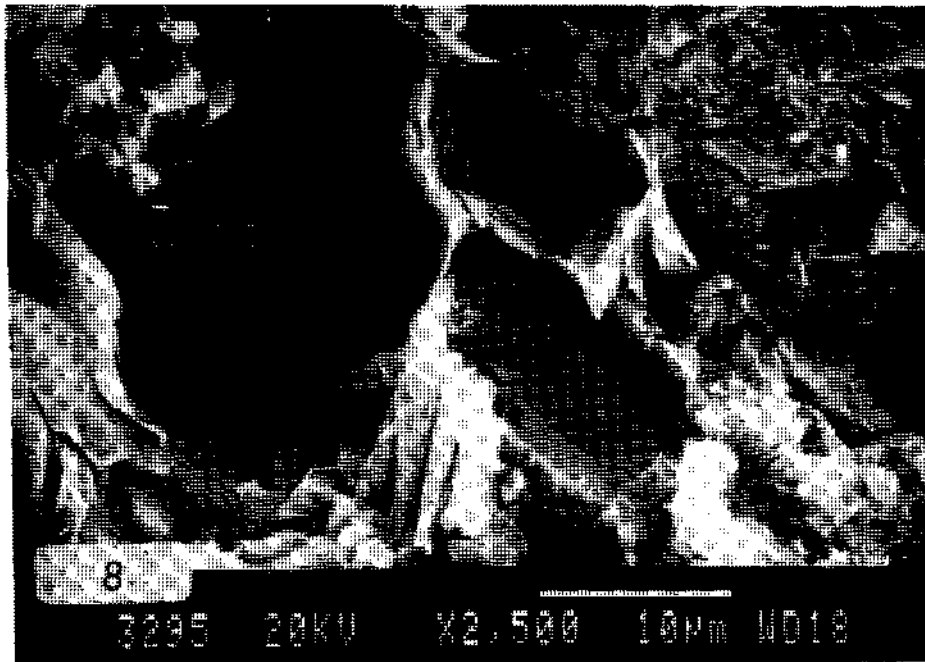
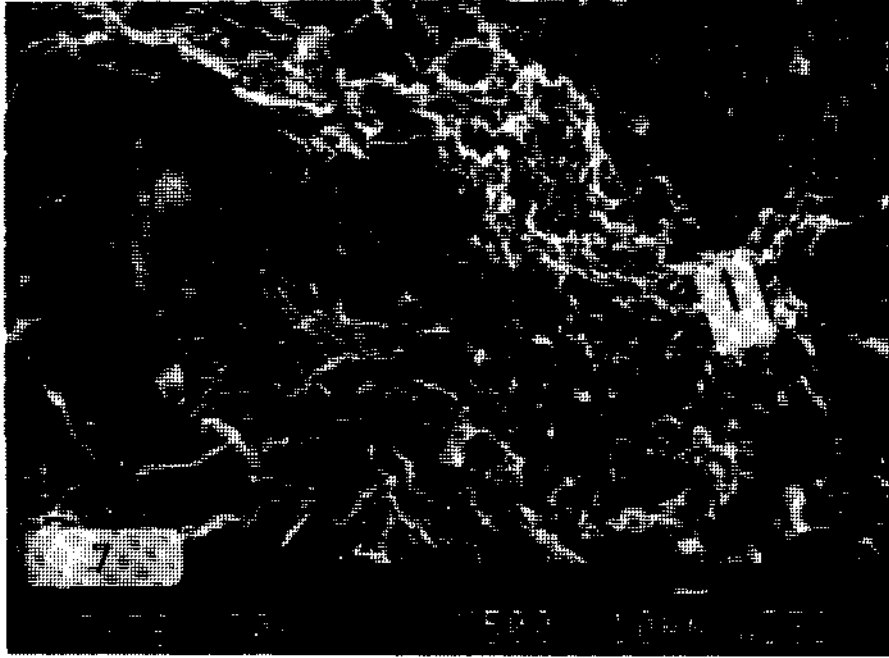


**PLATE -V**

Photo 9- SEM images of kaolinite, smectite, and calcite  
(kaolinite (k); smectite (s), and calcite (kls)).

Photo 10- SEM image of semi-booklet kaolinittes.

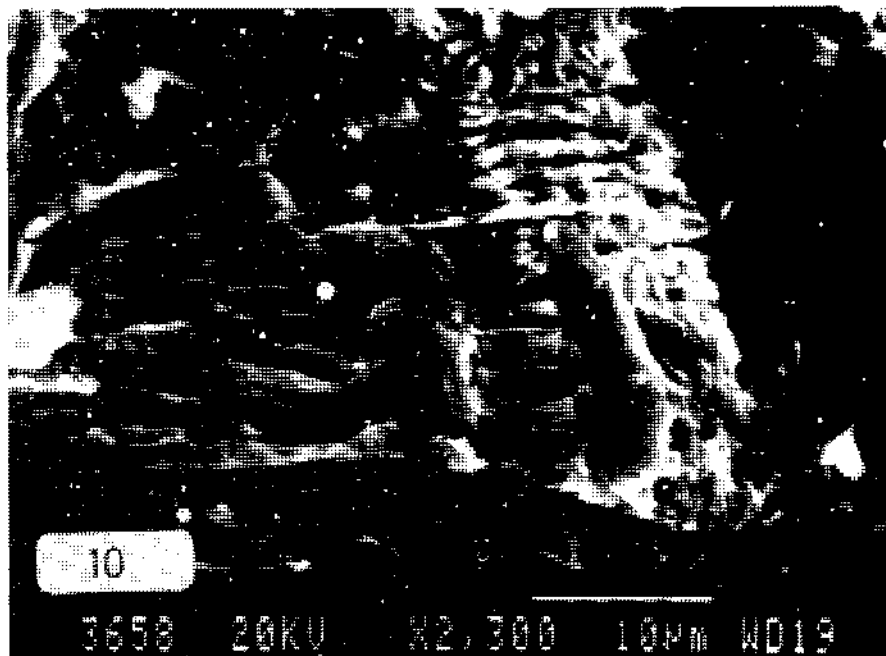
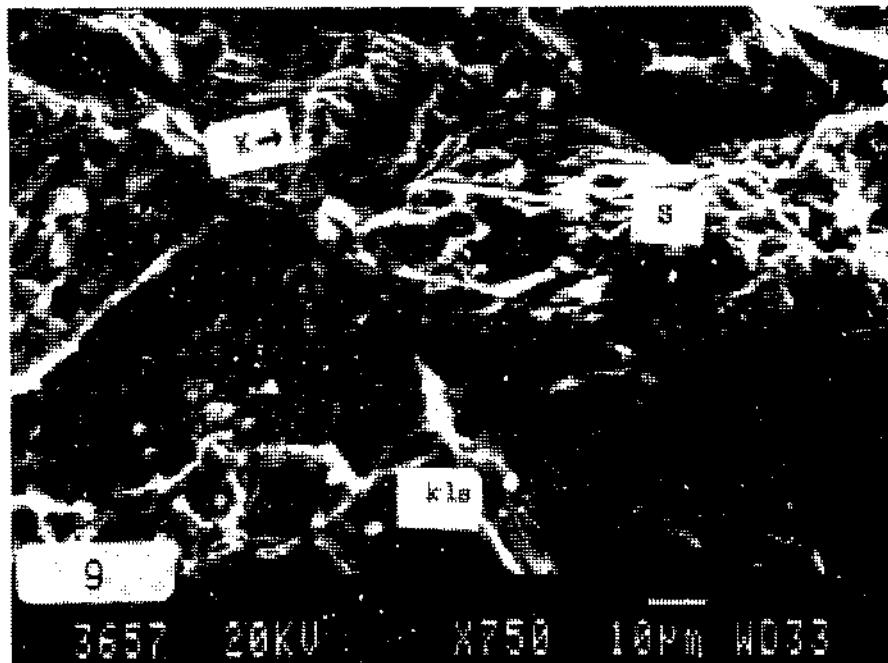
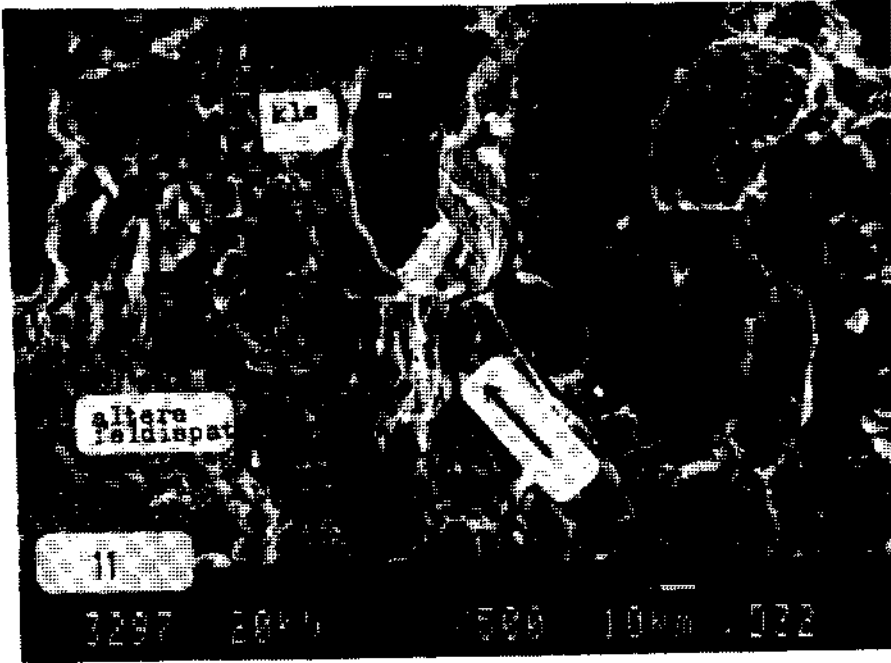


**PLATE -VI**

Photo 11- SEM image of porosity developments in calcite and altered feldspars within the fractured zone.

Photo 12- SEM image of fracture filling iron oxide (dmr) and chlorites.



## NEW PETROGRAPHICAL DATA AT THE EASTERN PART OF ALANYA METAMORPHITES (ANAMUR, S.TURKEY)

Veysel IŞIK\* and Okan TEKELİ\*

**ABSTRACT** - Investigated area is situated at the eastern part of Alanya metamorphites. Common rock types consist of metapelites, metabasites, marbles and quartzites. Field observations and petrographical investigations indicate that metamorphism and deformation histories of Alanya metamorphites in the studied area reveal considerably different features from the western part. Mineral compositions show that these rocks are affected from a Barrovian type metamorphism. The existence of staurolite and kyanite minerals especially in metapelitic rocks suggests that the metamorphism conditions in Alanya metamorphites have been reached to high grade amphibolite facies.

### INTRODUCTION

Investigated area is located at approximately 10 km northwest of Anamur and is geologically at the eastern part of Alanya metamorphites which crop out between Alanya and Anamur in western part of the middle Taurus (Fig. 1a). First detailed geological studies in Alanya metamorphites are carried out by Blumenthal (1942; 1951); Later on, structural characters and stratigraphic relationships at the western part of middle Taurus is essentially documented by Peyronnet (1967; 1971), Brunn et al., (1973), Özgül (1976), Monod (1977) and Demirtaşlı (1983; 1986; 1988) (Fig. 1b). Structure, stratigraphy and metamorphism of western part of Alanya metamorphites are investigated by Özgül (1983; 1984), Okay and Özgül (1984) and Okay (1989).

In these studies, it is suggested that a nappe structures including three slices and two type of metamorphism, developed in the late Upper Cretaceous at the western part of Alanya metamorphites. First metamorphism type developed under HP/LT conditions have been determined in one of the nappe and the second type greenschist facies metamorphism in all three nappe slices. It is also suggested that greenschist facies metamorphism conditions in the central part of Alanya metamorphites are similar to the western part of Alanya (Ulu, 1989).

The metamorphites in eastern part of Alanya metamorphites are divided into two parts as Tatlısu çayı metasediments and Azı Tepe marble by

İşgüden (1971). Tatlısu çayı metasediments are composed of feldspar, mica and quartz bearing-schist series at the basement and continuing upward by sandy schists, phillite, metasediments and recrystallized limestone which are unconformably covered by Azı Tepe marble. Baydar et al., (1981) have reported fossil findings of Permian age in crystalline limestones at the upper part of this metamorphites and thus, lower part of metamorphites should be older than Permian.

The main objective of this study is the determination of rock types and general metamorphic features of metamorphites at the eastern part of Alanya metamorphites. For this reason, it is especially investigated if the nappe structure and metamorphism characteristics described at the western part, also dominate at the eastern part.

### GEOLOGY

Metamorphites in the investigated area comprise the basement of this section. The dominant rock type of metamorphites is metapelites secondly followed by marbles. Metabasites and quartzites are interbedded with these units (Fig. 2).

Metapelitic rocks, forming slight topography, extensively crop out around Çaltıbükü, Sanağaç, Ormançık and Güney districts at northern and northeastern part of investigated area. Macroscopically and mesoscopically, they show green, yellowish green and yellowish gray colors, and their phillitic and schistose texture are dominant. Phillitic rocks especially crop out Güney district. Foliation



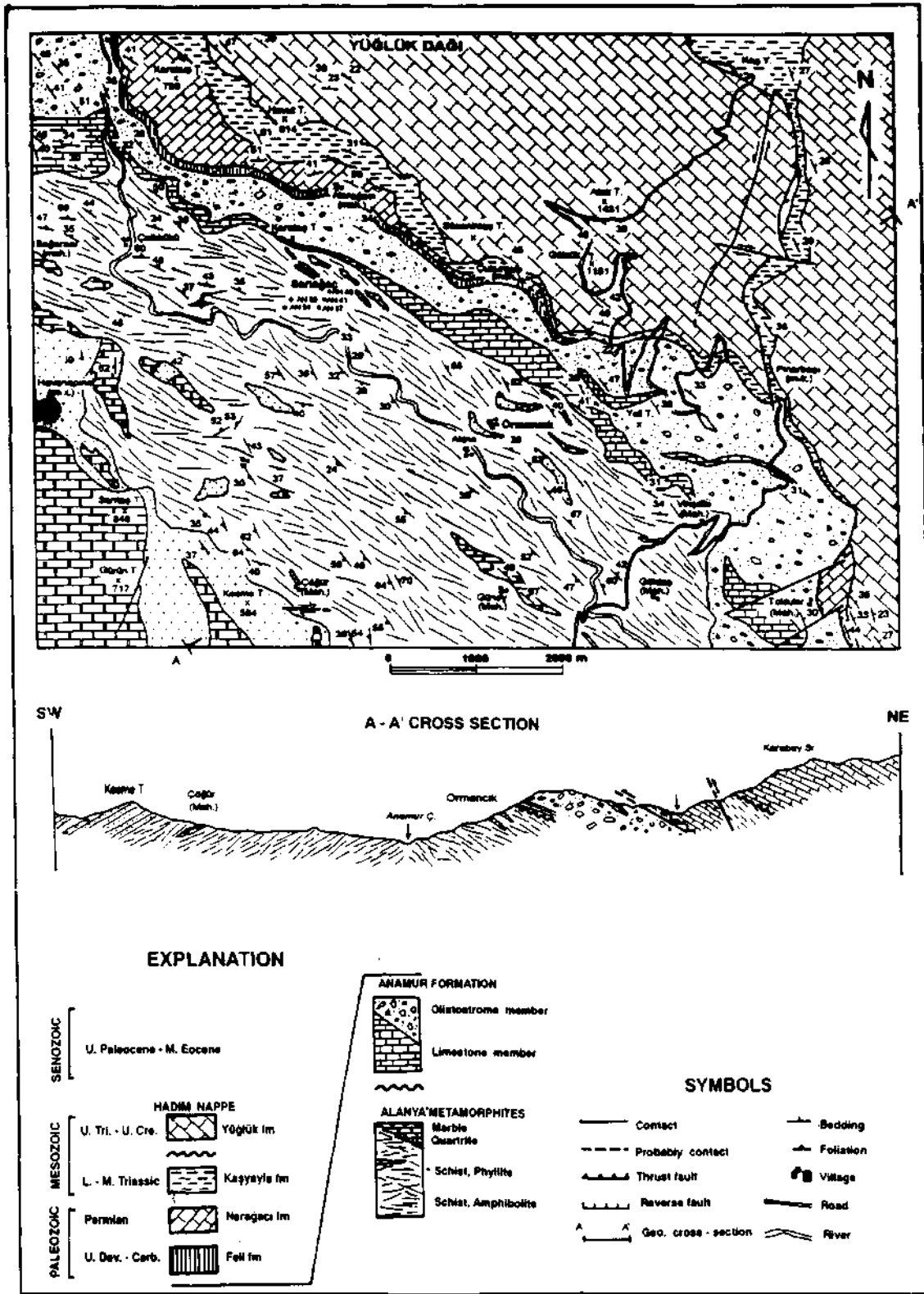


Fig. 2- Geological map of the study area (Işık, 1992).

can be observed at rocks with schistose texture. Coarse-grained muscovite is typically developed along the foliation planes. Brown, medium grained garnet crystals can easily be recognised at the schists around Sariağaç and Ormancık.

Fine to coarse, elongated structures are developed by quartz rich parts of metapelitic rocks. Folds and faults which reach up from cm to m sizes can clearly be observed at intensively deformed sections. Metabasites are commonly located in metapelitic rocks as intercalations. They are in colours of green, dark-green, greenish black. Greenschist up to 40 cm thicknesses are intercalated in phyllitic metabasites of Güney district. On the other hand, amphibolite type metabasites are especially common as interbeds in micaschists around Sariağaç.

Marble and quartzites cropping out in the western and southwestern parts of investigated area, forming the upper section of metamorphites, exhibit lateral and vertical relationships (Fig. 2). This unit is observed as lenses together with schists around Ormancık. The colour of marbles is white and of quartzites gray, white, purple and cream. Both marble and quartzite show medium to thick bed thicknesses. These medium to coarse grained rocks reveal weak foliation.

#### PETROGRAPHIC FEATURES OF ALANYA METAMORPHITES

##### Metapelitic rocks

The rocks consisting phyllite and schist texture by petrographic studies are determined as chlorite-sericite-albite phyllite, chlorite-muscovite-albite schist, chlorite-mica schist, and staurolite-kyanite-garnet-mica schist. Staurolite and kyanite-bearing schists are not widespread and crop out in a limited area (Fig. 2).

Lepidoblastic texture is common in the rocks with phyllitic textures; however, porphyroblastic texture formed by plagioclases are frequently observed. The main mineral components of these rocks are biotite, chlorite, muscovite, quartz and plagioclase. Opaque minerals, tourmaline with idioblastic, prismatic habits and small amounts of apatite are found as accessory components.

General texture of pelitic rocks which are characterized by schistosity is lepidoblastic. Small amounts of porphyroblastic texture are also recognized. The porphyroblasts are usually formed by plagioclase, and less amount of garnet. Staurolite, kyanite, garnet, biotite, muscovite, quartz, and plagioclase are the dominant minerals of pelitic rocks. Opaque minerals and tourmaline exist in these rocks as accessory minerals.

*Plagioclase.* - It constitutes the 15-40 volume % of the metapelitic rocks. Plagioclases appear as xenoblast porphyroblasts and elongated grains to foliation direction. Crystals showing polysynthetic twinning is rare. Abundant quartz and opaque mineral inclusions are located in the crystals. In some samples, plagioclases surround the garnets. This is also important for the mineral growth. The relationships between internal foliation, forming inclusion trails in plagioclase porphyroblasts, and external foliation imply syntectonic growth (Spry, 1976).

*Quartz.* - Quartz, consisting of 10-35 volume % of rock, is xenoblastic. Elongated grains are parallel to foliation. It shows clear undulatory extinction and cataclastic deformation textures.

*Muscovite-Biotite.* - These minerals in metapelitic rocks generally extend parallel to foliation planes and vary between 20 and 50 volume % of the rock. Muscovites with hypidioblast and tabular crystal forms constitute two characteristic foliation planes called  $S_1$  and  $S_2$  indicating that rock is at least subjected to two different deformation events. However, biotites which have idioblastic and tabular forms and distinctly pleochroic with light brown to dark brown colours are less than muscovite in amount. Biotites in metapelitic rocks usually are fine grained and extend parallel to  $S_2$  foliation planes.

*Garnet.* - It forms 5-25 volume % of the rocks and is usually idioblastic or hypidioblastic and is made of from medium to coarse sized porphyroblasts. Quartz, chlorite and biotite are found in garnets as inclusions.

*Kyanite.* - Kyanite is hypidioblast and bent prismatic and bladed parallel to  $S_2$  foliation plane. It consists of 5-10 volume % of the rock together with Staurolite.

*Staurolite*— It can be easily recognized by pale honey yellow colours. It is found in the rock less than other minerals and forms fine crystals (Fig. 3). Staurolite is usually hypidioblast and prismatic, and extends as elongated grains parallel to  $S_2$  foliation.

#### Metabastte rocks

Metabasites predominantly consist of chlorite-albite-actinolite schist, garnet-hornblende schist and garnet amphibolite due to the microscopic investigations. General texture of chlorite-actinolite schist is nematoblastic. The main mineral components of these rocks are chlorite, plagioclase and actinolite while titanite, opaque minerals and epidote are other associated minerals. Garnet-hornblende schist and garnet amphibolite represent the metabasites of higher metamorphism conditions. These rocks exhibit nematoblastic-granoblastic textures. Biotite, quartz, garnet, plagioclase and hornblende constitute the main mineral composition and opaque minerals and epidote also exist (Fig. 4).

*Hornblende*- This mineral with prismatic to tabular forms shows pleochroism colours varying from yellowish green to green. Their abundance varies between 35-60 volume % Hornblendes in foliated metabasites reveal parallelism to the foliation.

*Actinolite*— Actinolite, consisting of 30-45 volume % of the rock, has prismatic forms. Pale green pleochroism colours and lower extinction angles distinguish actinolite from hornblende.

*Plagioclase*- Plagioclases with intensive sericitization in metabasite make up of 10-35 volume % of the rocks.

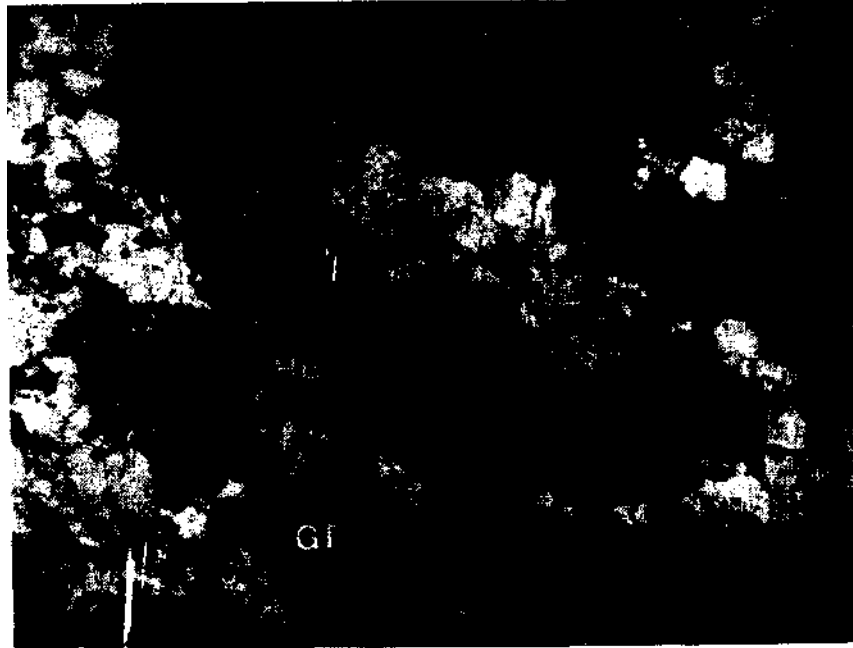
*Garnet*— Garnets exhibit generally rounded elliptic or angular grain forms and their abundance varies between 5-10 volume%. Atoll texture is typical. Chloritization in the cracks or at the borders of garnet is common.

#### Marble

Unique mineralogical composition is dominant, created by calcite crystals, in weakly oriented



Fig. 3- Staurolite kyanite garnet mica schist. KY= kyanite; GT= garnet; ST= staurolite. Magnification: 63, Parallel nicol.



**4- Garnet amphibolite. GT= garnet; HBL= hornblende; PL= plagioclase. Magnification: 63, Parallel nicol.**

marbles. General texture is granoblastic. Polysynthetic twinning in calcite minerals is also very common. Small amounts of quartz and opaque minerals occur in marbles.

#### Quartzite

General texture of quartzites is granoblastic. Its main mineral component is quartz. Quartzes usually show undulatory extinction. Coarse-grained plagioclase minerals are also observed with quartz inclusions. In some thin section, sericitization are developed in and around the plagioclases while sometimes they become as muscovite occurrences.

#### METAMORPHISM

Mineral components of common metapelitic rocks in the studied area represent different metamorphic degree conditions. In particular, while mineral composition of rock with phyllite texture and a part of schists typically represent greenschist facies, index minerals found in schists point out existence of amphibolite facies.

Mineral components of pelitic rocks underwent greenschist facies metamorphism show that metamorphism is reached to garnet zone in Barrovian type metamorphism and is developed under 3-6 kbar pressure and 350-500°C temperature conditions (Winkler, 1979; Yardley, 1989; Barker, 1990). Staurolite and kyanite occurrences, representing amphibolite facies, indicate that the metamorphism in this region has reached to kyanite zone. This shows that metamorphism conditions in this part had been developed at temperatures of 540-600°C, at pressure of 5-8 kbar temperature (Winkler, 1979; Yardley, 1989; Barker, 1990) (Fig. 5).

Metabasic rocks in greenschist facies of the studied area are represented by presence of actinolite. Garnet and green hornblende mineral assemblages appear in the regions with the absence of actinolite. These mineral assemblages show that the metamorphism is developed under amphibolite facies conditions (Barker, 1990).

Field and petrographical studies in studied area, suggest the conclusion that Alanya metamorphites has been affected by Barrovian type pro-

gressive metamorphism. Staurolite and kyanite minerals documented in this study reveal that metamorphism in eastern part of Alanya metamorphites has reached the amphibolite facies conditions.

#### CONCLUSION and DISCUSSION

According to the studies Okay and Özgül (1984) and Okay (1989), three metamorphic nappe slices can be separated. These nappes with different sequences are named from bottom to top as Mahmutlar nappe, Sugözü nappe and Yumrudağ nappe. Mahmutlar nappe consists of mica schists, with quartzite and marbles intercalations and the deposition age of this nappe is Permian. Sugözü nappe, overlying Mahmutlar nappe, contains garnet

mica schist and eclogite and blueschists inherited from basic rocks (Okay, 1989). On the other hand, recrystallized limestones are the common rock with calcschist and chlorite schist intercalations in the Yumrudağ nappe.

According to the studies of Okay (1989), a metamorphism with two different phases has been developed in the western part of Alanya metamorphites. First phase is characterized by blueschist and eclogite facies HP/LT metamorphism in only one nappe, namely Sugözü nappe, during Upper Cretaceous. Greenschist facies Barrovian type metamorphism is affected all three nappe slices in the second phase.

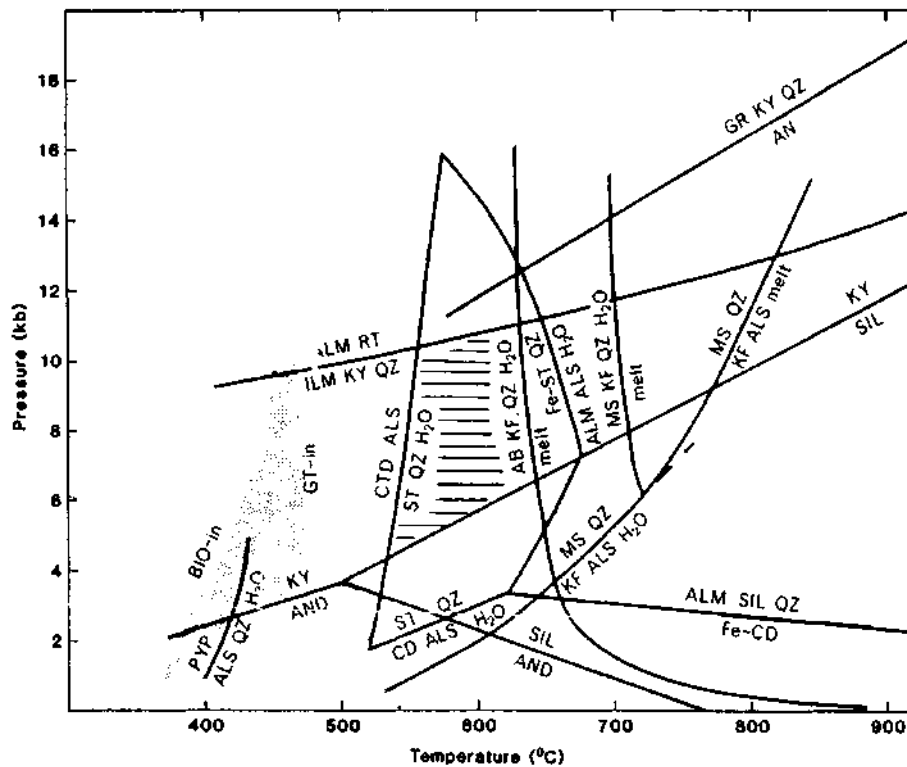


Fig. 5- Petrogenetic grid for pelitic metasediments with  $P = \text{H}_2\text{O}$  (Simplified from Yardley, 1989). Abbreviations: AB= albite; ALM= almandine; ALS= Al-silicate; AN= anorthite; AND= andalusite; BIO= biotite; CD= cordierite; CDT= chloritoid; GT= garnet; ILM= ilmenite; KF= K-feldspar; KY= kyanite; MS= muscovite; PYP= pyrophyllite; QZ= Quartz; RT= rutile; SIL= sillimanite; ST=staurolite. Stippled bands are approximate conditions of the biotite and garnet isograds. The hatched region represents the stability field of bearing-staurolite and kyanite metapelites.

At the eastern part of Alanya metamorphites, however, single phased Barrovian type regional metamorphism is defined by greenschist to amphibolite facies and probably by a progressive metamorphism. In addition, there has been found no implications to a structure consisting nappes in this parts of Alanya metamorphites. Thus, both parts of Alanya metamorphites has different metamorphic and structural character. For this reason, at this stage it is not possible to make any comparison for the metamorphism and deformation histories between both regions. Additionally, another difficulty is raised from the large central region between two metamorphites because of lack of enough information.

However, Barrovian type metamorphism thought developed in different grades and characters in both regions at Upper Cretaceous time makes a possible comparison. With some critical approach, it can be evaluated that the metamorphism at the eastern part is comparable with the second phase of metamorphism developed under greenschist metamorphism conditions at the western part. So, it can be concluded that the metamorphism at the eastern part represents the one of more advanced parts of second phase metamorphism of the western part of Alanya metamorphites.

#### ACKNOWLEDGEMENT

This study supported financially by Research Fond of Ankara University (Project number: 90250021) consists of a part of a Master Theses. Authors thank to the General Directorate of the Mineral Research and Exploration (MTA) and Regional Branch Office of Adana MTA for their field supports. Our thanks are also for the constructive criticism of Dr. Sönmez Sayılı from Ankara University and Prof. Dr. Cemal Göncüoğlu from METU.

*Manuscript received, December 26, 1994*

#### REFERENCES

- Barker, A.J., 1990, Introduction to metamorphic textures and microstructures: Blackie, New York, 162.
- Baydar, O.; Erdoğan, B.; Kengil, R.; Kaynar, A. and Selim, M., 1981, Uçarı-Teniste-Kaşayayla-Sazak-Bozyazı ve Anamur Arasındaki Bölgenin Jeolojisi: MTA Rep., 82, Ankara, Turkey.
- Blumenthal, M.M., 1942, Cenubi Anadolu Toroslarının Sahil Sıradağlarında Silifke-Anamur arasındaki Jeolojik İncelemeler: MTA Rep., 2833 (unpublished), Ankara-Turkey.
- , 1951, Batı Toroslarda Alanya Ard Ülkesinde Jeolojik İncelemeler: MTA Bull., 5, 134.
- Brunn, J.H.; Argynadı, I.; Marcoux, J.; Monod, O.; Poisson, A. and Ricou, L., 1973, Antalya'nın Ofiyolit Naplarının Orijini Lehide ve Aleyhindeki Kanıtlar: Cumhuriyetin 50. Yılı Yerbilimleri Kongresi, 58-69, Ankara, Turkey.
- Demirtaşlı, E., 1983, Stratigraphy and tectonics of the area between Silifke and Anamur, Central Taurus Mountains: Tekeli, O. and Göncüoğlu, M.C., ed., International Symposium on the Geology of the Taurus Belt, 101-118, Ankara-Turkey.
- , 1986, Ermenek Batısında Göktepe, Dumlugöze ve Tepebaşı Arasında Kalan Bölgenin Jeolojisi: MTA Rep., 8753 (unpublished), Ankara-Turkey.
- , 1988, Orta Toroslar'da Seydişehir ve Silifke Otoktonlarının Antalya, Alanya ve Hadim Naplarıyla Olan İlişkilerinin Stratigrafik ve Tektonik Açısından İncelenmesi: TPAO Rep. 2457, Ankara-Turkey.
- Işık, V., 1992, Alanya metamorfiterinin doğu kesiminin yapısı, stratigrafisi ve petrografisi (Anamur): Ms. S. Thesis, The Graduate School of Natural and Applied Sciences of Ankara, University, 81 (unpublished), Ankara-Turkey.
- İşgüden, Ö., 1971, Anamur Bölgesinin Jeolojik Etüdü: I.U. Fen Fakültesi Yayl., 103, İstanbul-Turkey.
- Monod, O., 1977, Recherches geologique dans le Taurus Occidental au sud de Beyşehir (Turquie): These Univ. Paris-Sud Orsay, 442.
- Okay, A., 1989, An exotic eclogite/blueschist slice in a Barrovian-style metamorphic terrain, Alanya Nappes, Southern Turkey: J. Petrology, Vol. 30, Part 1, 107-132.
- Okay, A. and Özgül, N., 1984, HP/LT metamorphism and the structure of the Alanya Massif, Southern Turkey: an allochthonous composite tectonic sheet: Robertson, A.H.F. and Dixon, T.E., ed., The Geological Evolution of the Eastern Mediterranean, Geol. Soc. Lond. Spec. Publ., 14, 429-439.

- Özgül, N., 1976, Toroslar'ın bazı temel jeoloji özellikleri: TJK Bull., 19, 65-78.
- , 1983, Stratigraphy and tectonic evolution of the Central Taurides: Tekeli, O. and Göncüoğlu, M.C., ed., International Symposium on the Geology of the Taurus Belt, 77-90, Ankara-Turkey.
- , 1984, Alanya tektonik penceresi ve batı kesiminin jeolojisi: Ketin Simpozyumu, 97-120, TJK Publication.
- Peyronnet, P., 1967, Alanya bölgesinin petrografi ve mineralojisi ile Alanya masifindeki boksitlere bitişik kloritoidli şistlerin kökeni: MTA Bull., 68, 154-173, Ankara-Turkey.
- Peyronnet, P., 1971, Alanya bölgesinin (Güney Toroslar) jeolojisi, metamorfik boksitin kökeni: MTA Bull., 76, 98-123.
- Spry, A., 1976, Metamorphic Textures: Pergamon Press, 350, New York.
- Ulu, Ü., 1989, Gazipaşa (Antalya İli) Bölgesinin Jeolojisi: Ph. D. Thesis, I.Ü. Fen Bilimleri Enst., 209, İstanbul-Turkey.
- Winkler, H.G.F., 1979, Petrogenesis of metamorphic Rocks: Springer-Verlag, 120, New York.
- Yardley, B.W.D., 1989, An introduction to metamorphic petrology: Longman Scientific and Technical, 248, New York.

## PETROGRAPHY AND ORIGIN OF DOLOMITES OF YANIKTEPE FORMATION (UPPER CRETACEOUS) IN GÜRÜN AUTOCHTHONOUS, EASTERN TAURUS TURKEY

Eşref ATABEY\*

**ABSTRACT.-** The purpose of this study was to reveal the petrography and origin of the Upper Cretaceous dolomites in the Gürün autochthonous in eastern Taurus. The Upper Cretaceous (Upper Santonian-Campanian) dolomites in the Gürün autochthonous belong to the Yanıktepe formation and are restricted to outcrops near Salyurt Yaylası, southern slope of Kavunağılı Tepe and Toycu Tepe. The Yanıktepe formation is represented by the interfingering limestone and dolomite facies, which can be identified in the field. The limestones are massive and exhibit texture of wackestone that contains foraminifera-macro shells (rudist). The dolomites formed as a result of dolomitization of foraminifera-macro shell-bearing wackestones. Three types of texture can be petrographically identified in these dolomites: Type 1: Clear dolomite crystals, Type 2: Filthy (blurry) dolomite crystals, Type 3: Zoned dolomite crystals. Of these, Type 1 is euhedral and subhedral, and very fine-to fine-grained; Type 2 anhedral and subhedral, and fine-to medium-grained; Type 3 subhedral and euhedral, and fine-to medium-grained. These data support that the Upper Cretaceous dolomites in the study area could have been formed at two different stages, early and late diagenetic. The early diagenetic dolomites (Type 1 and Type 2) are likely to form as a result of structural changes that occurred concurrently with sedimentation in the basin during the Upper Cretaceous. The sea water fresh water mixing zones over uplifted submarine masses (rudist-bearing limestones) are probably the most favoured environments for dolomitization. The late diagenetic ones (Type 3 texture) are wholly tectonically controlled and correspond to the dolomites which are controlled by fractures associated with nappe tectonics in the region.

### INTRODUCTION

The occurrence of dolomite is rather complicated and problematic matter. Different models have been established for dolomitization, and many theories have been put forward on this subject. These were separately evaluated and discussed by Hardie (1986).

Dolomitization may occur at two stages, early and late diagenetic stages. The early diagenetic dolomites form concurrently with deposition or immediately after this process and reflect the conditions of environment in which they occur. Evaporitic dolomites (Deffeyes et al., 1964; Illing et al., 1965; Behrens and Land, 1972; Patterson and Kinsman, 1982), mixing water dolomites (Hanshaw et al., 1971) and marine dolomites (Land, 1985) are examples for this type. Evaporitic dolomites occur widespread in supra-tidal environments (sabkha) characterized by excessive evaporation under continental climatic conditions. They can be found in a mineral association of gypsum-anhydrite dolomite or can form as cavity dolomites by leaching of evaporites (Illing et al., 1965). Mixing water dolomites

(sea water-fresh water) have been formerly proposed as a theoretical model (Dorag type dolomitization: Badiozamani, 1973) and afterwards modern and fossil examples of this type have been identified. This type is mostly used to explain the dolomitization of platform-type limestones that are not accompanied by evaporites. In addition to these, some workers put forward that high Mg rate required for the formation of thick and massive platform dolomites is directly supplied from sea water and established a dolomitization model by sea water (Varol and Magaritz, 1992).

Dolomitization by Mg-rich waters percolating through stylolites and micro fractures which were developed at epigenetic stage or during burial dolomitization (Zenger, 1983). Mg-bearing solutions removed from shales during burial process (Mc Harque and Price, 1982) and Mg-rich solutions of hydrothermal origin (Matsumoto et al., 1988; Radke and Mathis, 1980) can cause dolomitization in adjacent limestones. Among all these dolomitization mechanisms, the dolomites of Upper Devonian, Upper Permian, Upper Triassic and Middle Jurassic-Cenomanian age defined by Atabey (1993) in

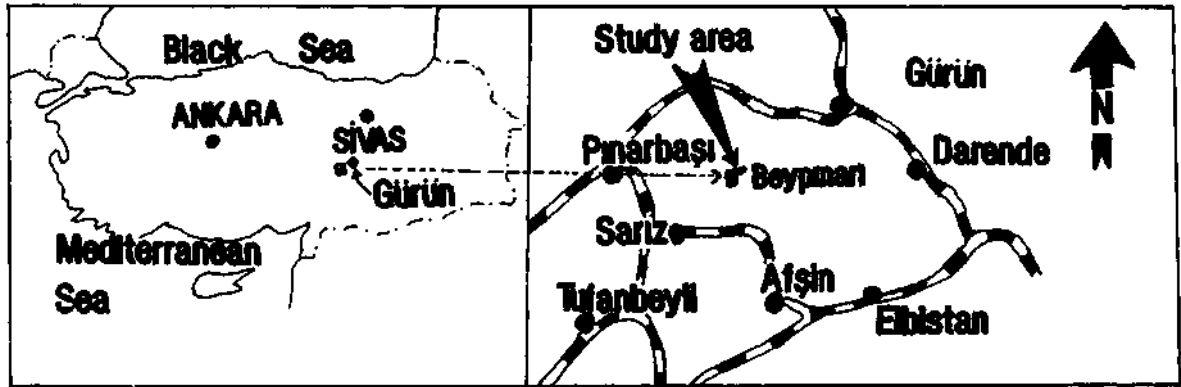
the study area as well as the Upper Cretaceous (Upper Santonian-Campanian) dolomites whose petrographic features will be described in detail are of the same type and included in the dolomite group without evaporites. The Upper Cretaceous dolomites that were aimed in this study exhibit textural features which reflect the effects of mixing water during the early diagenetic stage and effects of Mg-bearing waters percolating through the fracture systems and burial effects during the late diagenetic stage.

The geology, petrography and geochemistry of dolomite were evaluated together in order to elucidate the above mentioned mechanisms that resulted in the formation of dolomites. The geochemical studies based on stable isotopes ( $O^{18}$ ,  $C^{13}$ ) are underway. In this study, the emphasis will be placed on the geology and petrography of the Upper Cretaceous dolomites that crop out to the 30 km W of Gürün (SW Sivas) (Fig. 1). For this purpose, a detailed study was carried out near Salyurt Yaylası, southern slope of Kavunağılı Tepe and

Using field and laboratory data, a mechanism for dolomitization was proposed and a model was established.

#### YANIKTEPE FORMATION

The study area which is situated in the Gürün autochthonous, Eastern Taurus is characterized by a thick sedimentary sequence ranging in age from Paleozoic to Tertiary. The dolomites belong to a unit called the Yanıktepe formation in this sequence. The Yanıktepe formation crops out over an extensive area that covers K37-c<sub>1</sub>, c<sub>2</sub>, c<sub>3</sub> and c<sub>4</sub> sheets. It is typically exposed near Salyurt Yaylası and southern slope of Kavunağılı Tepe in the west of Beypinarı village (K37-c<sub>1</sub> sheet), near Toycu Tepe, between Camiliyurt and Yolgeçen villages, near Bölücek Tepe (K37-c<sub>2</sub> and c<sub>3</sub> sheets), and to the northwest of Arpaçukuru village (K37-c<sub>4</sub> sheet). The dolomite formations are restricted to small outcrops of this unit in K37-c<sub>1</sub> and c<sub>2</sub> sheets. As seen from figure 2A, the Yanıktepe formation is bounded by the Soğanlı allochthonous rock units in



Toycu Tepe (K37-c<sub>1</sub> and c<sub>2</sub> sheets) where the dolomites are best exposed (Fig. 2A). The petrological microscopic and scanning electron microscopic (SEM) studies were made on thin section specimens. Additionally, a dyeing technique which employs a mixture of alizarine Red-S and potassium ferrocyanide was utilized for calcite and dolomite tests on thin sections (Dickson, 1965).

the north (Tekeli et al., 1983). Here, the outcrops were intensely affected by the Upper Cretaceous and post-Lutetian tectonisms.

The Yanıktepe formation consists of limestone and dolomite. At Bölücek Tepe (K37-c<sub>2</sub> sheet), it unconformably overlies the Yüceyurt formation of Middle Jurassic-Cenomanian age, which consists of limestone and dolomitic limestone. From

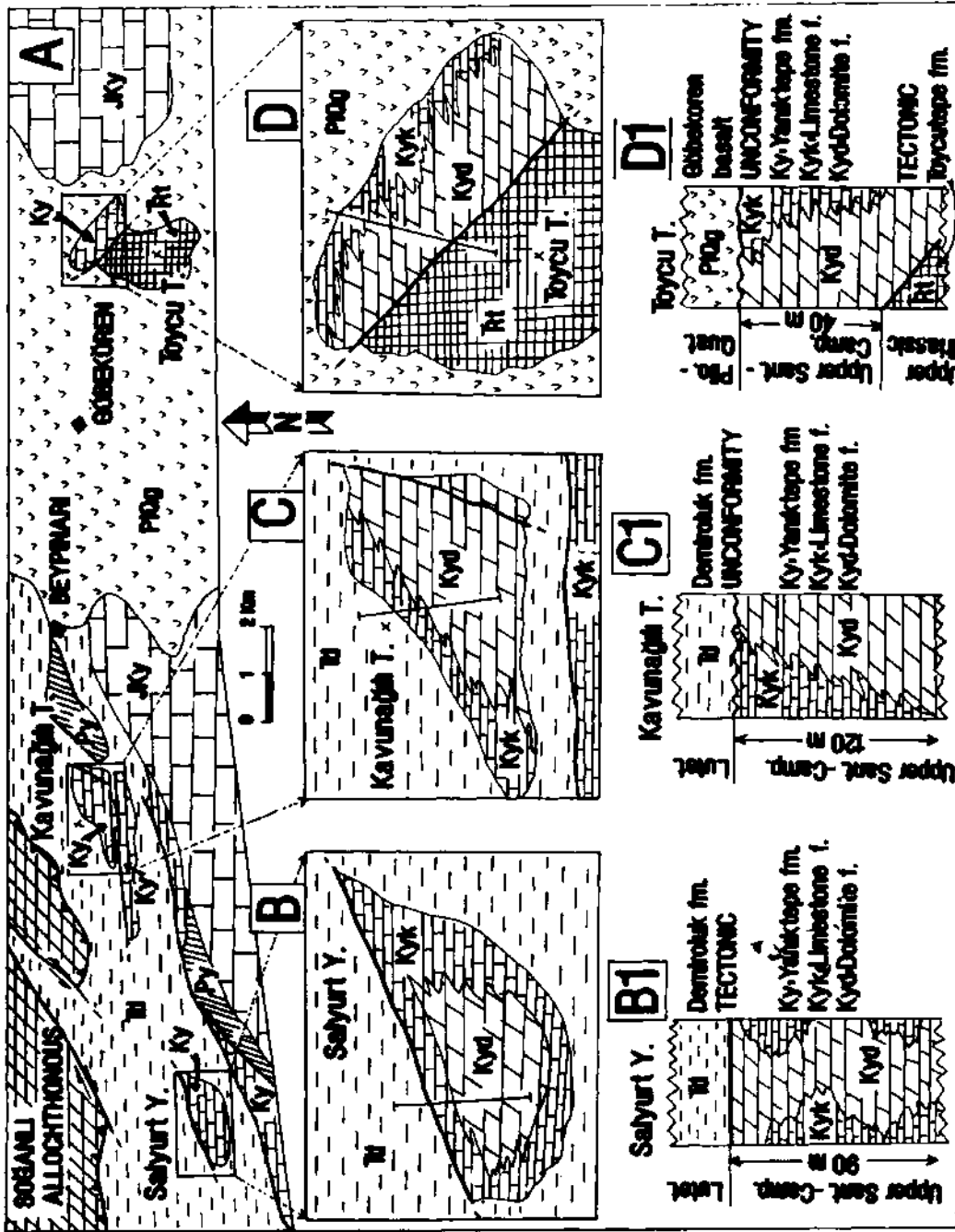


Fig. 2. A: Field view of Upper Cretaceous dolomites and their relationship with other units. Py-Yığıltepe fm. (Upper Permian); Tr-Toy-cutepe fm. (Upper Triassic); JKy-Yuçeyurt fm. (Dogger-Cenomanian); Ky- Yaniktepe fm. (Upper Santonian-Campanian); Td-Demirobruk fm. (Lutetian); PİÖg-Göbekören basalt (Pliocene-Quaternary); B, C and D-Yaniktepe fm. facies; Kyk- Limestone fa-cies; Kyd-Dolanite facies; B1, C1 and D1-Columnar sections.

the base upward, it consists of conglomerate breccia, massive and thickly bedded rudist-bearing limestone, and semi-pelagic and pelagic sequences (Atabey, 1993). It is overlain by the pelagic rocks that constitute the Upper Campanian-

Maestrichtian Akdere formation. Near Beypinari vil-lage (Fig 2A), the appearance is different from the southern part. Here, the Yaniktepe formation is represented by only horizons of rudist-bearing lime-stone, and dolomite. It is surrounded by the Tertiary



Fig. 3- Field view of dolomites yellowish, pinkish and light gray colored, form highrelief topography, overlying by Tertiary unit (Demiroluk fm.: Td). Kyk-Limestone fades, Kyd-Dolomite facies, 3 km west of Beypinarı village, south slope of Kavunağlı Tepe.

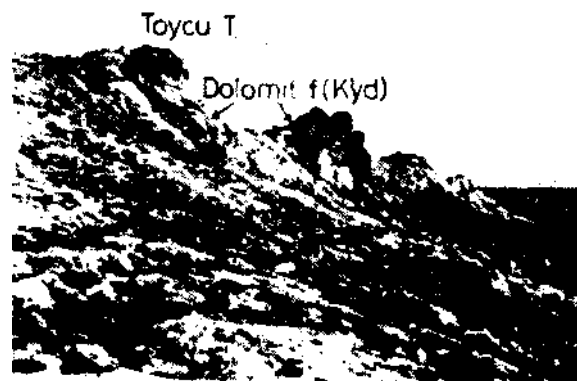


Fig. 4- Field view of pinkish, light colored dolomite forming high-relief topography with respect to limestones. Faulted contact with Upper Triassic unit (TRt) and (Toycutepe fm.). Kyd-Dolomite, 1 km east of Göbekören village, Toycu Tepe.

unit (Demiroluk fm.) and in part covered by this unit near Salyurt Yaylası and southern slope of Kavunağlı Tepe (Fig. 3). At Toycu Tepe, its contact with the underlying Upper Triassic rock unit (Toycutepe fm.) is a fault, and it is in part covered by the Göbekören basalt (Fig. 2A and 4).

The fossils identified from the limestones and pelagic rocks of the Yaniktepe formation are *Aeolisaccus kotori Radocic*, *Rotalia aff. skourensis Pfender*, *Siderolites vidali Schlumberger*, *Globotruncana stuartiformis Dalbiens*, *Globotruncana bulloides Vogler* and *Hippurites* sp. all of which represent a time span of Upper Santonian-Campanian.

According to the sections shown in figures 2B1, C1 and D1, the total thickness of levels of limestone and dolomite was estimated to be approximately 90 m, near Salyurt Yayla, 120 m at southern slope of Kavunağlı Tepe, and 40 m near Toycu Tepe, respectively. The thicknesses are not certain due to a variety of faults which the dolomites are found, limestone and dolomite facies (Fig. 2B, C and D).

#### Limestone facies

It is light gray and pinkish gray in a appearance. It is massive and thickly bedded. Its thickness is variable, 60 m near Salyurt Yayla, 70 m at

southern slope of Kavunağlı Tepe and 30 m at Toycu Tepe (Fig. 2A). The limestones interfinger with the dolomites laterally. This interfingering is locally interrupted by faults.

It exhibits a texture of foraminiferous wackestone-packstone, macro shell-bearing (rudist-bearing) mudstone-wackestone under the microscope. In this mudstone texture, rudist shells that are locally rounded and floating are observed. The mudstone-wackestone texture laterally grades into foraminifera-pellet and macro shell-bearing wackestone-packstone mud-supported texture reflects back-reef shelf lagoon in which relatively low energy conditions prevail (Flügel, 1982), while packstone texture characterizes reef environments in which medium-high energy conditions prevail.

#### Dolomitefacies.

It differs markedly from the limestone facies in that its color is whitish, pinkish, and yellowish white and it forms high reliefs (Fig. 3 and 4). It is massive and fractured and displays a sugary texture. It is locally brecciated dissolution hallows and cavities developed on rock surfaces. Its thickness was measured to be 30 m near Salyurt Yayla, 50 m at southern slope of Kavunağlı Tepe and 10 m at Toycu Tepe (Fig. 2 B1, C1 and D1). The most important feature of dolomites is that they laterally in-



Fig. 5- Close-up view of yellowish, pinkish gray colored dolomite rock. Dolomitized rudist and cast fragments observed within it (arrow), 3 km west of Beypinari village, south slope of Kavunağılı Tepe.

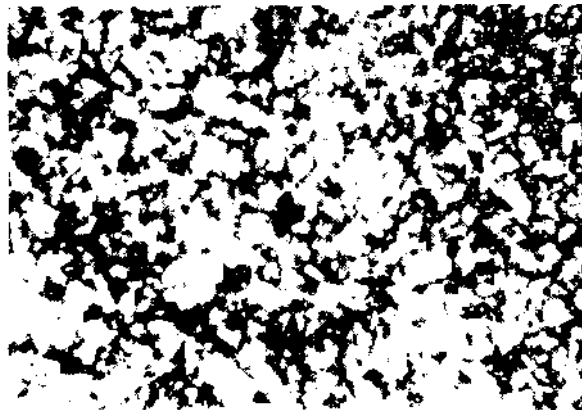


Fig. 6- Euhedral and regular sided fresh dolomite crystals (Type 1). Lime mud in the rock causes cloudy structure. Intercrystal areas filled with calcite (black areas). X63

terfinger with limestones. Some relics of undolomitized limestone are locally observed within dolomites and at boundaries with limestones. The dolomites were formed as a result of partial dolomitization of foraminifera-macro shell-bearing (rudist-bearing) mudstone-wackestone-packstone, as evidenced by dolomitized complete rudist shells in dolomite (Fig. 5).

PETROGRAPHY

The Upper Cretaceous dolomites in the study area petrographically differ from the dolomites of Upper Devonian, Upper Permian, Upper Triassic and Dogger age. Three types of dolomite crystal were identified on the basis of textural changes, internal structure and crystal shape. Type 1, clear dolomite crystals, Type 2, filthy (blurry) dolomite crystals, Type 3, zoned dolomite crystals.

Clear dolomite crystals (Type 1)

These are mostly light colored and represented by a dolosparitic mosaic. Dolomite crystals are euhedral and subhedral, very fine-to fine-grained (0.10-0.15 mm). The crystal boundaries are well-developed. They have a character similar to limpid dolomite crystal type defined by Folk and Land (1975). Interlocking is poorly-developed in crystals. This resulted in high porosity. Intergranu-

lar spaces are filled with calcite matrix (black areas in Fig. 6). This type of dolomites are best seen near Salyurt Yayla and at southern slope of Kavunağılı Tepe.

Filthy (blurry) dolomite crystals (Type 2)

These are dark gray, subhedral and anhedral (Fig. 7). They are fine-to medium-grained (C.15-0.34 mm). Although they are usually disseminated,

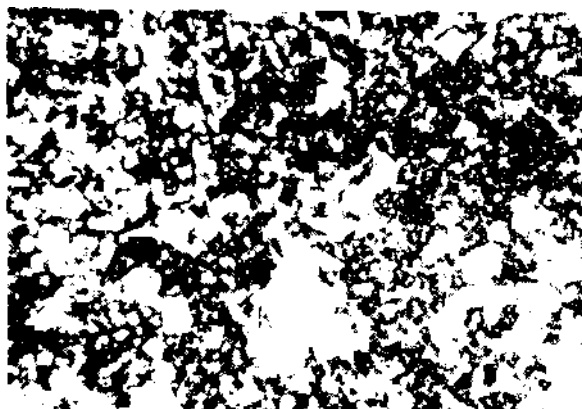


Fig. 7- Dirty (cloudy) appearance dolomite crystals (Type 2). Some crystals are euhedral (D), some are anhedral and dirty. This dirty appearance formed by lime mud escaped from dolomitization. Calcite filling in intergrain (K). Within the rock ooid or fossil-like structures are present, X63

they locally form interlocked aggregates. Large spaces are present between grains. These spaces are filled with calcite (black areas). Porosity is medium-to high. The crystals become more filthy (blurry) from the center outward. This filthiness is caused by relics of undolomitized lime mud. As a result, the rock gained a cloudy appearance.

This type of dolomites crop out at Toyçu Tepe and at southern slope of Kavunağılı Tepe.

#### Zoned dolomite crystals (Type 3)

These dolomites are light gray and light colored. The crystals are anhedral and rarely euhedral.



Fig. 8- Zoned dolomite crystals (Type 3). There are euhedral-subhedral and partly anhedral with cloudy center (B) fresh framework (Ç) dolomite crystals. Crystals are sutured. Sometimes rudist cast or allochem like structures observed (A). Dolomite crystals cut by late stage fracture and microfractures (Mç) and there are filled with calcite cement (Ç), X63.

(Gregg and Sibley, 1984). They are fine-to medium-grained (0.24-0.37 mm). The crystal boundaries are regular and found in contact with each other (Fig. 8). Porosity is extremely low or undeveloped. The dolomite crystals are intersected by fractures and microfractures. These microfractures are filled with calcite (black areas along fractures). Fossil shells or allochem-like structures are locally seen in the rock. This type of dolomites are usually found at Toyçu Tepe.

#### SCANNING ELECTRON MICROSCOPE (SEM)

The dolomites where crystal types were petrographically defined above, exhibit similar textural features in scanning electron microscopic (SEM) images. The SEM images (664 and 665) of the sample 905 collected from a dolomite outcrop near Salyurt Yayla are given in figures 9 and 10. The image 661 belonging to the same sample (Fig. 9) indicates an euhedral clear dolomite crystal (Type 1: Limpid dolomite). The intergranular spaces that are not filled with dolomite are abundant. The im-



Fig. 9- Fresh dolomite crystals (Type 1) SEM view. Euhedral regular sided, intergrain areas not filled with dolomite cement. Sample no: 905 from Salyurt Yaylası.



Fig. 10 Fresh dolomite crystals (Type 1) SEM view. Euhedral and anhedral crystals. Grains are in contact with each other, porosity decreased. Sample no: 905 from Salyurt Yaylası.

age 665 shows that euhedral crystals as well as subhedral crystals are found (Fig. 10). The crystals are found in contact with each other. As a result, the porosity is poorly developed relative to that in the image 664. A partial dissolution started in dolomite crystals. Consequently, they were replaced by calcite. Figures 11 and 12 show the SEM images of a sample (images 666 and 667), taken from the southern slope of Kavunağılı Tepe. These images belong to filthy (Type 2) dolomite crystals. The leaflike structures in figure 11 are undolomitized

rudist shells. Figure 12 (image 667) shows a subhedral crystal type and dissolution cavities. Both images have filthy and blurry appearance. The presence of undolomitized areas and formation of dolomicrites which represent the early stage of dolomitization caused this filthiness. The SEM images (images 662 and 663) of dolomite sample (sample 905) collected from Salyurt Yaylası are given in figures 13 and 14. These images belong to zoned dolomite crystals (Type 3). The crystals tend to grow inward into the center of hollows. Figure 13



Fig. 11- Dirty (cloudy) appearance dolomite crystals (Type 2) SEM view. Crystal shape and dimension is not clear. The leaf-like structures are rudist casts escaped from dolomitization. Sample no: 560 from south slope of Kavunağılı Tepe.

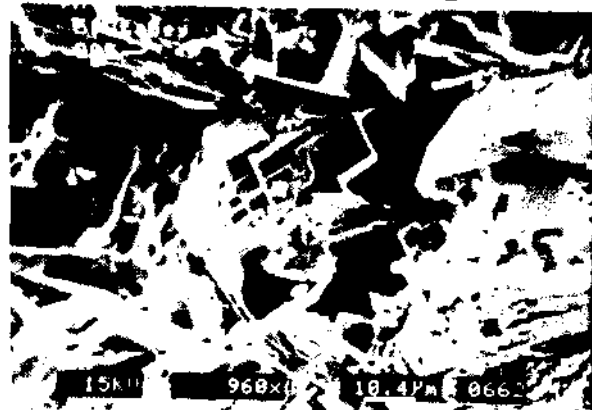


Fig. 13- Zoned growth dolomite crystals (Type 3) SEM view. Increasing growth tendency toward empty center, Euhedral and regular sided. Sample no: 905 from Salyurt Yaylası.

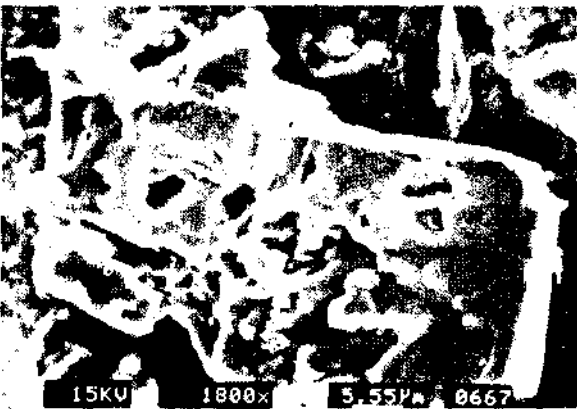


Fig. 12- Dirty-appearance dolomite crystals (Type 2) SEM view. Partly euhedral and anhedral dolomite crystals with dissolve surfaces.

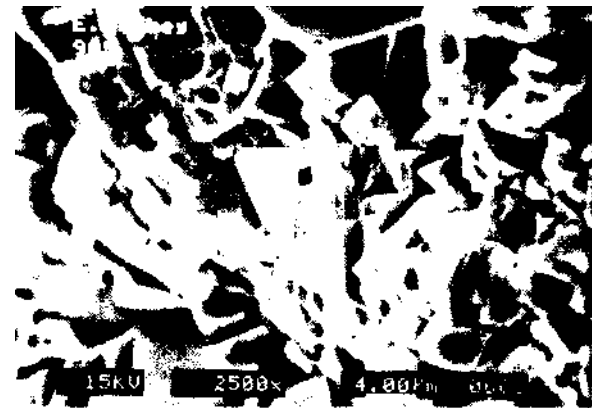


Fig. 14- Zoned growth dolomite crystals (Type 3) SEM view. Increasing growth tendency toward empty crystal center. Anhedral and subhedral crystals with dissolve surfaces. Sample no: 905 from Salyurt Yaylası.

shows euhedral, regular sided dolomite crystals, whereas figure 14 shows anhedral and subhedral dolomite crystals. Dissolution seems to have started in these crystals indicates a multi-stage crystallization rather than a single-stage one.

#### DISCUSSION and CONCLUSIONS

The Upper Cretaceous Yanıktepe formation that belongs to the Gürün autochthonous in Eastern Taurus is represented by limestone and dolomite facies. These facies laterally interfinger with each other. The dolomites formed by dolomitization of limestone facies which consists of foraminifera and macro sholl-bearing (rudist-bearing) mudstone-wackestone-packstone. This is well documented by the presence of dolomitized complete rudist shells in dolomite rocks and of relics of undolomitized limestone in the field.

Having regard the facies features, crystal shapes and texture features of dolomites it is suggested that dolomitization has taken place at early and late diagenetic phases. The absence of evaporite minerals from the collected samples is not reconciled with the model of dolomitization which takes place in evaporitic supra tidal environments, discussed by Illing et al., (1965) and Patterson and Kinsman (1982). Thin section studies reveal that no evaporite minerals formed and no hollows which may be developed by leaching of evaporite minerals as a result of influx of fresh water, are found. The formation model of the Upper Cretaceous dolomites generally fits the model of dolomitization by mixing water, common in reef facies. The Yanıktepe formation is locally composed of rudist-bearing reefs. These rudistiferous reef facies lie on active continental slopes. This activity provided favorable conditions for mixing of fresh water-sea water. It is most likely that a contemporaneous fault tectonics that had been active throughout the Upper Cretaceous played a role on this process. The areas that became shallower during sea level fluctuations (probably short lived lowering and raising of sea level) triggered by fault tectonics concurrent with deposition, were invaded by fresh water. This fresh water was mixed with sea water to make brackish water favorable for dolomitization. The ground water which, becomes brackish by this process can cause dolomitization. At the beginning, dolomitiza-

tion has rapidly taken place in Mg-rich terrains of back-reef shelf lagoon and resulted in the formation of clear dolomite crystals (Type 1). The limestones remained undolomitized when Mg supply was occasionally interrupted and as a result, cloudy textures developed. The solutions which give rise to dolomitization can hardly replace the fossil shells such as rudist and foraminifera at early stages (Sibley, 1980,1982). At more advanced stages, these fossil shells dissolve and Ca deficiency in dolomitizing solutions is compensated in this way. The balancing Mg/Ca ratio (approximately 1/1) results in the formation of dolomite crystals having cloudy centers and clear rims (Type 2), as evidenced by our samples. This type of dolomite crystals discussed here reflect feeding from a local source. This local source can have been originated by dissolution of rudist shells by fresh water effect. Zoned dolomite crystals (Type 3) developed along fractures at late diagenetic stage. The solutions which have arisen possibly recrystallization of early formed dolomites along fractures or in open spaces. The dolomite matrix filling the dissolution spaces resulted in the formation of zoned dolomite crystals (Type 3) in these parts. The trace element analyses on collected samples yielded Sr values between 60 and 90 ppm. These low Sr values has taken place in dolomites in the study area.

#### ACKNOWLEDGEMENT

The writer wishes to thank Prof. Dr. Baki Varol of Ankara University, for critics and contributions during the preparation of this paper.

*Manuscript received February 9, 1995*

#### REFERENCES

- Atabay, E., 1993, Gürün otoktonunun stratigrafisi (Gürün-Sarız arası), Doğu Toroslar, GB Sivas, Türkiye: Türkiye Jeol. Bull.. 36/2, 99-113.
- Badiozamani, K., 1973, The dorag dolomitization model. Application to the Middle Ordovician of the Wisconsin: J. Sed. Petr., 43, 965-986.
- Behrens, E.W. and Land, L.S., 1972, Subtidal Holocene dolomite, Baffin Bay, Texas: Sedimentary Geol., 42, 155-161.

- Deffeyes, K.S.; Lucia, F.J. and Weyl, P.K., 1964, Dolomitization: Observations on the Island of Bonaire, Netherlands Antilles: *Science*, 143, 678-679.
- Dickson, J.A.D., 1965, A modified staining technique for carbonates in thin section: *Nature*, 205: 587.
- Flügel, E., 1982, *Microfacies Analysis of limestones*: pp. 633, Springer-Verlag, Berlin.
- Folk, R.L. and Land, L.S., 1975, Mg/Ca ratio and salinity: Two controls over crystallization of dolomite: *Amer. Assoc. of Petrol. Geol. Bull.*, 59, 60-68.
- Gregg, J.M. and Sibley, D.F., 1984, Epigenetic dolomitization and the origin of xenotopic dolomite texture: *J. Sed. Petr.*, 54, 908-931.
- Hanshaw, B.B.; Back, W. and Dieke, R.G., 1971, A geochemical hypothesis for dolomitization by groundwater: *Econ. Geol.*, 66, 710-724.
- Hardie, L.A., 1986, Perspectives dolomitization: A critical view of some current views: *Sedimentary Geol.*, 57, 166-183.
- Illing, L.V.; Wells, A.J. and Taylor, J.C.M., 1965, Penecontemporary dolomite in the Persian Gulf, in dolomitization and limestone diagenesis: *Soc. Econ. Paleontol. Minerol. Spec. Publ.*, 23, 13, 89-111.
- Land, L.S., 1985, The origin of massive dolomite: *J. Geol. Educ.*, 33, 112-125.
- Matsumoto, R.; Iijima, A. and Katayama, T., 1988, Mixed-water and hydrothermal dolomitization of the Pliocene Shirahama Limestone, Izu Peninsula, central Japan: *Sedimentology*, 35, 979-998.
- McHargue, T.R. and Price, R.C., 1982, Dolomite from clay in argillaceous or shale-associated marine carbonates: *Sedimentary Geol.*, 52, 873-886.
- Patterson, R.J. and Kinsman, D.J.J., 1982, Formation of diagenetic dolomite in coastal sabkha along Arabian (Persian) Gulf: *Amer. Assoc. of Petrol. Geol. Bull.*, 66, 28-43.
- Radke, B.M. and Mathis, R.L., 1980, On the formation and occurrence of saddle dolomite: *Sedimentary Geol.*, 50, 1149-1168.
- Sibley, D.F., 1980, Climatic control of dolomitization, Serro Domi Formation (Pliocene), Bonaire, NA: *Soc. Econ. Paleontol. Minerol. Spec. Publ.*, 28, 247-258.
- , 1982, The origin of common dolomite fabrics: clues from the Pliocene: *J. Sed. Petr.*, 52, 1087-1101.
- Tekeli, O.; Aksay, A.; Ürgün, B.M. and Işık, A., 1983, Geology of the Aladağ Mountains, in: Tekeli, O., and Göncüoğlu, M.C., eds. *Geology of the Taurus Belt*, 143-158.
- Varol, B. and Magaritz, M., 1982, Dolomitization time boundaries and unconformities: examples from the dolostone of the Taurus Mesozoic sequence, south-central Turkey: *Sedimentary Geol.*, 76, 117-133.
- Zenger, D.H., 1983, Burial dolomitization in the Lost Burro Formation/Devonian, eastcentral California and the significance of late diagenetic dolomitization: *Geology*, 11, 519-522.

## GEOLOGY OF THE AKDAĞ MASSIF AND SURROUNDINGS

Ali YILMAZ\*; Şükrü UYSAL\*; Yavuz BEDI\*; Halil YUSUFOĞLU\*; Talat HAVZOĞLU\*; Ahmet AĞAN\*; Deniz GÖÇ\* and Nihal AYDIN\*

ABSTRACT.- The study area is located in the eastern part of Akdağ massive and its surrounding area. The purpose of this paper is to contribute in understanding of the regional geology. In the study area, Akdağmadeni Lithoderm represents basement rocks consisting mainly of gneiss, amphibolite, schist, marble and quartzite. The metamorphic assemblage underwent metamorphism in the higher temperature part of amphibolite facies and was intruded by granitoids and gabbro. The contact between metamorphics and Paleocene volcanics is tectonic. The units showing different sedimentary environments were deposited during Eocene. For example, in the northern part of the area, Eocene units were represented by hemipelagic elastics which overlie Paleocene volcanics conformably and olistostromal rocks composed of Upper Cretaceous mega olistolithes. Within some of the olistolithes there is a sharp facies change between Campanian pelagic limestone and Maastrichtian turbidites. Maastrichtian turbidites pass to the Maastrichtian-Paleocene (?) volcanics conformably. Ophiolitic melange overlies the olistostrome by a northward-dipping overthrust and, passing to the Campanian hemipelagic limestone in the upper levels, in the southern part of the area, the Eocene units are represented by shallow marine deposits and overlie the metamorphic rocks unconformably. This sequence is followed by Oligocene and Lower-Middle Miocene continental deposits respectively. The Upper Miocene-Pliocene fluvial and lacustrine deposits overlie the rest of the older units unconformably. In the neotectonic period, in the study area, the faults showing left lateral-reverse oblique slip in NE-SW trending, right lateral oblique slip in NNW-SSE trending and dip-slip faults in N-S trending, were developed under the control of N-S compression.

## FEATURES AND ORIGIN OF THE KOÇKALE-ELAZIĞ MANGANESE MINERALIZATIONS

Mehmet ALTUNBEY\*\* and Ahmet SAĞIROĞLU\*\*

ABSTRACT.- Koçkale and its vicinity (Elazığ) is composed of four different units. These are; Upper Jurassic-Lower Cretaceous Guleman Group, Campanian-Maastrichtian Yüksekova Complex, Maastrichtian-Lower Eocene Hazar Group and Middle Eocene Maden Complex. The Mn mineralizations of Koçkale are situated in volcanosedimentary rocks of Maden Complex and occur in two types: (1) The mineralizations conformable with volcanosedimentary rocks, are syngenetic and volcanosedimentary type. This type of mineralizations occur within mudstone and as a constituent of this unit The mineralized bodies are tense and stratiform shaped. Any alteration related to mineralization is absent. Ore mineral assemblage is pyroiusite, psilomelane, rodokrosite, braunttite, manganite, limonite, hematite, magnetite, chromite, pyrite and baryite. In places baryite forms silica rich lenses. (2) Vein type mineralizations are epigenetic and are products of hydrothermal solutions circulating through fault and openings. The vein type mineralizations are also situated in different levels and places of mudstone. The mineral assemblage is; pyrolusite, psilomelane, rodokrosite, limonite, hematite, magnetite, chromite and a significant alteration associated with the mineralizations is present.

## TERTIARY MOLLUSK FAUNA AND STRATIGRAPHY OF PINARHISAR (KIRKLARELI) AREA

Yeşim İSLAMOĞLU\* and Güler TANER\*\*\*

ABSTRACT.- A paleontologic-stratigraphic study based primarily on the pelecypod and gastropod fauna was carried out at Pınarhisar (Kırklareli) and its surrounding, for which previous researchers have put forward various ideas, by taking into consideration the ages of the Tertiary sediments and their relation with the Tethys which crop out in the region. In the stratigraphic cross-section made using 8 measurements; 15, 5 and 6 species of molluscan fauna were observed in the İslambeyli formation, Kırklareli limestone and Pınarhisar formation respectively. The ages of the formations were once again taken into consideration under the light of all paleontologic data, and an approximated age was given by evaluating both the paleontological and stratigraphic conditions. The following conclusions were made: The age of the İslambeyli formation which represents the base of the Tertiary sediments is Early Priabonian, the age of the Kırklareli limestone which conformably overlies the İslambeyli formation and which represents the reef carbonates is Late Priabonian and the age of the Pınarhisar formation which unconformably overlies the Kırklareli limestone and which has shelf-margin and shallow sea properties, is Stampian. It was also concluded that the age of the Balıklı serie, which conformably continues over the Pınarhisar formation, is -Stampian as well, according to the paleogeographic distribution of the present molluscan fauna, It can be seen that the majority of it is completely the same with those in the Balcan countries; a minority of it is also seen in the Western European countries in Eocene. In the Oligocene, where it is not abundantly seen, the fact that the basin contains completely the same fauna with Bulgaria shows that it is, within the area of spread of the Paratethis.